Performance Assessment of Global Climate Models for Thailand and Southeast Asia

Suchada Kamworapan

A Thesis Submitted in Fulfillment of the Requirements for the Degree of Doctor of Philosophy Program in Earth System Science (International Program)

Prince of Songkla University

2021

Performance Assessment of Global Climate Models for Thailand and Southeast Asia

Suchada Kamworapan

A Thesis Submitted in Fulfillment of the Requirements for the Degree of Doctor of Philosophy Program in Earth System Science (International Program)

Prince of Songkla University

2021

Thesis Title	Performance Assessment of Global Climate Models for Thailand and Southeast Asia
Author	Miss Suchada Kamworapan
Major Program	Earth System Science (International Program)

Major Advisor

……
(Asst. Prof. Dr. Kritana Prueksakorn)

Co-advisor

…….
(Prof. Dr. Shabbir H. Gheewala)

Co-advisor

…….
(Dr. Pham Thi Bich Thao)

Examining Committee:

……Chairperson
(Asst. Prof. Dr. Sittichai Pimonsree)

…… Committee
(Asst. Prof. Dr. Kritana Prueksakorn)

…… Committee
(Prof. Dr. Shabbir H. Gheewala)

…… Committee
(Dr. Kiyota Hashimoto)

…… Committee
(Dr. Pham Thi Bich Thao)

…… Committee
(Dr. Tanwa Arpornthip)

The Graduate School, Prince of Songkla University, has approved this thesis as fulfillment of the requirements for the Doctor of Philosophy Degree in Earth System Science (International Program)

……
(Prof. Dr. Damrongsak Faroongsarng)
Dean of Graduate School

This is to certify that the work here submitted is the result of the candidate's own investigations. Due acknowledgement has been made of any assistance received.

……..……. Signature
(Asst. Prof. Dr. Kritana Prueksakorn)
Major Advisor

……. Signature
(Miss Suchada Kamworapan)
Candidate

I hereby certify that this work has not been accepted in substance for any degree and is not being currently submitted in candidature for any degree.

……. Signature

(Miss Suchada Kamworapan)

Candidate

ชื่อวิทยานิพนธ์ Performance Assessment of Global Climate Models for Thailand and Southeast Asia
ผู้เขียน นางสาวสุชาดา ขำวรพันธ์
สาขาวิชา วิทยาศาสตร์ระบบโลก (หลักสูตรนานาชาติ)
ปีการศึกษา 2564

บทคัดย่อ

เอเชียตะวันออกเฉียงใต้ถือว่าเป็นภูมิภาคที่มีความเสี่ยงจากการเพิ่มความถี่และความรุนแรงของภัยพิบัติทางธรรมชาติ ประเทศไทยเป็นหนึ่งในประเทศที่ตั้งอยู่ในเอเชียตะวันออกเฉียงใต้ ย่อมได้รับผลกระทบเป็นอย่างมากจากภัยพิบัติทางธรรมชาติเหล่านี้ แบบจำลองสภาพภูมิอากาศโลก (GCM) ได้รับการพัฒนาขึ้นมาเพื่อจำลองลักษณะภูมิอากาศในอดีตและปัจจุบัน รวมทั้งถูกนำมาใช้ประโยชน์ในการทำนายสภาพภูมิอากาศในอนาคต อย่างไรก็ตาม GCM ถูกสร้างขึ้นมาจากสถาบันทางด้านภูมิอากาศหลายแห่งทั่วโลก ส่งผลให้ผลการจำลองสภาพภูมิอากาศของแต่ละ GCM มีความแตกต่างกันอันเนื่องมาจากการกำหนดค่าพารามิเตอร์ที่ต่างกัน ดังนั้นจุดมุ่งหมายของการศึกษานี้คือเพื่อค้นหา GCM ที่มีประสิทธิภาพดีที่สุดในรุ่น Coupled Model Intercomparison Project Phase 5 (CMIP5) และ Coupled Model Intercomparison Project Phase 6 (CMIP6) ในการจำลองสภาพภูมิอากาศในเอเชียตะวันออกเฉียงใต้และประเทศไทยตามลำดับ CMIP5 GCM จำนวน 40 รุ่น ถูกนำมาประเมินประสิทธิภาพในการจำลองอุณหภูมิและหยาดน้ำฟ้าสำหรับช่วงเวลาระยะสั้น (1960 - 1999) และระยะเวลาระยะยาว (1901 - 1999) ครอบคลุมพื้นที่เอเชียตะวันออกเฉียงใต้ ผลลัพธ์ที่ได้จากการจำลองจะถูกนำประเมินประสิทธิภาพโดยใช้ตัวชี้วัดทางสถิติ 10 ตัวและตรวจสอบความถูกต้องโดยเปรียบเทียบกับชุดข้อมูล ground-based และ reanalysis ผลการศึกษาพบว่า CNRM-CN5-2 คือ GCM ที่มีประสิทธิภาพดีที่สุดในการจำลองอุณหภูมิและหยาดน้ำฟ้าบริเวณเอเชียตะวันออกเฉียงใต้เมื่อเปรียบเทียบกับ GCM รุ่นอื่นๆ รองลงมาคือ CNRM-CM5, BNU-ESM, CESM-CAM5 และ CCSM4 ตามลำดับ ในขณะที่ CMIP6 GCMs จำนวน 13 รุ่น ถูกนำมาประเมินประสิทธิภาพในการจำลองอุณหภูมิสำหรับช่วงเวลาที่ใกล้เคียงปัจจุบัน (2000 - 2014) ครอบคลุมพื้นที่ประเทศไทย ผลการจำลองจะถูกนำประเมินประสิทธิภาพโดยใช้ตัวชี้วัดทางสถิติ 5 ตัว และตรวจสอบความถูกต้องโดยเปรียบเทียบกับชุดข้อมูล ground-based และ reanalysis ผลการศึกษาพบว่า CNRM-CM6-1, CNRM-CM6-1-HR และ CNRM-ESM2-1 สามารถจำลองอุณหภูมิได้ดีกว่า GCMs รุ่นอื่นๆ โดยเฉพาะอย่างยิ่ง CNRM-ESM2-1 ในขณะเดียวกัน MIROC6 ถูกพบว่าเป็น GCM ที่มีประสิทธิภาพแย่ที่สุดในจำลองอุณหภูมิพื้นที่ประเทศไทย

คำสำคัญ: Global climate models, CMIP5, CMIP6, Temperature, Precipitation, Southeast Asia, Thailand

Thesis Title Performance Assessment of Global Climate Models for Thailand and Southeast Asia
Author Miss Suchada Kamworapan
Major Program Earth System Science (International Program)
Academic Year 2021

ABSTRACT

Southeast Asia is a region vulnerable to climate variability that increases the frequency and intensity of natural disasters. Thailand, one of the Southeast Asia countries, is also highly affected by these natural disasters. Global climate models (GCMs) are developed to simulate the past and present climatic characteristics and predict the climate in the future. However, there are a variety of GCMs developed by many climate institutes around the world and their GCMs have different performances due to different parameterizations. Therefore, the aim of this study is to find the best GCMs in CMIP5 and CMIP6 that work over Southeast Asia and Thailand, respectively. In Southeast Asia, temperature and precipitation simulated by 40 CMIP5 GCMs are evaluated for the short-term period (1960 - 1999) and the long-term period (1901 - 1999). Simulation results are compared with ground-based and reanalysis data using ten statistical metrics. The results show that CNRM-CN5-2 has the best performance with the lowest total error, followed by CNRM-CM5, BNU-ESM, CESM-CAM5, and CCSM4, respectively. In Thailand, the temperatures simulated by 13 CMIP6-GCMs are evaluated for the near-to-current term period (2000 - 2014). The simulation results are compared with the ground-based and reanalysis data using five statistical metrics. The results show that CNRM-CM6-1, CNRM-CM6-1-HR and CNRM-ESM2-1 perform better than the other models in temperature simulation over Thailand. In particular, CNRM-ESM2-1 perform best for all study cases, while MIROC6 perform worst for all study cases in this study area.

Keywords: Global climate models, CMIP5, CMIP6, Temperature, Precipitation, Southeast Asia, Thailand

ACKNOWLEDGEMENT

I would like to convey my sincere gratitude and thanks to my advisor, Asst. Prof. Dr. Kritana Prueksakorn, for his guidance, teaching, and support. I am grateful for all his advice, not only for the research but also for life. Without his encouragement, I would not have been able to complete my research.

Also, I would like to thank my co-advisor, Prof. Dr. Shabbir H. Gheewala, and Dr. Pham Thi Bich Thao for their consistent guidance, helpful and constructive suggestions. Their insightful feedback helped me to improve my research.

I would like to thank Asst. Prof. Dr. Chinnawat Surussavadee for his teaching on climate model and Matlab techniques.

I would like to extend my gratitude to my chairman, Asst. Prof. Dr. Sittichai Pimonsree, also, I thank all my committees, Prof. Dr. Kiyota Hashimoto and Dr. Tanwa Arpornthip for their valuable time spent on my study.

I would like to thank the staffs of the Faculty of Technology and Environment at Prince of Songkla University, Phuket Campus for their great support.

I would also like to thank all my friends, especially Ms. Thanchanok Noosook and Ms. Hong Anh Thi Nguyen who always helped me during my dissertation.

Finally, I would like to express my grateful thank to my parents who gave me the opportunity to be educated in the best institutions and supported me throughout my life.

Suchada Kamworapan

CONTENTS

CONTENTS (Continued)

CONTENTS (Continued)

Page

LIST OF FIGURES

LIST OF FIGURES (Continued)

LIST OF FIGURES (Continued)

LIST OF FIGURES (Continued)

LIST OF FIGURES (Continued)

LIST OF TABLES

LIST OF TABLES (Continued)

LIST OF TABLES (Continued)

LIST OF ABBREVIATION

ADW	The angular-distance weighting
AGCMs	Atmospheric general circulation models
AOGCMs	Atmosphere-ocean general circulation models
APHRODITE	Asian Precipitation – Highly Resolved Observational Data Integration Towards Evaluation
AR6	Intergovernmental Panel on Climate Change Sixth Assessment Report
BCC	Beijing Climate Center
BNU	Beijing Normal University,
CAI	Climatologically aided interpolation
CAMS	Chinese Academy of Meteorological Sciences
CanAM4	The Canadian Fourth Generation Atmospheric Global Climate Model
CCA	Canonical correlation analysis
CCCM	Canadian Center for Climate Modeling and Analysis
CCSR	the Center for Climate System Research
CDR	Climate Data Record
CERFACS	Centre Europeen de Recherche et Formation Avancees en Calcul Scientifique
CFCs	Chlorofluorocarbons
CH_4	Methane
CICE	The Los Alamos Sea-Ice Model
CMAP	Climate Prediction Center Merged Analysis of Precipitation
CMCC	Centro Euro-Mediterraneo per I Cambiamenti Climatici

LIST OF ABBREVIATION (Continued)

CMIP	Coupled Model Intercomparison Project
CMIP1-6	Coupled Model Intercomparison Project Phase 1-6
CMIP5-6	Coupled Model Intercomparison Project Phase 5 and 6
CNRM	Centre National de Recherches Meteorologiques
CN05	The China Region 05
COCO	CCSR Ocean Component Model
CoLM	The Common Land Model
CO_2	Carbon dioxide
CPC	Climate Prediction Center
CPC-UNI	Climate Prediction Center unified rain gauge
CRU	Climatic Research Unit
CRU TS	Climate Research Unit Time Series
CSIRO-QCCCE	Organization/Queensland Climate Change Center of Excellence
CTEM	The Canadian Terrestrial Ecosystem Model
CV	Coefficient of variation
DAS	Data assimilation system
DECK	Diagnostic Evaluation and Characterization of Klima
DEM	Digital-elevation-model
ECMWF	European Centre for Medium-Range Weather Forecasts
EC-EARTH	A European community Earth-System Model
ENSO	The El Niño-Southern Oscillation

LIST OF ABBREVIATION (Continued)

EOF	Empirical orthogonal function
ERA-Interim	European Centre for Medium-Range Weather Forecasts Interim reanalysis
ERA40	European Centre for Medium-Range of Weather Forecasts 40 Year Re-analysis
FAMIL	The Finite-volume Atmospheric Model of the IAP/LASG
FIO	The First Institute of Oceanography
FMA	February, March, April
GCMs	Global circulation/climate models
GELATO	Global Experimental Leads and ice for Atmosphere and Ocean
GEOS	Goddard Earth Observing System
GFDL	Geophysical Fluid Dynamics Laboratory
GHGs	Greenhouse gases
GMAO	Global Modeling and Assimilation Office
GPCP	Global Precipitation Climatology Project
HYCOM	The Hybrid Coordinate Ocean Model
IFS	The Integrated Forecasting System
INM-CM4	Institute for Numerical Mathematics
IPCC	Intergovernmental Panel on Climate Change
IPSL	Institut Pierre Simon Laplace
ISBA	Interaction Sol-Biosphère-Atmosphère
JULES	The Joint UK Land Environment Simulator

LIST OF ABBREVIATION (Continued)

KS-test	Kolmogorov-Smirnov test
LICOM	LASG/IAP Climate system Ocean Model
LIM	Louvain-la-Neuve sea ice model
MA	Mean Annual
MATSIRO	The Minimal Advanced Treatments of Surface Interaction and Runoff
MBE	Mean bias error
MDTR	Mean diurnal temperature range
MERRA2	The Modern-Era Retrospective Analysis for Research Applications, Version 2
MJJASO	May, June, July, August, September, October
mm	millimeter
MMM	the season designation
MOM	The Modular Ocean Model
MPI	Max Planck Institute for Meteorology
MRI	Meteorological Research Institute
NASA	The National Aeronautics and Space Administration
NCAR	National Center of Atmospheric Research
NCC	Norwegian Climate Center
NCEP	National Center for Environmental Prediction/National Center for Atmospheric Research Reanalysis Reanalysis
NDJ	November, December, January

LIST OF ABBREVIATION (Continued)

NEMO	The Nucleus for European Modelling of the Ocean
NMSs	National Meteorological Services
NOAA	The National Oceanic and Atmospheric Administration's National Climatic Data Center
NSD	Normalizated Standard deviation
N_2O	Nitrous oxide
OGCMs	Oceans general circulation models
OPA	The Océan PArallélisé
ORCHIDEE	Organizing Carbon and Hydrology in Dynamic Ecosystems Environment
O_3	Ozone
P	Precipitation
PNW	Pacific Northwest
POP	Parallel Ocean Program
P1	The period 1901 to 1940
P2	The period 1941 to 1970
P3	The period 1971 to 2014
P4	The period 1901 to 2014
r	The correlation coefficient
RCP	A Representative Concentration Pathway
RMSE	Root mean squared error
SD	Standard deviation

LIST OF ABBREVIATION (Continued)

SeasonAmp	Mean seasonal cycle amplitude
SIS	Sea Ice Simulator
SVD	Singular value decomposition
T	Temperature
Tas	Near-Surface Air Temperature
TESSEL	The Tiled ECMWF Scheme for Surface Exchanges over Land
Trend	Linear trend
TRMM	Tropical Rainfall Measuring Mission
UD	University of Delaware Air Temperature and Precipitation
UNFCCC	United Nations Framework Convention on Climate Change
Var	Variance
WCRP	World Climate Research Program
WGCM	Working Group of Coupled Modelling
WMO	The World Meteorological Organization
6-MODEL ENSEMBLE	The multi-model ensembles of the top-six GCMs
13-MODEL ENSEMBLE	The multi-model ensembles of the 13 GCMs
40-MODEL ENSEMBLE	The multi-model ensembles of the 40 GCMs

CHAPTER 1
INTRODUCTION

1.1 Problem statement

Climate change is one of the most discussed environmental issues. It not only increases the magnitude and frequency of natural disasters, but also seasonal weather changes. A number of serious events have been attributed to climate change. For example, 30% of glaciers at European Alps were lost between 1912 and 2003, while glaciers in the North Caucasus region of Russia shrank by 50% between 1998 and 2001 (Zemp et al. 2007). The temperature in Europe reached a record 40 °C in 2003 (De Bono et al. 2004). Between 2000 and 2012, global mean sea level rose by 1.1 - 2.1 mm/year compared to the 1880 – 1980 average (Dasgupta and Meisner 2009 and Warrick et al. 1990). In the early 2000s, the coral bleaching had been found especially in the tropical oceans (Wilkinson 2000). Nowadays, extreme natural events are becoming more frequent (Khalid et al. 2017). As a result, humanity is suffering from more life hazards and property damage. Understanding the changing climate on Earth could be a first step to curb the devastation.

The climate system is an interactive system that consists of the atmosphere, hydrosphere, cryosphere, land surface, biosphere, and solar energy (Treut et al. 2007). The interactions between the components make the climate system even more complex. Before it was affected by human activities, the climate was changing steadily and regularly (Cubasch et al. 2013). In 2017, the Earth's temperature was found to have warmed by about 1 °C more than in the pre-industrial era, primarily due to human activities. This leads to a change in the composition of the atmosphere (Trenberth et al. 1996; Hoegh-Guldberg et al. 2018). These events and historical data could help climate scientists understand how the climate is changing. Research centers around the world are working to develop climate models, also known as global climate models (GCMs), not only to simulate the climate characteristics of the past and recent, but also to achieve another development: predicting climate in the future with high accuracy (Randall et al. 2007).

GCMs are mathematical models useful for the study of climate. They can demonstrate the components of the climate system of the atmosphere, oceans, cryosphere, biosphere, and geosphere. In addition, the new generation of GCMs adds more complex components such as the carbon cycle, aerosol processes, and atmospheric chemistry (Trenberth et al. 1996; Flato et al. 2019). Climate scientists from many countries have worked from 1995 to the present to develop them to simulate climate as closely as possible to the real climate system (Flato et al. 2019).

Coupled Model Intercomparison Project (CMIP) is a project under the World Climate Research Programme (WCRP) Working Group on Coupled Modelling (WGCM). GCMs participating in this project are determined framework by standard experimental of CMIP (Haarsma et al. 2016; Stouffer et al. 2017). In 2008, twenty climate modeling groups agreed to the new coordinated set of GCM experiments that formed the framework for CMIP5 implementation. These experiments were designed to focus on both the long-term (century) and short-term (10–30 years) time frames to represent the multi-faceted nature of climate change and variability. Moreover, they can highlight gaps in change in past climate as well as in future climate scenarios (Taylor et al. 2012; Su et al. 2013). Thus, the model results of CMIP5 provide a deeper understanding of the climate system. Recently, the latest phase of CMIP, CMIP6, has become available. Although it was developed based on CMIP5, it has improved the process of physical parameterization and has higher spatial resolution and more components of Earth system processes than CMIP5 (Fan et al. 2020). The critical question is whether the improvement of GCMs in CMIP6 has been sufficiently developed and solved to simulate the climate. Another issue is that the GCMs participating in the CMIP projects are produced by different climate institutes around the world (Taylor et al. 2012), therefore there are different physical parameterizations and strategies of each GCM (Hourdin et al. 2006). The fact remains that the topography and climate characterization of each region are different (White et al. 2010). Hence, the internal determinations of GCMs are the key to show the different performance of GCMs for different regions because it is difficult to input the topography and climate datasets that cover the entire globe. For this reason, researchers have evaluated the performance of GCMs in different regions of the world (Kumar et al. 2013; Rupp et al. 2013; Su et al. 2013; Miao et al. 2014; Moise et al. 2015; Lovino et al. 2018; Raghavan,

et al. 2018). This study focuses on Southeast Asia and Thailand, areas with high climate sensitivity and variability (Tan et al. 2010).

Southeast Asia is one of the most vulnerable regions in the world. In recent decades, it has experienced frequent extreme natural disasters, probably due to climate change. For example, heat waves that occurred between 1961 and 1998 (Khalid et al. 2017). Drought events caused forest fires, crop failures, and water shortages in the period from 1997 to 1998, and the increasing frequency of cyclones and typhoons had caused major floods in many countries in 1990, 2000, and 2004 (Tan et al. 2010). Thailand is a country in Southeast Asia and highly affected by climate variability. It is frequently hit by floods and droughts without being prepared for them. Besides, the temperature in Thailand has increased by about 1.04-1.80 °C per century (Tan and Pereira 2010; Haraguchi and Lall 2015). These examples show that natural disasters in the study areas are related to the climate variables. As a result, the economies of Southeast Asia and Thailand are extremely affected because their principal economies are mainly based on agriculture and natural resources, as well as economic activities in coastal areas (Tan et al. 2010).

Weather-related natural disasters that occur in the study areas are mainly related to the variables of temperature and precipitation (Seneviratne et al. 2012). Both variables are important climate factors that directly influence the occurrence of floods, storms, landslides, droughts and extreme temperatures (CRED and UNISDR 2015). These natural disasters damage human lives and property (Handmer et al. 2012). In addition, the increasing frequency of natural disasters has a strong impact on human occupations, especially agriculture, as it is mainly dependent on climate for its production (Nastis et al. 2012). Since agriculture is considered as one of the major occupations of the population of Southeast Asia, the study areas could not escape the impacts of these climate variability. Hence, the evaluation of GCMs of this study is useful because these results show the best GCMs for temperature and precipitation simulation in Southeast Asia and for temperature simulation in Thailand. They also show the changes of temperature and precipitation that occurred in the past in the study area.

Subsequently, the current CMIP is used for climate simulation at Southeast Asia (CMIP5 was the latest version at that time). In addition to the regional

level, it is further investigated whether the best GCM for the national level is still the same for the regional level or not. Therefore, CMIP6 (the latest version) is used for climate simulation, and Thailand was selected as the study area for national simulation. Moreover, the result of this study is a preliminary guide to support climate studies in Southeast Asia and Thailand. Therefore, this work aims to evaluate and find suitable GCMs for climate simulation in Southeast Asia and Thailand.

1.2 Research objectives

- To evaluate the performance of GCMs for temperature and precipitation simulation over Southeast Asia and for temperature simulation over Thailand.
- To find the best GCM for climate simulation over Southeast Asia and Thailand

1.3 Research scope

The study evaluates the performance of 40 different global climate models in CMIP5 for temperature and precipitation simulations of the 20th century. The results of the global climate models are evaluated using observations and reanalysis data from University of East Anglia Climatic Research Unit (CRU) TS3.10.01, University of Delaware Air Temperature and Precipitation (UD) v.3.01, National Center for Environmental Prediction/National Center for Atmospheric Research Reanalysis (NCEP), European Centre for Medium-Range of Weather Forecasts 40 Year Re-analysis (ERA40). Besides, this study employs 13 different global climate models in CMIP6 for temperature simulations at the beginning of the twenty-first century (2000-2014). All GCMs CMIP6 results were compared with observational data from the University of Delaware (UD) Air Temperature V5.01, the University of East Anglia Climatic Research Unit Time Series (CRU TS) V4.02; also, reanalysis datasets from the Modern-Era Retrospective Analysis for Research Applications, Version 2 (MERRA2), and the European Centre for Medium-Range Weather Forecasts (ECMWF) Interim Reanalysis (ERA-Interim) were used for model evaluation.

CHAPTER 2
LITERATURE REVIEW

2.1 Climate change

Climate is weather in the sense of the average and its variability over a long-term period (decade, centuries) of a place or region. Climate data are temperature, humidity, precipitation, clouds and wind. The climate of each place varies and depends on latitude, intensity of solar radiation, wind and ocean currents, distance to the sea, vegetation and mountains, and surface variables such as temperature and precipitation (IPCC, 2007; Bauer et al. 2016; Shepardsona et al. 2011; Houghton 2002).

United Nations Framework Convention on Climate Change (UNFCCC) reports that climate change is mainly caused by changes in atmospheric components such as carbon dioxide (CO_2), methane (CH_4), nitrous oxide (N_2O), chlorofluorocarbons (CFCs), and ozone (O_3). These gases are known as greenhouse gases and are produced to a significant extent by human activities such as fossil fuel burning (transportation), deforestation, heating and cooling of buildings, production of cement and chlorofluorocarbons, especially after the industrial revolution (Trenberth et al. 2000; Bitz and Marshall 2008; UNFCCC 1992; IPCC 2007). The increase in greenhouse gases causes the greenhouse effect, which leads to changes in the global system, especially an increase in global temperature.

Figure. 2.1 shows temperature records from NASA's Goddard Institute for Space Studies (NASA), the National Oceanic and Atmospheric Administration's National Climatic Data Center (NOAA), the Met Office Hadley Centre (UK), the Berkeley Earth research group, and Cowtan and Way's analysis. They show a graph of temperature anomalies from 1880 to 2019 compared to the baseline average temperature for the period 1951-1980. Their records also show that past temperature has increased dramatically since the 1980s, especially in the last decade (NASA/NOAA 2020).

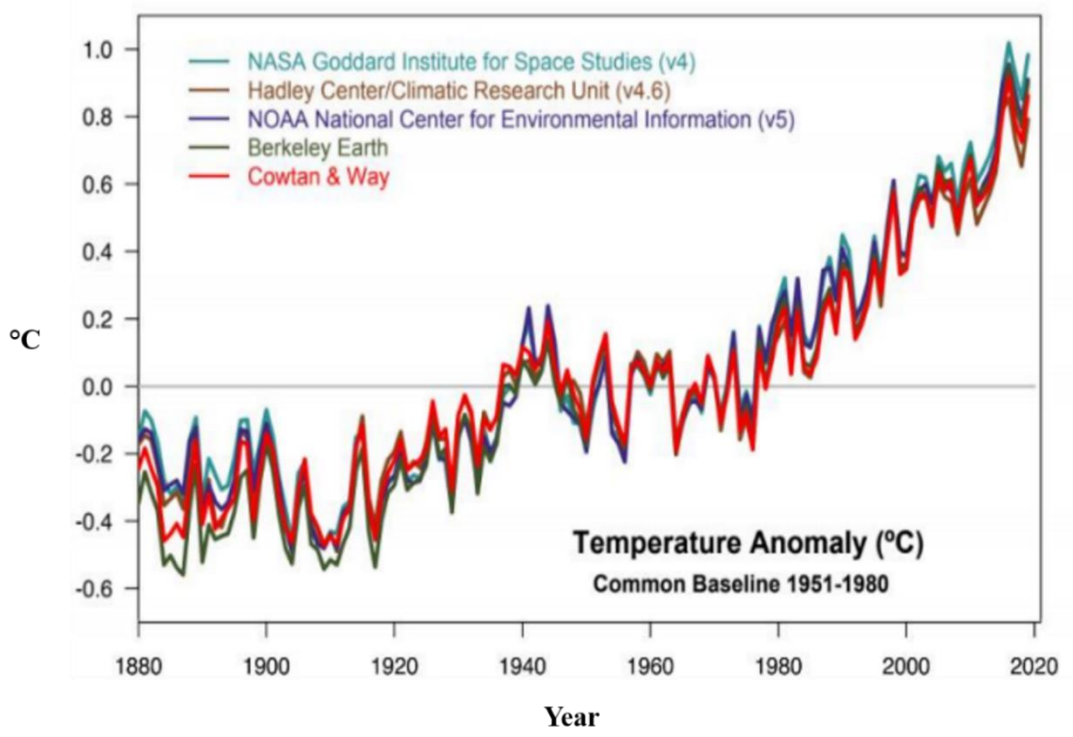

Figure 2.1 Annual anomalies in global surface temperature from 1880 to 2019 recorded by five climate agencies (NASA /NOAA, 2020)

2.2 Global climate models

General Circulation Model or Global Climate Models (GCMs) are a complex model developed to represent the physical, chemical, and biological processes in the atmosphere, oceans, land surface, and cryosphere components and their interactions (Figure 2.2) (Dunlea and Elfring 2012).

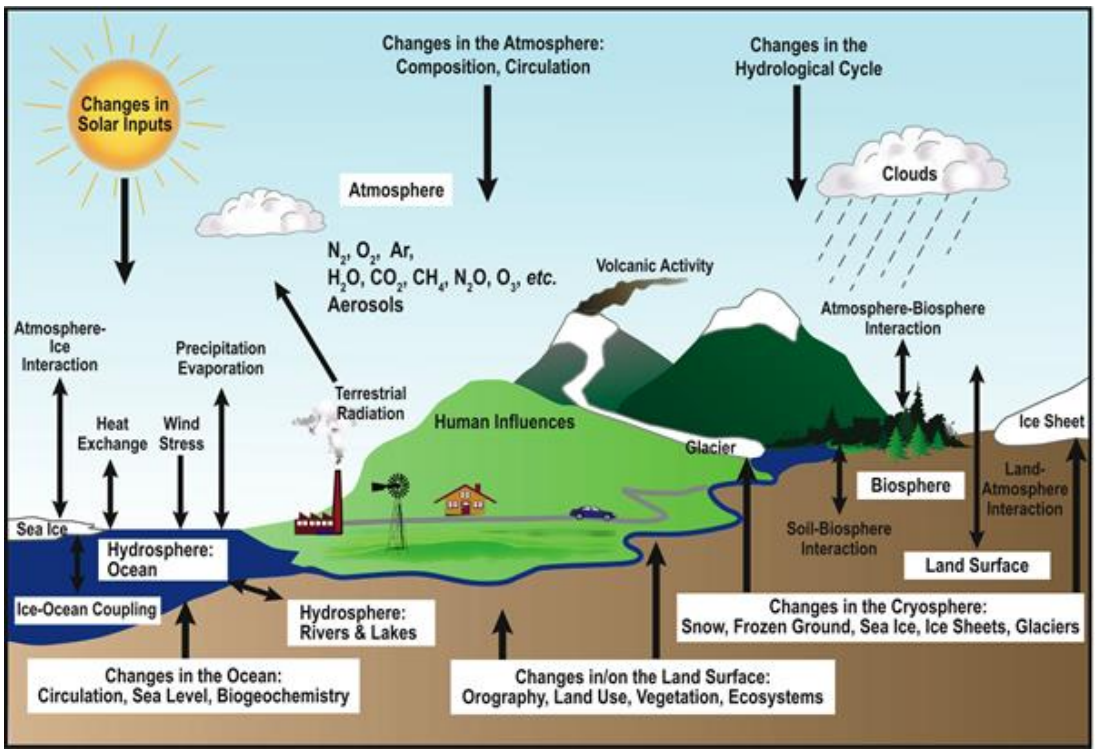

Figure 2.2 Schematic representation of the major processes and components of the global climate system (IPCC 2007)

The internal climate sub-models of the GCMs focus on simulating the individual components of the climate system, which consist of the atmospheric model, the ocean model, the land model, and the sea-ice model (Figure 2.3) (Gent 2012). To simulate these climate components, GCMs use mathematical equations and physical laws, including the conservation laws for momentum, energy, mass, and humidity, and the ideal gas law (Schneider 1992). These are the main equations used by GCMs to describe the motion of fluids and gases in the atmosphere and ocean. GCMs require some input data derived from observations or other modeling studies, including

- Earth's properties: Earth's radius and rotation period, land topography, ocean coastline and bathymetry, land/soils properties
- Boundary conditions: Distribution of vegetation, topography of ice sheets
- Solar influences: Monthly or annual solar radiation
- Emissions: Monthly or annual CO_2 emissions in the grid

- Concentrations of GHGs and aerosols: global mean time series (e.g., black carbon, organic carbon, CH_4, sulfur)
- Volcanic forcing: Dust and sulfur emissions
- Ozone: Time-evolving 3d concentrations for forcing in models
- Land use: emissions from changes in land cover

GCMs represent the Earth through three-dimensional spatial grids of the atmosphere, oceans, and land that include both horizontal and vertical grids for representing the most realistic climate possible (Figure 2.4). Grid boxes containing climate information are built in, and the resolution of the GCMs is defined by the size of the grid boxes (Edwards 2011; Gettelman and Rood 2016). In each grid cell, GCMs compute basic physical variables such as temperature, precipitation, pressure, winds, and humidity. In addition, GCMs produce a variety of output data, such as soil layer moisture content, soil moisture content, surface eastward stress, surface downward northward stress, surface snow thickness, surface temperature, surface air pressure, snowfall flux, surface upward latent heat flux, surface upward sensible heat flux, runoff flux, land surface snow amount, etc. (Meehl et al. 2007).

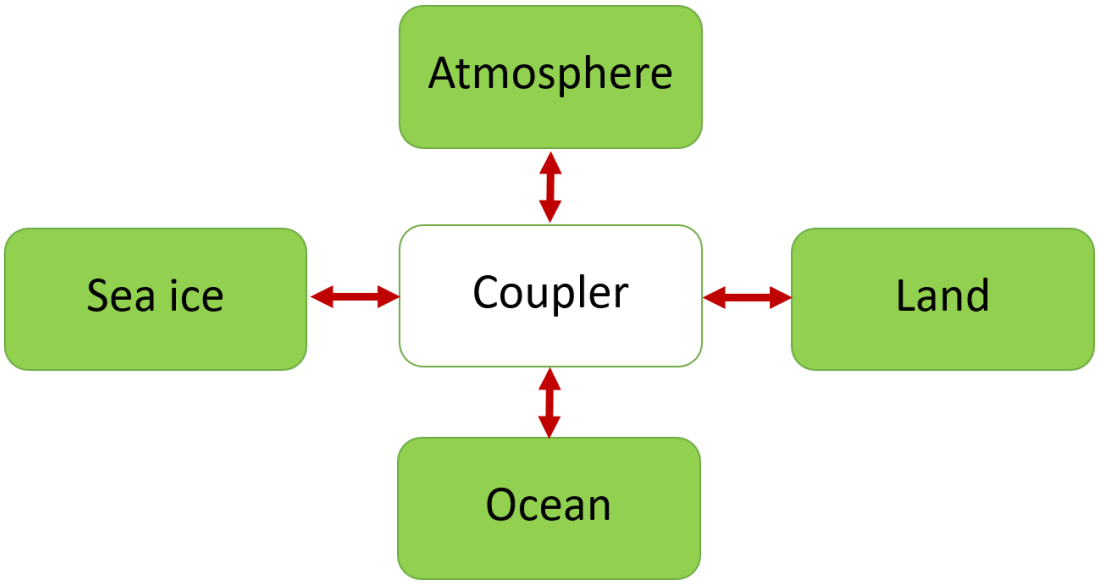

Figure 2.3 Key components of GCMs (adapted from Gent 2012)

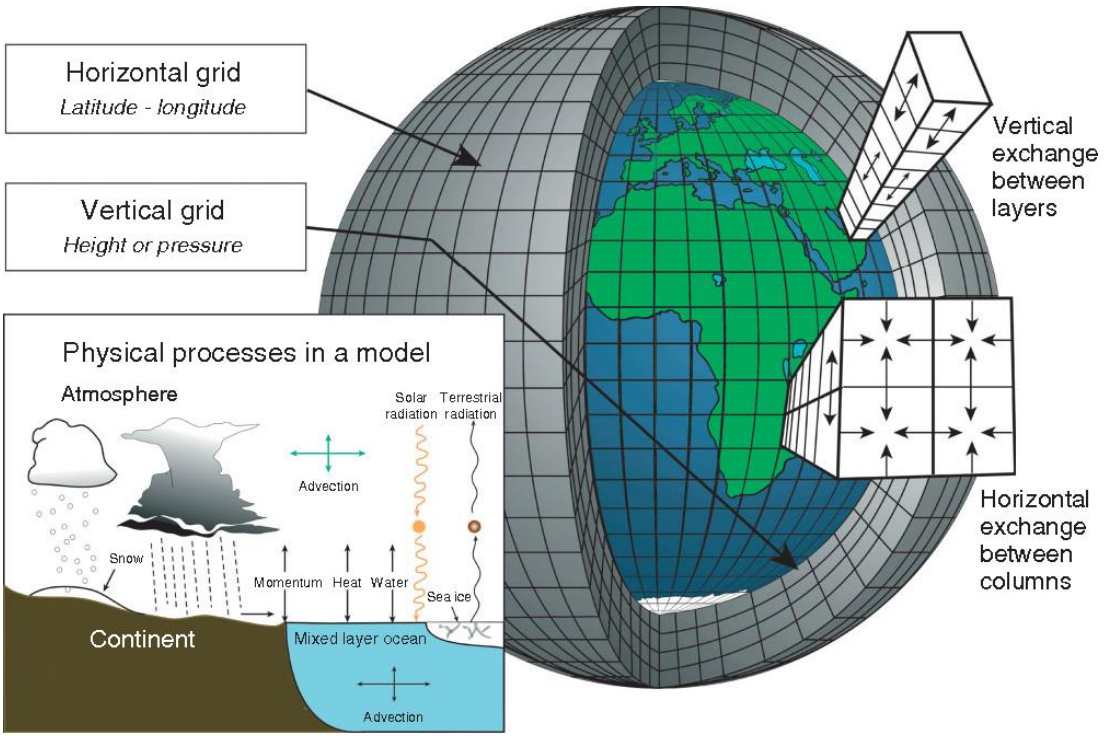

Figure 2.4 Schematic representation of physical processes and grid structure in global climate models (Edwards 2011)

GCMs are divided into 3 types, namely atmospheric general circulation models (AGCMs), ocean general circulation models (OGCMs), and atmosphere-ocean general circulation models (AOGCMs). These models can predict future climate based on emission scenarios that describe the amount of greenhouse gas emissions, aerosols, and other pollutants including land use and land cover. AOGCMs are a more complex calculation because this model adds sea ice and land components. Therefore, AOGCMs is a full version climate model and is currently used as the basis for climate models. GCMs are typically run on a high performance computer to simulate past, present, and future climate (Randall et al. 2007; Symon 2013).

In summary, GCMs are the most appropriate and useful tool to understand the complex climate system and climate change around the world used for climate simulations and projections. (Voldoir et al. 2013; Lauer et al. 2013; Vigaud et al. 2009). According to Cubasch et al. (2013), GCMs have been developed over time with more components and higher resolutions, resulting in more complex processes in GCMs from 1992 to the present (Figure 2.5). Nowadays, GCMs have a spatial

resolution of about 100-300 km, while the temporal resolution is 1-hourly to monthly data.

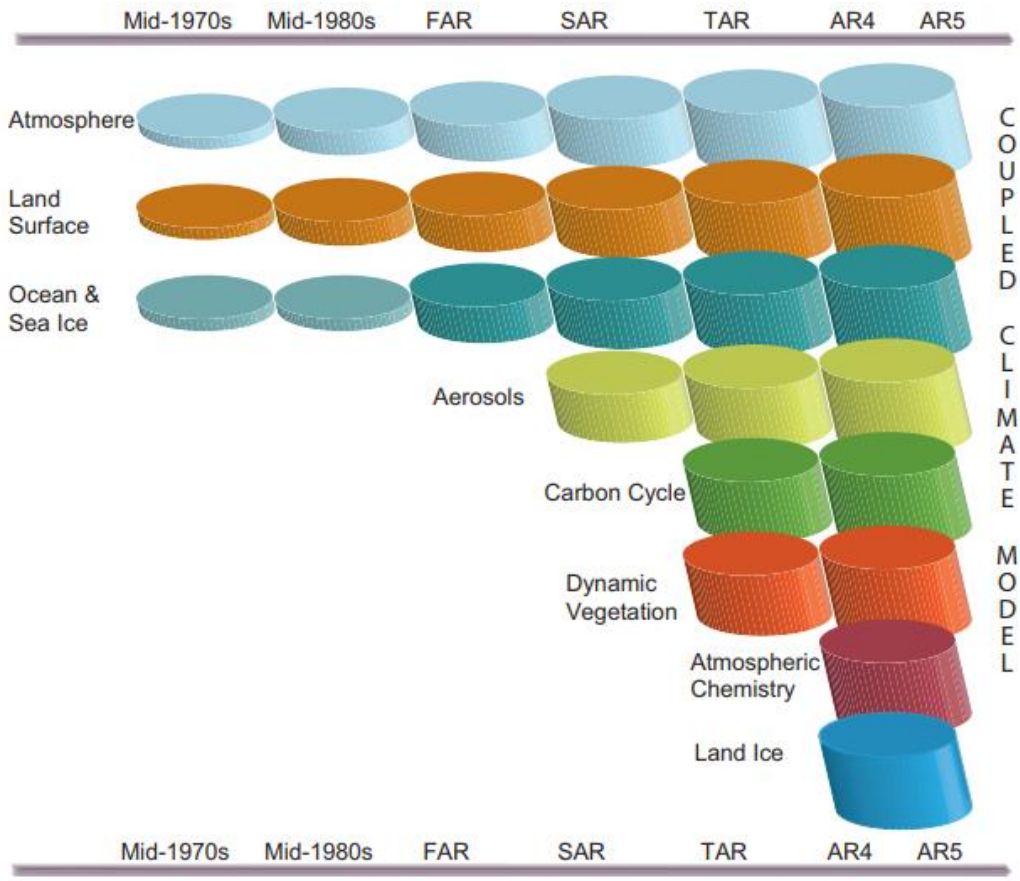

Figure 2.5 The development of climate models (IPCC 2013)

2.3 Coupled Model Intercomparison Project (CMIP)

The World Climate Research Program (WCRP) and the World Meteorological Organization (WMO) build CMIP to collect GCMs from climate research centers around the world. CMIP phases are continuously released to develop the performance of GCMs (Bock et al. 2020). The experimental design of CMIP1 and CMIP2 is simple (Stouffer et al. 2017), while CMIP3 is increasingly complex and represent the first phase of atmospheric and ocean general circulation models (AOGCMs) (Meehl el al. 2007).

CMIP5 was developed based on CMIP3, but added land and ocean biogeochemical processes and experiments with future climate scenarios (Stouffer et al. 2017). The goal of CMIP5 is set to assess the past climate of GCM as it realistically occurs. The experiments were designed to focus on both long-term (century) and short-term (10–30 years) experiments to represent the multiview of climate change and variability as well as climate projections. Thus, the GCM results in CMIP5 have a deeper understanding of the climate system than in earlier phases (Taylor et al. 2012).

Figure 2.6 shows all CMIP5 experiments in which the length of the experiment portion indicates the length of the simulation. The highest priority experiments are in the core, while the tier 1 and tier 2 experiments are lower priority. The main CMIP5 experiments are divided into 4 types, including climate projections (blue), model understanding (yellow), model evaluation (red), carbon cycle experiments (green) (Jones et al. 2011).

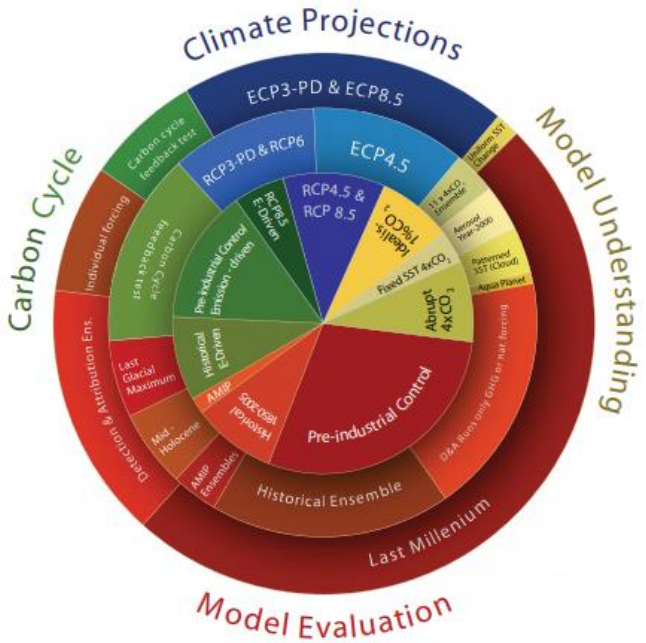

Figure 2.6 A schematic summary of the CMIP5 model experiments (Jones et al. 2011)

CMIP6 is the current phase. It improves the process of physical parameterization and higher spatial resolution; there are also more components of Earth system processes than in CMIP5 (Fan et al. 2020). The results of CMIP simulations are used to evaluate climate for several international projects, such as the 2001, 2007, and

2013 assessment reports of the Intergovernmental Panel at Climate Change (IPCC) (IPCC 2014; Taylor et al. 2012). Simulation results from CMIP6 are expected to appear in IPCC Sixth Assessment Report (AR6). Figure 2.7 shows a schematic representation of the CMIP6 experimental design, which focuses on specific themes. The core consists of the standardized functions of all CMIP Diagnostic Evaluation and Characterization of Klima (DECK) experiments, as well as the CMIP6 historical simulation. The middle and outer ring consists of science questions and challenges used to determine CMIP6. Table 2.1 and 2.2 show the sub-model components of each CMIP5 and CMIP6 GCMs used in this study, respectively.

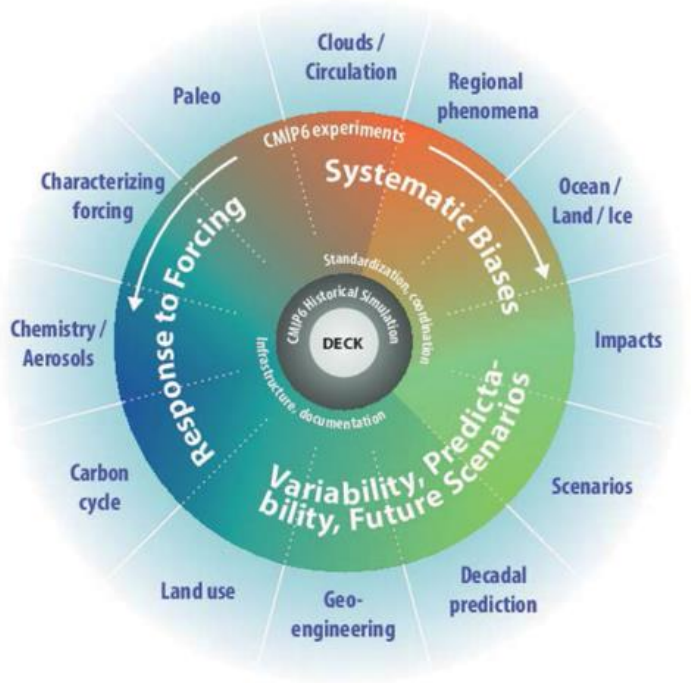

Figure 2.7 Schematic representation of the CMIP6 experiment design (Stouffer et al. 2017)

Table 2.1 List of climate system model for 40CMIP5 GCMs used in this study

Model	Center	Atmosphere model	Ocean model	Land model	Ice model	Reference
1. BCC-CSM1-1	BCC/ China	BCC−AGCM 2.1	MOM4−L40v1	BCC−AVIM1.0	SIS	Wu et al. (2014)
2. BCC-CSM1-1-M	BCC/ China	BCC−AGCM 2.2	MOM4−L40v2	BCC−AVIM1.0	SIS	Wu et al. (2014)
3. BNU-ESM	BNU/ China	CAM4	MOM4p1	CoLM	CICE4.1	Ji et al. (2014)
4. CanESM2	CCCM/ Canada	CanAM4	CanOM4	CTEM	CanSIM1	Lionello and Scarascia (2018)
5. CCSM4	NCAR/ USA	CAM4	POP2	CLM4	CICE4	Hurrell et al. (2013)
6. CESM1-BGC	NCAR/ USA	CAM4	POP2	CLM4	CICE4	Hurrell et al. (2013)
7. CESM1-CAM5	NCAR/ USA	CAM-CHEM	POP2	CLM4	CICE4	Hurrell et al. (2013)
8. CESM1-FASTCHEM	NCAR/ USA	CAM4	POP2	CLM4	CICE4	Hurrell et al. (2013)
9. CESM1-WACCM	NCAR/ USA	WACCM4	POP2	CLM4	CICE4	Hurrell et al. (2013)
10. CMCC-CESM	CMCC/ Italy	CAM–5.2	NEMO3.4	CLM4	CICE4	Fogli and Iovino (2014)
11. CMCC-CM	CMCC/ Italy	ECHAM5	OPA8.2	SILVA/PELAGOS	LIM	Lionello and Scarascia (2018)
12. CMCC-CMS	CMCC/ Italy	ECHAM5	OPA8.2	SILVA/PELAGOS	LIM	Lionello and Scarascia (2018)
13. CNRM-CM5	CNRM-CERFACS / France	ARPEGE-Climat v5.2.1	NEMO v3.2	ISBA	GELATO v5.3	Voldoire et al. (2013)
14. CNRM-CM5-2	CNRM-CERFACS / France	ARPEGE-Climat V5.2.3	NEMO v3.2	ISBA	GELATO v5.4	Voldoire et al. (2013)
15. CSIRO-Mk3-6-0	CSIRO-QCCCE/Australia	MK3.6 At.Co	MK3.6 Oc.Co.	MK3.6	Mk3.6 Part of OGCM	Rotstayn et al. (2010); Lionello and Scarascia (2018)

Table 2.1 List of climate system model for 40CMIP5 GCMs used in this study (Continued)

Model	Center	Atmosphere model	Ocean model	Land model	Ice model	Reference
16. EC-EARTH	EC- EARTH/ Europe	IFS	NEMO v2	TESSEL	LIM2TESSEL	Hazeleger et al. (2011)
17. FGOALS-g2	LASG/ China	GAMIL2	LIOCM2	CLM3	CICE4-LASG	Zhang and Yu (2011); Zhou et al. (2018)
18. FIO-ESM	FIO/ China	CAM3.5	POP2	CLM	CICE	Qiao et al. 2013
19. GFDL-CM3	GFDL/ USA	AM3p9	MOM4p1	LM3p7	SISp2	Griffies et al. (2011)
20. GFDL-ESM2G	GFDL/ USA	AM2p14	TOPAZ1p2	LM3p7	SISp2	Dunne et al. (2012)
21. GFDL-ESM2M	GFDL/ USA	AM2p14	MOM4p1	LM3p7	SISp2	Dunne et al. (2012)
22. GISS-E2-H	NASA/ USA	GISS-E2	HYCOM	GISS	HYCOM	Sanderson et al. (2017)
23. GISS-E2-H-CC	NASA/ USA	GISS-E2	HYCOM	GISS	HYCOM	Sanderson et al. (2017)
24. GISS-E2-R	NASA/ USA	GISS-E2	Russell	GISS	Russel	Sanderson et al. (2017)
25. GISS-E2-R-CC	NASA/ USA	GISS-E2	Russell	GISS	Russell	Sanderson et al. (2017)
26. HadCM3	Hadley Center/ UK	HadAM3	HadOM3	MOSES1	Sea ice component of HadOM3	Collins et al. (2001)
27. HadGEM2-AO	Hadley Center/ UK	HadGAM2	HadGOM2	MOSES2	Sea ice component of HadOM3	Collins et al. (2001)
28. HadGEM2-CC	Hadley Center/ UK	HadGAM2	HadGOM2	JULES + TRIFFID	Inspired from CICE	Martin et al. (2010)
39. HadGEM2-ES	Hadley Center/ UK	HadGAM2	HadGOM2	JULES + TRIFFID	Inspired from CICE	Martin et al. (2010)

Table 2.1 List of climate system model for 40CMIP5 GCMs used in this study (Continued)

Model	Center	Atmosphere model	Ocean model	Land model	Ice model	Reference
30. INMCM4	INM-CM4/Russia	INM-CM4 At.Co	INM-CM4 Oc.Co	Simple model into INMCM4	INM-CM4 Oc.Co	Volodin et al. (2010); Lionello and Scarascia (2018)
31. IPSL-CM5A-LR	IPSL/ France	LMDZ4A v5	NEMO v2.3	ORCHIDEE	LIM2	Dufresne et al. (2013)
32. IPSL-CM5A-MR	IPSL/ France	LMDZ4A v5	NEMO v2.3	ORCHIDEE	LIM2	Dufresne et al. (2013)
33. IPSL-CM5B-LR	IPSL/ France	LMDZ5B	NEMOv3. 2	ORCHIDEE	LIM2	Dufresne et al. (2013)
34. MIROC5	MIROC/ Japan	CCSR/NIES/FR CGC AGCM	COCO v4.5	MATSIRO	COCO v4.5	Sakamoto et al. (2012)
35. MIROC-ESM	MIROC/ Japan	CCSR/NIES/FR CGC AGCM	COCO v3.4	MATSIRO	COCO v3.4	Watanabe et al. (2011)
36. MIROC-ESM-CHEM	MIROC/ Japan	CCSR/NIES/FR CGC AGCM	COCO v3.4	MATSIRO	COCO v3.4	Watanabe et al. (2011)
37. MPI-ESM-LR	MPI/ Germany	ECHAM6	MPI-OM	JSBACH	Sea ice component of MPI-OM	Raddatz et al. (2007)
38. MPI-ESM-MR	MPI/ Germany	ECHAM6	MPI-OM	JSBACH	Sea ice component of MPI-OM	Giorgetta et al. (2013)
39. MRI-CGCM3	MRI/ Japan	GSMUV	MRI.CO M3	HAL	MRI.COM3	Yukimoto et al. (2011)
40. NorESM1-M	NCC/ Norway	CAM4-Oslo	MICOM	CLM4	CICE4	Bentsen et al. (2012)

Table 2.2 List of climate system model for 13CMIP5 GCMs used in this study

Model	Center	Atmosphere model	Ocean model	Land model	Ice model	Reference
1.BCC-CSM2-MR	BCC-CMA/ China	BCC-AGCM3-MR	MOM4-L40v2	BCC-AVIM2	SISv2	Wu et al. (2019)
2. CAMS-CSM1-0	CAMS/China	ECHAM5_CAMS	MOM4	CoLM 1.0	SIS1	Rong et al. (2019)
3. CanESM5	CCCMA/Canada	CanAM5	CanNEMO	CLASS-CTEM	LIM2	Swart et al. (2019)
4. CESM2	NCAR/ USA	CAM6	POP2	CLM5	CICE5	Danabasoglu et al. (2020)
5. CNRM-CM6-1	CNRM-CERFACS / France	ARPEGE-Climat v6.3	NEMO v3.6	SURFEX	GELATO v6	Voldoire et al. (2019)
6. CNRM-CM6-1-HR	CNRM-CERFACS / France	ARPEGE-Climat v6.3	NEMO v3.6	SURFEX	GELATO v6	Voldoire et al. (2019)
7. CNRM-ESM2-1	CNRM-CERFACS / France	ARPEGE-Climat v6.3	NEMO v3.6	SURFEX	GELATO v6	Séférian et al. (2019)
8. FGOALS-f3-L	LASG/ China	FAMIL2.2	LICOM3	CLM4	CICE4	HE et al. (2019)
9. FIO-ESM-2-0	FIO-QLNM/China	CAM5	POP2	CLM4	CICE4	Bao et al. (2020)
10. GFDL-CM4	GFDL/ USA	AM4.0	LM4.0	OM4.0	SIS2	Held et al. (2019)
11. IPSL-CM6A-LR	IPSL/France	LMDZ6	NEMOv3.6	ORCHIDEE	NEMO-LIM	Boucher et al. (2020)
12. MIROC6	MIROC/ Japan	CCSR/NIES/FRCGC AGCM	COCO v4.5	MATSIRO	COCO v4.5	Tatebe et al. (2019)
13.MRI-ESM2-0	MRI / Japan	MRIAGCM3.5	MRI. COMv4	MRIAGCM3.5	MRI. COMv4	Yukimoto et al. (2019)

2.4 Reference data for evaluating GCMs

2.4.1 The Climatic Research Unit gridded Time-series

Climatic Research Unit gridded Time Series (CRU TS) is the monthly dataset of a gridded climate product with high-resolution in space and time. It was developed by the Climatic Research Unit (CRU) at the University of East Anglia. The climate sources were derived from the World Meteorological Organization (WMO). This is supplemented by national-level climate data from National Meteorological Services (NMSs). These global climate data collected from climate stations were interpolated in the spatial pattern 0.5° × 0.5° over the land area. To produce climate data without missing values, CRU TS3.10.01 used the triangulation method to interpolate the values, while CRU TS v4.02 used the angular-distance weighting (ADW) method. (Harris et al. 2014; Harris et al. 2020). The CRU TS dataset is available in NetCDF and ASCII formats and can be downloaded from the Centre for Environmental Data Analysis website.

2.4.2 The University of Delaware Air Temperature and Precipitation (UD)

UD is a global air temperature and precipitation dataset produced by the University of Delaware. Stations records from Global Historical Climatology Network and Legates and Willmott are used as input data to create the UD climate dataset. The datasets cover the period 1901-2010 (v3.01) (Matsuura and Willmott 2012) and 1900-2017 (v5.01) (Willmott and Matsuura 2018). The horizontal resolution of both versions is 0.5° × 0.5° 3 using three interpolation methods, including digital elevation model (DEM), assisted interpolation, traditional interpolation, climatologically aided interpolation (CAI) (Willmott et al. 1985; Willmott and Matsuura 1995; Willmott and Robeson 1995). The UD dataset can be downloaded from the Physical Sciences Laboratory’s website.

2.4.3 The National Centers for Environmental Prediction (NCEP)-National Center for Atmospheric Research (NCAR) 40-Year Reanalysis (called NCEP)

NCEP is a joint product of NCEP and NCAR. It is produced to record retrospective data from 40 years of global atmospheric analyses for climate research and monitoring. The data sources that feed into this reanalysis model are data from land surface, rawinsonde, ship, pibal, aircraft, satellite, and various other data, using a state-of-the-art data assimilation system to assimilate the input data. The NCEP dataset includes data from 1948 to the present (Kalnay et al. 1996). The NCEP dataset is available on a 2.5° × 2.5° grid and can be downloaded from the Physical Sciences Laboratory's website.

2.4.4 The European Centre for Medium-Range Weather Forecasts (ECMWF)

ERA40 is a reanalysis dataset of meteorological observations from the European Centre for Medium-Range Weather Forecasts (ECMWF). Their surface observations are from land stations and ships, and soundings from radiosonde and pilot balloons. The ERA40 products also receive many observations to create the dataset, which consists of aircraft, buoys, satellite wind, satellite radiance, scatterometer, and PAOB. A data assimilation system is used to create these reanalysis datasets. This dataset covers the period from 1957 to 2002 (Uppala et al. 2005). The ERA40 dataset is available on a 2.5° × 2.5° grid and can be downloaded from the European Centre for Medium-Range Weather Forecasts' website.

ERA-Interim is the most recent global atmospheric reanalysis produced by ECMWF. It covers the period from 1979 to the present and is continuously updated in real-time. The ERA-Interim project was to prepare a new global atmospheric reanalysis for the future and to replace the data of the ERA-40 reanalysis. Compared to ERA40, ERA-Interim uses an improvement of some key aspects of ERA40-, such as the representation of the hydrological cycle, the quality of the stratospheric circulation, and the treatment of biases and changes in the observing system (Dee et al. 2011; Balsamo et al. 2012; Gao et al. 2012). The spatial resolution of the latest ECMWF ERA-Interim model has a spectral resolution at T255 with a 0.75° × 0.75° latitude-

longitude grid or about 80 km on 60 vertical levels from the surface to uppermost level at 0.1 hPa, 37 pressure levels and uses a reduced Gaussian grid N128 (Balsamo et al. 2012; Berrisford et al. 2011; Gao et al. 2012). The ERA40 dataset is available on a 2.5° × 2.5° grid and can be downloaded from European Centre for Medium-Range Weather Forecasts' website.

2.4.5 The Modern-Era Retrospective Analysis for Research Applications, Version 2 (MERRA2)

MERRA2 is a reanalysis product generated using the Goddard Earth Observing System (GEOS) data assimilation system (DAS) from NASA's Global Modeling and Assimilation Office (GMAO). MERRA version 2 (MERRA2) is produced using version 5.12.4 of the GEOS DAS (Rienecker et al. 2011). Many types of observational data are used in this product, derived from various data sources, including land surface observations, ground-based remotely sensed, satellite-derived wind, satellite retrieved, radio occultation, satellite radiance (Gelaro et al. 2017). The MERRA2 dataset is available on a 0.5° × 0.625° grid and can be downloaded from National Aeronautics and Space Administration Goddard Space Flight Center's website.

2.5 Previous Studies of evaluation of CMIP GCMs

There are several studies that have used climate variables from GCMs to simulate past, present and future climate trends in different regions of the world.

Gleckler et al. (2008) developed a set of climate model metrics to evaluate CMIP3 GCMs for atmospheric fields during the period 1980–1999 over Northern Hemispheres, the extratropical zones of the South, tropics, and globe. They used statistical metrics to assess the performance of the models and employed the relative error method to rank the models. The usefulness, limitations, and robustness of the metrics are evaluated by examining whether the information provided by each metric correlates in any way with the others. Besides, the evaluation of the metrics (spatial and temporal variability, RMSE, correlation coefficient, bias error) of the

performance of the model considered limitations and robustness in the correlation between each metric and the climate variable, and considered metrics with multiple factors (spatial scale, study area, time series). Their results revealed that the performance of each GCM evaluated is not equal in simulating the climatology of the annual cycle and the variance of monthly anomalies. When a multi-model ensemble is considered, its performance in the climatology of the annual cycle for several variables and regions is better than that of the individual models.

Yan et al. (2013) assessed twenty-five historical CMIP5 simulations of temperature over China. The simulation results of CMIP3 and CMIP5 are compared with the observations of CRUT3v and CN05. The temperature results were evaluated in three expressions, which include the mean, the spatial distribution of the mean, and spatial distribution of the linear trend. They found that the multi-model ensemble of CMIP5 can simulate the spatial pattern of temperature well.

Kumar et al. (2013) analyzed the trends and long-term persistence of temperature and precipitation of nineteen CMIP5 GCMs over continental areas (608S–608N) during 1930–2004 with good agreement between simulation and observational results. This result shows that CCSM4.0 has the highest pattern correlation for temperature trends, while GFDL and MIROC models show the highest pattern correlation for precipitation trends. The relative performance of this study shows that CMIP5 models are not equally good for precipitation and temperature. They concluded that the best simulation of temperature trend does not necessarily provide the best simulation of precipitation trend. Therefore, determining the best model depends on the purpose of the analysis.

Rupp et al. (2013) evaluated the performance of forty-one CMIP5 GCMs in simulating temperature and precipitation over the Pacific Northwest United States (PNW) using performance metrics. Metrics used to evaluate the GCMs consisted of 40-year simulations (mean, diurnal temperature range, seasonal cycle amplitude, seasonal correlation, and seasonal variance) and twentieth-century simulations (variance, trend, and ENSO related-teleconnections). GCM results were compared with average observations. The ranking of the models was calculated based on the total error score of all performance metrics. Based on the design criteria and results, CNRM-CM5 performed best among the selected models.

Su et al. (2013) assessed the performance of 24 GCMs available in CMIP5, which evaluated both monthly surface air temperature and precipitation over eastern Tibetan Plateau, and compared the model outputs with 176 meteorological stations for 1961–2005. When evaluating GCMs by bias metrics, the results indicate that GFDL-ESM2M, MPI-ESM-LR, GFDL-ESM2G, CanESM2, and CanCM4 ranked top in temperature, while IPSL-CM5A-LR, MRI-CGCM3, IPSLCM5A-MR, HadCM3, and CanESM2 led in precipitation. However, they concluded that the result of model performance depends on the climate variable.

Miao et al. (2014) used the criteria of correlation, RMSE, and amplitude of standard deviations to evaluate twenty-four CMIP5 GCM simulations and projections over Northern Eurasia which found that most of the simulations overestimated the annual mean T, especially in the winter season. Although most of the GCMs in this study can capture decadal temperature trends, their accuracy is quite low. When skill scores are taken into account, the results simulated by a multi-model ensemble method perform better than a single model.

Siew et al. (2014) evaluated the performance of ten CMIP5 GCMs of winter monsoon precipitation over Southeast Asia. All the models were evaluated in terms of annual cycle, spatial distribution and interannual variability. They found only 8 GCMs simulating average annual cycle of precipitation well, while all models simulating winter monsoon precipitation had large biases. In addition, CNRM, IPSL and NorESM1 were the top 3 GCMs simulating the present climate. These GCMs were selected to simulate precipitation in future projections under 3 RCP scenarios (RCP2.5, RCP4.5, and RCP8.5). Their projection of RCP 8.5 scenario shows the most significant changes in winter monsoon precipitation.

Ahmadalipour et al. (2017) evaluated the performance of daily records of precipitation and temperature from 20 CMIP5 GCMs datasets over the Columbia River Basin (CRB) in the Pacific Northwest USA from 1970 to 2000. To select the appropriate model, they employed the univariate (mean, standard deviation, coefficient of variation, relative change (variability), Mann-Kendall trend, Kolmogorov-Smirnov test (KS-test), and multivariate (principal component analysis (PCA) or empirical orthogonal function (EOF), singular value decomposition (SVD) or maximum covariance analysis, canonical correlation analysis (CCA), and cluster analysis)

techniques. All metrics were treated equally. A ranking of GCMs based on performance assessed against gridded observational data at daily, monthly and seasonal levels. The ranking of GCMs in this study shows that their results can provide insight into climate variables.

Xu et al. (2017) evaluated the ability of 14 CMIP5 GCMs in simulating air T, specific humidity, geopotential height, and wind over Tibetan Plateau using criteria such as spatial correlation efficiency, spatial mean error, and standard deviation. Their ranking shows that CCSM4 and CNRM-CM5 perform better than the other models.

Xuan et al. (2017) evaluated the maximum and minimum air T, precipitation, wind speed, solar radiation, and relative humidity from 1971 to 2000 over Zhejiang Province in China using eighteen CMIP5 GCMs ranked by correlation coefficient, root mean square error, and percent bias of model estimation. Six variables of all GCMs exhibited different spatial patterns, while five variables (except wind speed) had similar representation of seasonal variations in most simulations.

Bannister et al. (2017) evaluated the change in recent and future temperature over the Sichuan Basin in China using forty-seven CMIP5 GCMs and found that most GCMs could not adequately represent temperature trends, especially for seasonal cases.

Agyekum et al. (2018) evaluated eighteen CMIP5 GCMs in simulating different time scales of precipitation over Volta Basin and concluded that the ensemble mean of all selected models performed better than individual models in simulating at annual, seasonal and monthly time scales.

Huang et al. (2019) analyzed the vector winds for the performance assessment of thirty-seven CMIP5 GCMs and multi-model ensembles in the monsoon region Asian-Australian using mean, annual cycle and interannual variability criteria and found that the best performance belonged to the multi-model ensembles.

However, the CMIP 6 GCMs are the last release of the project. As a result, there are few CMIP6 evaluation. Xin et al. (2020) simulated the summer precipitation of eight CMIP6 GCMs over China and the summer of East Asian during 1961–2005; they also compared the simulations of all CMIP6 GCMs with those of eight previous CMIP5 GCMs. The climatology of their study was assessed based on

interannual variation and linear trends. It was found that most of the CMIP6 GCMs were better at simulating the interannual precipitation pattern over Eastern China than the earlier CMIP5 GCMs. Also, their study found that the multi-model ensemble of CMIP6 is better than the multi-model ensemble of CMIP5 in terms of performance. Almazroui et al. (2020) analyzed the projected changes in temperature and precipitation over Africa from twenty-seven CMIP6 GCMs for the period 2030–2059 as well as for the period 2070–2099, comparing the two future periods with the historical climate (1981–2010). Under SSP5-8.5, they showed that the mean annual temperature at the end of 2100 will increase by 5.6 °C over the Sahara region and by 3.5 °C over Central East Africa.

Watanabe et al. (2014) studied monsoon precipitation in Thailand, a tropical country, using nine CMIP5 models over Thailand and compared the projections of all GCMs with three reference datasets (CMAP, GPCP and APHRODITE). They found that the September monthly river discharge projection of the ensemble was 60% to 90% higher than that of the retrospective simulation. Supharatid (2015) analyzed the performance of CMIP3 and CMIP5 GCMs for simulating precipitation over Chao Phraya River Basin, Thailand, and found that the mean precipitation of GCMs CMIP5 is more similar to the observed data than that of GCMs CMIP3.

Since the GCMs involved in the CMIPs project are generated by different climate institutes around the world (Taylor et al. 2012), there are different physical parameterizations and strategies of each GCM (Hourdin et al. 2006). Moreover, the topography and climate characterization of each region varies (White et al. 2009). The internal determinations of GCMs are the keys to the different performances of GCMs for different regions, because it is difficult to input the topography and climate datasets that cover the entire globe. For this reason, researchers have evaluated the performance of GCMs in different regions of the world (Kumar et al. 2013; Rupp et al. 2013; Su et al. 2013; Miao et al. 2014; Moise et al. 2015; Lovino et al. 2018; Raghavan et al. 2018).

CHAPTER 3
MATERIALS AND METHODS

3.1 Research framework

The research framework for this study is shown in Figure 3.1. The results of GCMs CMIP and CMIP6 and the reference datasets evaluated in this study were linearly interpolated on the same grid with a resolution of $0.15°$. When it comes to climate analysis, the study area is a major consideration since the larger the region, the more time and resources are required for computation and processing. As Southeast Asia is the main study area in this work, the CMIP5 GCMs have been published since 2013, which provides sufficient time for the analysis of the precipitation and temperature data. In the first part of the study, the historical temperature and precipitation data from 40 CMIP5 GCMs over Southeast Asia 1901- 1999 and 1960 - 1999 were analyzed using 9 statistical metrics. The GCMs evaluated for a long-term period are computed over land only, while that for the short-term is computed separately for land, ocean, and both land and ocean.

However, during the evaluating of the CMIP5 GCMs, the CMIP6 GCMs, a new version, was released. Although the CMIP6 GCMs were released in 2017 (Stouffer et al. 2017), few modeling organizations participated (Rivera and Arnould, 2020). By 2020, there were a sufficient number of models that could be studied. Because of the limited time to analyze these recently published CMIP6 GCMs, Thailand was selected as the preliminary study region for assessing CMIP6 GCMs. For these reasons, the temperature and area of Thailand were chosen as preliminary variables and study areas for assessing and updating the performance of the CMIP6 GCMs. In the second part, the history of 13 CMIP6 GCMs over Thailand for the near-to-current term (2000 – 2014) of the early 21st century is evaluated using 5 statistical metrics. They are computed separately for land, ocean, and both land and ocean.

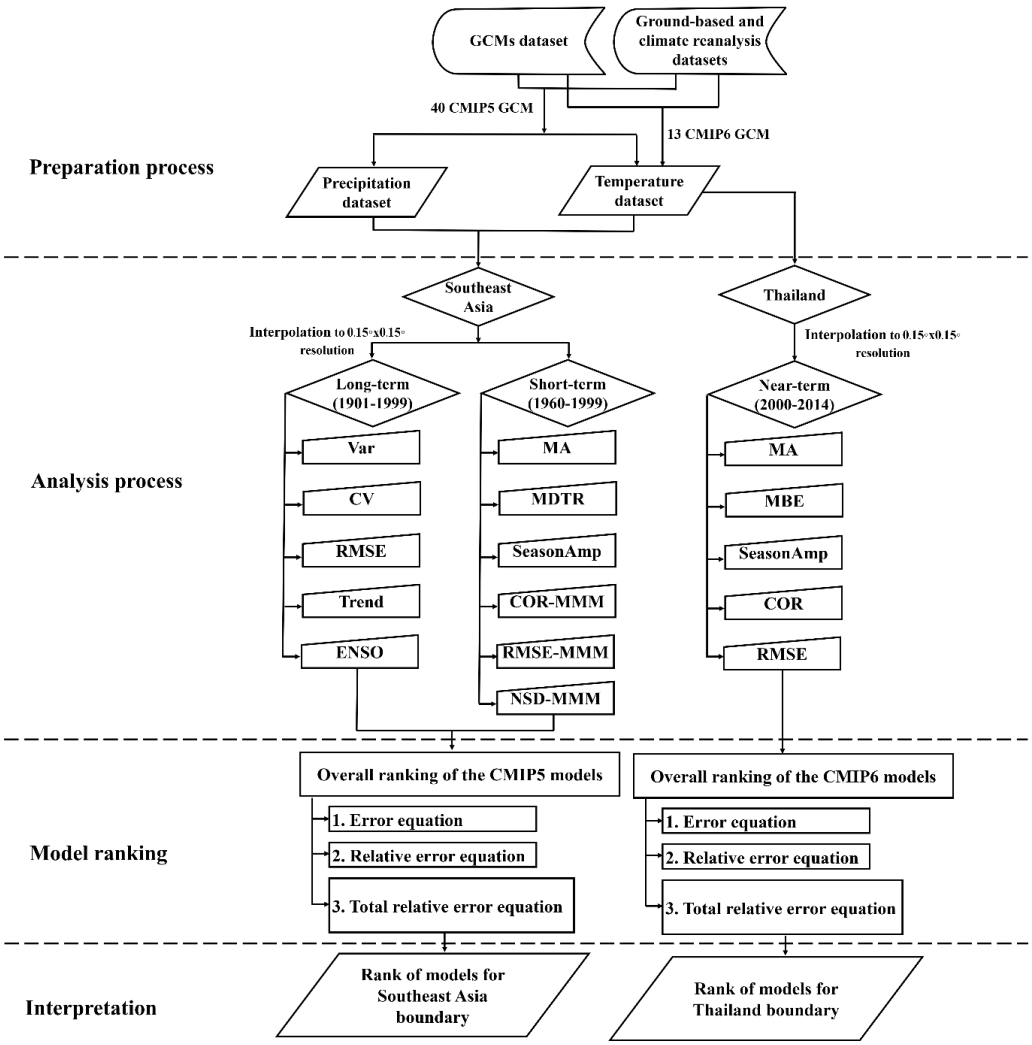

Figure 3.1 Research framework of this study

3.2 Study Area

The study areas of this study are Southeast Asia and Thailand. Southeast Asia is a group of countries located between Indian Ocean and Pacific Ocean. It has a total area of about 4.5 million km^2, which is almost 3% of the global land area (GIIN 2018). It can be divided into mainland and marine. The mainland covers 9 % of Southeast Asia, which consists of West Malaysia, Myanmar, Thailand, Laos, Cambodia, and Vietnam, while the marine areas account for 14 % of this region, which consists of Singapore, Brunei, Indonesia, East Timor, East Malaysia, Papua New Guinea and the Philippines. Most of the mainland is covered by extensive plains, hills

and high mountains, while the islands in the maritime area are covered by lowland plains and high mountains (Frenken 2012). Figure 3.2 shows the topography (m) of the first study area. It is located between latitude 12 .75°S and 24 .25°N and longitude 88 .25°E and 144 .75°E. The average annual precipitation in Southeast Asia between 1961 and 1990 is about 2,455 millimeters (UNISDR 2010), most of which is influenced by the southwest and northeast monsoons (Endo et al. 2009). Since most of this region is in the tropical climate zone, the average temperature is above 25 °C throughout the year (Yuen and Kong 2009).

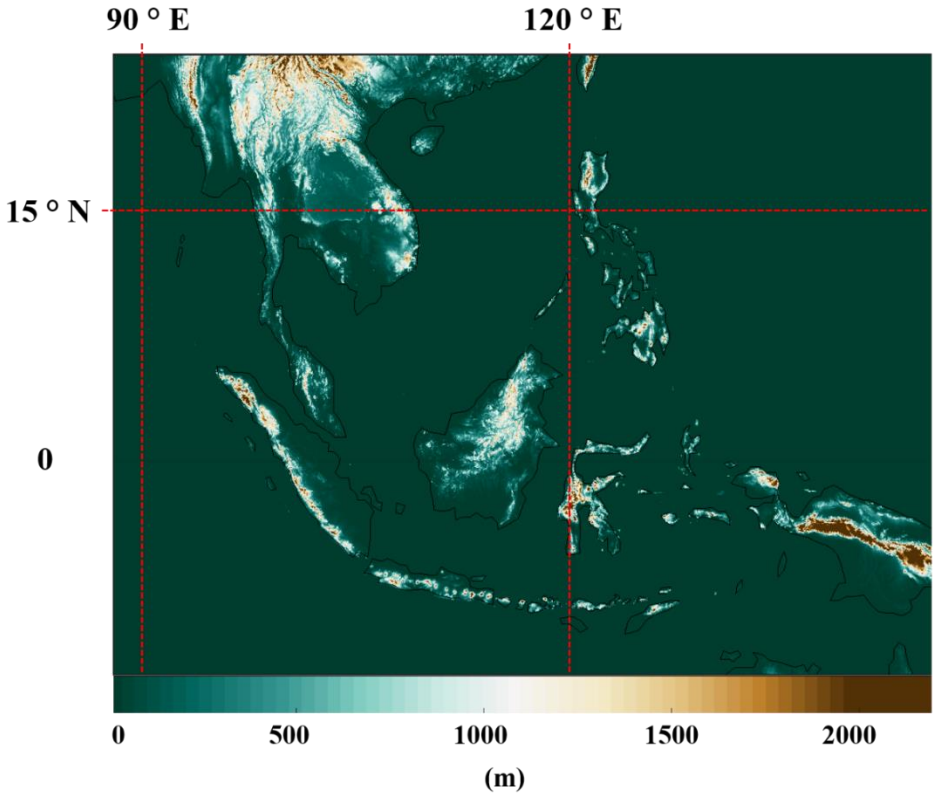

Figure 3.2 Topography in meters above mean sea level in the area Southeast Asia for evaluating the performances of 40 different CMIP5 GCMs

The second study area – Thailand – is located between latitude 5° S -21 ° N and longitude 96° E-107 °E (Figure 3.3). Thailand consists of land and marine areas. The topography of Thailand mainly consists of high mountains, a central plain, and a plateau. The land area is located in the middle of Southeast Asia, while the marine area is located between the Pacific and Indian Oceans (Tantrakarnapa 2018). The

annual mean temperature in Thailand between 1981 and 2007 reported by Thai Meteorological Department was 27.9 °C.

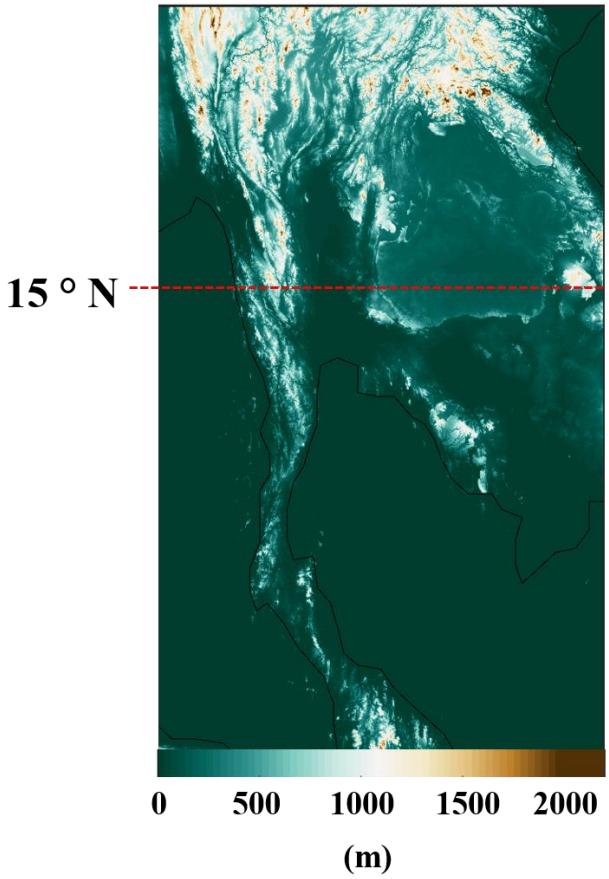

Figure 3.3 Topography in meters above mean sea level over Thailand for evaluating the performance of 13 different CMIP6 GCMs

3.3 CMIP5 and CMIP6 GCMs

In this study, GCMs of CMIP5 and CMIP6 were evaluated. A historical experiment of 40 CMIP5 and 13 CMIP6 GCMs was used to simulate the past climate characteristics. The historical experiment of the CMIP5 project covers the period from 1850 to 2005, while that of the CMIP6 covers the period from 1850 to 2014. The datasets of CMIP5 and CMIP6 are free and available online from the WCRP Coupled Model Intercomparison Project hosted on the Earth System Grid Federation (ESGF, 2017).

To find the best GCM from Southeast Asia, the results of CMIP5 are employed to simulate temperature and precipitation for the short-term (1960-1999) and long-term (1901-1999) periods. The results of CMIP6 were used to simulate only temperature for the recent period from 2000 - 2014 (near-to-current term) to find the best GCMs for Thailand. In this study, the monthly dataset was used to examine the capability of the model simulations, which are compared with reference datasets. Detailed information of each GCM in CMIP5 and CMIP6 are shown in Table 3.1 and Table 3.2, respectively.

Table 3.1 Details of the 40 CMIP5 GCMs used to evaluate model performance in Southeast Asia.

Model	Center	Resolution lon x lat	Number of Ensemble Members
1. BCC-CSM1-1	BCC/ China	2.8 × 2.8	3
2. BCC-CSM1-1-M	BCC/ China	1.12 x 1.12	3
3. BNU-ESM	BNU/ China	2.8 × 2.8	1
4. CanESM2	CCCM/ Canada	2.8 × 2.8	5
5. CCSM4	NCAR/ USA	1.25 × 0.94	6
6. CESM1-BGC	NCAR/ USA	1.25 × 0.94	1
7. CESM1-CAM5	NCAR/ USA	1.25 × 0.94	3
8. CESM1-FASTCHEM	NCAR/ USA	1.25 × 0.94	3
9. CESM1-WACCM	NCAR/ USA	2.5 × 1.89	4
10. CMCC-CESM	CMCC/ Italy	3.75 × 7.71	1
11. CMCC-CM	CMCC/ Italy	0.75 × 0.75	1
12. CMCC-CMS	CMCC/ Italy	1.88 × 1.87	1
13. CNRM-CM5	CNRM-CERFACS / France	1.4 × 1.4	10
14. CNRM-CM5-2	CNRM-CERFACS / France	1.4 × 1.4	4
15. CSIRO-Mk3-6-0	CSIRO-QCCCE /Australia	1.8 × 1.8	10
16. EC-EARTH	EC-EARTH/ Europe	1.13 × 1.12	14
17. FGOALS-g2	LASG/ China	2.8 × 2.8	5
18. FIO-ESM	FIO/ China	2.81 × 2.79	3
19. GFDL-CM3	GFDL/ USA	2.5 × 2.0	5
20. GFDL-ESM2G	GFDL/ USA	2.5 × 2.0	1
21. GFDL-ESM2M	GFDL/ USA	2.5 × 2.0	1
22. GISS-E2-H	NASA/ USA	2.5 × 2.0	6
23. GISS-E2-H-CC	NASA/ USA	2.5 × 2.0	1
24. GISS-E2-R	NASA/ USA	2.5 × 2.0	6

Table 3.1 Details of the 40 CMIP5 GCMs used to evaluate model performance in Southeast Asia (continued)

Model	Center	Resolution lon x lat	Number of Ensemble Members
25. GISS-E2-R-CC	NASA/ USA	2.5 × 2.0	1
26. HadCM3	Hadley Center/ UK	3.75 × 2.5	10
27. HadGEM2-AO	Hadley Center/ UK	1.88 × 1.25	1
28. HadGEM2-CC	Hadley Center/ UK	1.88 × 1.25	3
39. HadGEM2-ES	Hadley Center/ UK	1.88 × 1.25	4
30. INMCM4	INM-CM4/Russia	2.0 × 1.5	1
31. IPSL-CM5A-LR	IPSL/ France	3.75 × 1.8	6
32. IPSL-CM5A-MR	IPSL/ France	2.5 × 1.25	3
33. IPSL-CM5B-LR	IPSL/ France	3.75 × 1.8	1
34. MIROC5	CCSR/ Japan	1.4 × 1.4	1
35. MIROC-ESM	CCSR/ Japan	2.8 × 2.8	3
36. MIROC-ESM-CHEM	CCSR/ Japan	2.8 × 2.8	3
37. MPI-ESM-LR	MPI/ Germany	1.88 × 1.87	3
38. MPI-ESM-MR	MPI/ Germany	1.88 × 1.87	3
39. MRI-CGCM3	MRI/ Japan	1.1 × 1.1	5
40. NorESM1-M	NCC/ Norway	2.5 × 1.9	3

Table 3.2 Details of the 13 CMIP6 GCMs used to evaluate model performance in Thailand

Model	Center	Resolution lon x lat	Number of Ensemble Members
1. BCC-CSM2-MR	BCC-CMA/ China	1.12° × 1.12°	1
2. CAMS-CSM1-0	CAMS/China	1.12◦ × 1.12◦	3
3. CanESM5	CCCMA/Canada	2.8° × 2.8°	10
4. CESM2	NCAR/ USA	1.25°× 0.9°	3
5. CNRM-CM6-1	CNRM-CERFACS / France	1.4° × 1.4°	10
6. CNRM-CM6-1-HR	CNRM-CERFACS / France	0.5° × 0.5°	1
7. CNRM-ESM2-1	CNRM-CERFACS / France	1.4° × 1.4°	1
8. FGOALS-f3-L	LASG/ China	1.25° × 1°	3
9. FIO-ESM-2-0	FIO-QLNM/China	1.25°× 0.9°	3
10. GFDL-CM4	GFDL/ USA	1° × 1.3°	3
11. IPSL-CM6A-LR	IPSL/France	2.5°× 1.3°	20

Table 3.2 Details of the 13 CMIP6 GCMs used to evaluate model performance in Thailand (continued)

Model	Center	Resolution lon x lat	Number of Ensemble Members
12. MIROC6	MIROC/ Japan	1.4° ×1.4°	5
13.MRI-ESM2-0	MRI / Japan	1.12°× 1.12°	5

3.4 Reference datasets

Reference datasets are employed to compare the GCMs' performance. They are summarized in Table 3.3. The datasets in this study can be divided into 2 categories.

3.4.1 The ground-based products

The ground-based products are widely used as measuring instruments. They are meteorological instruments that have high accuracy because they can directly detect at the station and have a high temporal frequency of measurements (Gilewski and Nawalany 2019).

The ground-based dataset used to evaluate CMIP5 GCMs in Southeast Asia includes CRU TS3.10.01, with available data from 1901-2009 at a horizontal resolution of 0.5° × 0.5° (Harris et al. 2014), and UD v3.01, with available data from 1901-2010 at a horizontal resolution of 0.5° × 0.5° (Matsuura and Willmot 2012).

In addition to the CRU and UD dataset used to evaluate CMIP6 GCMs in Thailand, other versions of datasets are employed. Since the version of the two ground-based datasets does not cover the years 2000-2014, the evaluation of CMIP6 GCMs in Thailand is based on CRU TS v4.02, with the available data from 1901 to 2017 and a horizontal resolution of 0.5° × 0.5° (Harris et al. 2020) and UD v5.01, with the available data from 1900-2017 and a horizontal resolution of 0.5° × 0.5° (Willmott and Matsuura 2018). All ground-based datasets used in this study are monthly datasets and only available over global land areas. All ground-based datasets used in this study are monthly datasets and only available over global land areas.

3.4.2 The reanalysis products

The climate reanalysis product is a dataset that combines observations and satellites through the model to create climate variables with high resolution and long-term data record to simulate the best climate estimation for all locations in the world. Furthermore, climate reanalysis products can estimate historical climate over several decades or more (Decker et al. 2012; Wagan et al. 2017).

To evaluate CMIP5 GCMs in Southeast Asia, two reanalysis datasets (ERA40 with data from mid-1957 to mid-2002 and a horizontal resolution of ~2.5° × 2.5° (Uppala et al. 2005) and NCEP with data from 1948 to 2012 and a horizontal resolution of 2.5° ×2.5°) were used (Kalnay et al. 1996).

Two reanalysis datasets used to evaluate CMIP6 GCMs in Thailand are ERA-Interim (Dee et al. 2011), with data from 1979 to present and a horizontal resolution of 0.75° × 0.75° (Dee et al. 2011) and MERRA2, with data from 1979 to present and a horizontal resolution of 0.625°× 0.5° (Rienecker et al. 2011; Bosilovich and Coauthors 2015).

Table 3.3 Reference datasets used in this study

Area	Data	Resolution lon x lat	Source	Reference
Southeast Asia	CRU TS3.10.01	0.5° × 0.5°	Ground-based	Harris et al. 2014
	UD v.3.01	0.5° × 0.5°	Ground-based	Matsuura and Willmot 2012
	ERA40	~2.5° × 2.5°	Reanalysis	Uppala et al. 2005
	NCEP	2.5° ×2.5°	Reanalysis	Kalnay et al. 1996
Thailand	CRU TS v4.02	0.5° × 0.5°	Ground-based	Harris et al. 2020
	UD v5.01	0.5° × 0.5°	Ground-based	Willmott and Matsuura 2018
	ERA-interim	0.75° × 0.75°	Reanalysis	Dee et al. 2011
	MERRA2	0.625°× 0.5°	Reanalysis	Rienecker et al. 2011

3.5 Performance Metrics

The evaluation of CMIP5 and CMIP6 GCMs is divided into three study cases: land only, sea only, and both land and sea. The reason is that the characteristics of endothermy and an exothermy of land and sea are different and the consideration of the case of separate areas is interesting. This is because the temperature of the land area is higher than that of the sea area during the day and decreases rapidly at night; therefore, the air temperature over the land area changes more rapidly than over the sea area (Trenberth et al. 2007). Ocean currents also affect the temperature and P value (Reid et al. 2009), which show apparent differences in seasonal temperature (Crespo et al. 2019). Therefore, the climate variable from land-atmosphere and ocean-atmosphere interaction is an interesting variable for this research. Each study case uses different reference datasets because climate data from CRU and UDEL are only available over land. Hence, the datasets in the ocean case are from reanalysis datasets. The reference datasets from each study are averaged before being used for comparison with the GCMs.

Despite the fact that GCMs can provide important climate data, there are always uncertainties. Hence, statistical metrics have been employed to validate the correctness of the results of climate simulations from different perspectives. Statistical metrics are usually used to assess the difference between the model simulation and the reference dataset, as each metric can show the relative overall performance of the different model simulations (Gleckler et al. 2008). Therefore, the statistical metrics are often used to compare climate simulation results between GCMs and reference datasets (Rupp et al. 2013; Miao et al. 2014; McMahon et al. 2015; Xu et al. 2017; Raghavan et al. 2018; Li et al. 2019; Kamworapan and Surussawadee 2019).

3.5.1 CMIP5 in Southeast Asia

The first step in evaluating a model is to consider which statistical metric can reveal the uncertainty by comparing observed and simulated data. The performance metrics used in this study were selected from previous studies and are based on statistical reliability and the ability to analyze grid cell data from GCMs. The

results of each performance metric are averaged over 92,496 grid cells. The details of the statistical formulas used in this study are listed in Table 3.4, including

(1) Mean bias error (MBE) is a measure of bias that indicates positive and negative differences between the GCM data and the reference data. In other words, the GCM simulation overestimates or underestimates the mean reference data. When MBE = 0, it is assumed that there is no bias (Lovino et al. 2018).

(2) Mean diurnal temperature range (MDTR) is a measure of the difference between the daily maximum and minimum temperatures.

(3) Mean seasonal cycle amplitude (SeasonAmp) is a metric indicating the difference between the warmest and coldest month.

(4) Correlation coefficient (r) is used to check the degree of relationship or to assess the similarity between the spatial patterns of GCM data and reference data. Moriasi et al. (2007) suggested that for model performance evaluation, $r \leq 0.60$ = not satisfactory, $0.60 < r < 0.70$ = satisfactory, $0.70 \leq r \leq 0.75$ = good, and $r > 0.75$ = very good.

(5) Root mean squared error (RMSE) is the measure of the error value of the difference between the GCM data and the reference data (magnitude). Low RMSE values indicate that the GCMs can simulate the reference data well, and a RMSE value = 0 means that the GCMs can be used 100% for simulation because the simulation result has no error value. Thus, the RMSE is a statistical metric for calculating the magnitude of the error between the GCM data and the reference data (Lovino et al. 2018).

(6) Standard deviation (SD) is employed to measure the dispersion of individual data from their mean, which is the most detailed and reliable metric in terms of distribution measurements. Then, the normalization is calculated for the comparison of the SD between the model and the reference data (NSD). If it approaches 1, the meaning is that the data distribution of the GCM is very similar to the reference data.

(7) Variance (Var) is employed to measure the average of the dispersion characteristics from the mean, which is the commonly used measurement (Mishra et al. 2019).

(8) Coefficient of variation (CV) is a metric that indicates the ability of the GCM to measure how effective its simulation is, and is usually calculated in terms

of percentages (Mishra et al. 2019). The advantage of CV is that it measures dispersion without considering unity, which is a limitation of SD and Var.

(9) Linear trend (Trend) is employed to illustrate the trend of estimation of data with best-fit linearity to find a relationship between data and time series.

(10) The correlation of winter temperature and precipitation with Niño3.4 index (ENSO) is employed to verify the degree of relationship and assess the coupled atmosphere-ocean mode of variability on inter-annual timescales between GCM data and Niño3.4 index. The assessment of model performance for the Moriasi et al. (2007) ratings suggests that $r \leq 0.60$ = unsatisfactory, $0.60 < r < 0.70$ = satisfactory, $0.70 \leq r \leq 0.75$ = good, and $r > 0.75$ = very good.

The performance metrics are divided into two groups. It consists of a group of long-term and short-term performance metrics. The first group of performance metrics that are sensitive to record lengths (Rupp et al. 2013) includes Var, CV, Trend, and ENSO (Rupp et al. 2013). These metrics consider grid-based statistics that compute statistics between models and observations for each grid and then compute the spatial mean of these statistical values. Because observation datasets have been available since the start of the twentieth century, metrics in this group, such as Var, CV, RMSE, Trend, and ENSO, have been used to analyze climate variables throughout the twentieth century (Harris et al. 2014; Matsuura and Willmot 2012). Because observation data are available since the early twentieth century, metrics in this group were used to analyze climate variables throughout the twentieth century to quantify interannual variability and trend similarities between GCMs and observational data for long-term climate change (long-term period). The metrics in the second group were used to look at spatially averaged time series (Chhin and Yoden, 2018), such as MA, MBE, MDTR, SeasonAmp, r, NSD, RMSE. These metrics aimed to verify the ability of a GCM to replicate the mean annual climatology (short-term period). The reanalysis datasets were combined with the ground-based dataset to assess the climate across the study area (land and sea). However, the reanalysis datasets were accessible from the mid-twentieth century (Uppala et al. 2005; Kalnay et al. 1996). The metrics from in the second group were used to evaluate climate for a short-term period.

Table 3.4 Statistical formula of the performance metrics used to evaluate CMIP5 in Southeast Asia

Performance metrics	Equation	References
MA	$\frac{\sum_{y=1}^{N} T_y}{N}$	Ruan et al. 2019
MBE	$MA_m - MA_r$	Su et al. 2013
MDTR	$TAS_{max}-TAS_{main}$	Rupp et al. 2013
SeasonAmp	$M_{max} - M_{min}$	Rupp et al. 2013
r	$\frac{\sum_i \sum_j (MA_{m_{ij}} - \overline{MA_m})(MA_{r_{ij}} - \overline{MA_r})}{\sqrt{(\sum_i \sum_j (MA_{m_{ij}} - \overline{MA_m})^2)(\sum_i \sum_j (MA_{r_{ij}} - MA_$	Russ 1994
RMSE	$\sqrt{\frac{\sum_{p=1}^{n}(MA_{m_p} - MA_{r_p})^2}{n}}$	Hebeler 2020
NSD	$SD_m = \sqrt{\frac{\sum_{p=1}^{n} \lvert MA_{m_p} - \overline{MA} \rvert^2}{n}}$ $SD_r = \sqrt{\frac{\sum_{p=1}^{n} \lvert MA_{r_p} - \overline{MA} \rvert^2}{n}}$ $NSD = \frac{SDm}{SDr}$	Russ 1994
Var	$\frac{\sum_{p=1}^{n} \lvert MA_p - \overline{MA} \rvert^2}{n}$	Mishra et al.2019
CV	$\frac{SD}{MA}$	Mishra et al. 2019
Trend	$Y = ax + b$ when $b = \frac{\sum MA_y \sum T_y^2 - \sum T_y \sum T_y MA_y}{N * \sum T_y^2 - (\sum T_y)^2}$; $a = \frac{N * \sum T_y MA_y - \sum T_y \sum MA_y}{N * \sum T_y^2 - (\sum T_y)^2}$	Rahman et al. 2016

Note. if X_y is the annual X for year y. N is the total number of years. MA_m is mean annual of the model. MA_r is the mean annual of the reference data. Tas_{min} is the mean annual of the daily minimum temperature. Tas_{max} is the mean annual of daily maximum temperature. M_{max} is the mean of the warmest month of the model. M_{min} is the mean of the coldest month of the model. $MA_{m_{ij}}$ is the mean annual of the model in row i and column j. $MA_{r_{ij}}$ is the mean annual of the reference data in row i and column j. MA_{m_p} is the mean annual of the model for a pixel p. MA_{r_p} is the mean annual of the reference data for a pixel p. $\overline{MA_m}$ is the average mean annual of the model. $\overline{MA_r}$ is the average mean annual of the reference data. n is the total number of pixels. T_y is the time series studied in year y. MA_y is the annual mean for year y.

Table 3.5 shows the list of each performance metric and the reference datasets used in this study.

Table 3.5 List of performance metrics

Metric	Description	Reference datasets
MBE-T-Land	Mean annual temperature	CRU, UD, ERA40, NCEP
MBE-T-Sea		ERA40, NCEP
MBE-T-Land & Sea		CRU, UD, ERA40, NCEP
MBE-P-Land	Mean annual precipitation	CRU, UD, NCEP
MBE-P-Sea		NCEP
MBE-P-Land & Sea		CRU, UD, NCEP
MDTR-MMM-Land	Mean diurnal temperature range	CRU, NCEP
MDTR-MMM-Sea		NCEP
MDTR- MMM-Land & Sea		CRU, NCEP

Table 3.5 List of performance metrics (Continued)

Metric	Description	Reference datasets
SeasonAmp-T-Land	Mean seasonal cycle amplitude of temperature that indicates the difference between the warmest and coldest month.	CRU, UD, ERA40, NCEP
SeasonAmp-T-Sea		ERA40, NCEP
SeasonAmp-T-Land & Sea		CRU, UD, ERA40, NCEP
SeasonAmp-P-Land	Mean seasonal cycle amplitude of precipitation that indicates the difference between wettest and driest month	CRU, UD, NCEP
SeasonAmp-P-Sea		NCEP
SeasonAmp-P-Land & Sea		CRU, UD, NCEP
r -MMM-T-Land	Correlation coefficient between simulated and observed mean seasonal temperature	CRU, UD, ERA40, NCEP
r -MMM-Sea		ERA40, NCEP
r-MMM-T-Land & Sea		CRU, UD, ERA40, NCEP
r-MMM-P-Land	Correlation coefficient between simulated and observed mean seasonal precipitation	CRU, UD, NCEP
r-MMM-P-Sea		NCEP
r -MMM-P-Land & Sea		CRU, UD, NCEP
RMSE-T-Land	Root mean squared error of mean annual temperature	CRU, UD, ERA40, NCEP
RMSE-T-Sea		ERA40, NCEP
RMSE-T-Land & Sea		CRU, UD, ERA40, NCEP
RMSE-P-Land	Root mean squared error of mean annual precipitation	CRU, UD, NCEP
RMSE-P-Sea		NCEP
RMSE-P-Land & Sea		CRU, UD, NCEP40

Table 3.5 List of performance metrics (Continued)

Metric	Description	Reference datasets
NSD-MMM-T-Land	Standard deviation between simulated and	CRU, UD, ERA40, NCEP
NSD- MMM-T-Sea	observed mean seasonal temperature	ERA40, NCEP
NSD- MMM-T-Land&Sea		CRU, UD, ERA40, NCEP
NSD- MMM-T-Land	Standard deviation between simulated and observed mean seasonal precipitation	CRU, UD, NCEP
NSD- MMM-T-Sea		NCEP
NSD- MMM-T- Land & Sea		CRU, UD, NCEP
Var-Land	Variance of annual temperature	CRU, UD
CV-Land	Coefficient of variation of annual precipitation	CRU, UD
RMSE-T-Land	Root mean squared error of temperature	CRU, UD
RMSE-P-Land	Root mean squared error of precipitation	CRU, UD
Trend-T-Land	Linear trend of annual temperature over land	CRU, UD
Trend-P-Land	Linear trend of annual precipitation over land	CRU, UD
ENSO-T-Land	Correlation of winter temperature with Niño3.4 index	CRU, UD
ENSO-P-Land	Correlation of winter precipitation with Niño3.4 index	CRU, UD

*MMM is the designation of seasn: FMA (February, March, April), MJJASO (May, June, July, August, September, October), and NDJ (November, December, January)

3.5.2 CMIP6 in Thailand

The results of each performance metric are averaged over 7,738 grid cells using performance criteria similar to those used in Southeast Asia, including MBE, SeasonAmp, r, and RMSE. In addition, Mean Annual (MA) was added, which MA in this study refers to the sum of each mean annual temperature, then divided by the total number of years. Table 3.6 shows the list of each performance metric and the reference datasets used in this study.

Table 3.6 List of performance metrics

Metric	Description	Reference datasets
MA-Land	Mean annual temperature	CRU, UDEL, MERRA, ERA
MA-Sea		MERRA, ERA
MA-Land & Sea		CRU, UDEL, MERRA, ERA
MBE-Land	Mean bias errors of mean annual temperature	CRU, UDEL, MERRA, ERA
MBE-Sea		MERRA, ERA
MBE-Land & Sea		CRU, UDEL, MERRA, ERA
SeasonAmp-Land	Mean seasonal cycle amplitude of temperature	CRU, UDEL, MERRA, ERA
SeasonAmp-Sea		MERRA, ERA
SeasonAmp-Land & Sea		CRU, UDEL, MERRA, ERA
r -Land	Correlation coefficient between simulated and observed mean annual temperature	CRU, UDEL, MERRA, ERA
r -Sea		MERRA, ERA
r -Land & Sea		CRU, UDEL, MERRA, ERA
RMSE-Land	Root mean squared error of mean annual temperature	CRU, UDEL, MERRA, ERA
RMSE-Sea		MERRA, ERA
RMSE-Land & Sea		CRU, UDEL, MERRA, ERA

3.6 Model ranking by overall performance

All GCMs are ranked based on performance metrics that identify the strengths and weaknesses of each model. Because of the different objects and results of each metric, the relative error is used to rank the overall model in this study. The model ranking that considers several metrics and climate variables is the most widely used method (Gleckler et al. 2008; Waugh and Eyring 2008; Radić et al. 2011; Rupp et al. 2013; Xu et al. 2017; Kamworapan and Surussawadee 2019).

The first method to determine the error for each GCM *m* and each performance metric *y* ($E_{m,y}$) defined in formula 1, when $W_{r,y}$ and $W_{m,y}$ is the reference and GCMs for metric *y*, respectively. Next, the relative error of for each GCM *m* and each performance metric *y* ($R_{m,y}$) is calculated using formula 2. Last, formula 3 was used to calculate the sum of the relative error of GCM *m* ($E_{m,\mathrm{total}}$) by all performance metrics when N is the total number of performance metrics.

$$E_{m,y} = | W_{r,y} - W_{m,y} | \quad (1)$$

$$R_{m,y} = \frac{E_{m,y} - \min(E_{m,y})}{\max(E_{m,y}) - \min(E_{m,y})} \quad (2)$$

$$E_{m,total} = \sum_{y=1}^{N} R_{m,y} \quad (3)$$

The GCM has a lower relative error value, making it the best model. All performance metrics are equally weighted, which has been used to evaluate the GCMs in several previous studies (Gleckler et al. 2008; Rupp et al. 2013; Kamworapan and Surussawadee 2019), as well as the model ranking by overall performance metrics (Gleckler et al. 2008; Rupp et al. 2013; Kamworapan and Surussawadee 2019). The robustness or confidence for ranking the performance matrices in this study is categorized as “highest” and “higher” as recommended by Rupp et al. (2013).

CHAPTER 4
RESULTS AND DISCUSSION

The first part focuses on identifying the best CMIP5 GCMs for simulating temperature and precipitation over Southeast Asia. The second part focuses on identifying the best CMIP6 GCMs for simulating temperature over Thailand. In addition, the CMIP6 GCMs that perform best and worst in the study of the second part are compared with the results of the previous CMIP GCMs in the previous studies.

4.1 Evaluation of CMIP5 GCMs in Southeast Asia

4.1.1 Ranking of CMIP5 GCMs by all performance metrics

Figure 4.1 illustrates the aggregate errors of the GCMs calculated by performance metrics. This figure shows the ranking of the 40 GCMs in order from best to worst GCMs from left to right. The aggregate errors of the 40 GCMs range from 12.37 to 40.25. CNRM-CM5-2, CNRM-CM5, BNU-ESM, CESM1-BGC, CESM-CAM5, and CCSM4 are the best-performing groups across Southeast Asia. CNRM-CM5-2 is the best model with the least errors. The GCMs that perform the worst are the GISS models from NASA center, especially GISS-E2-R, whose error is 40.25.

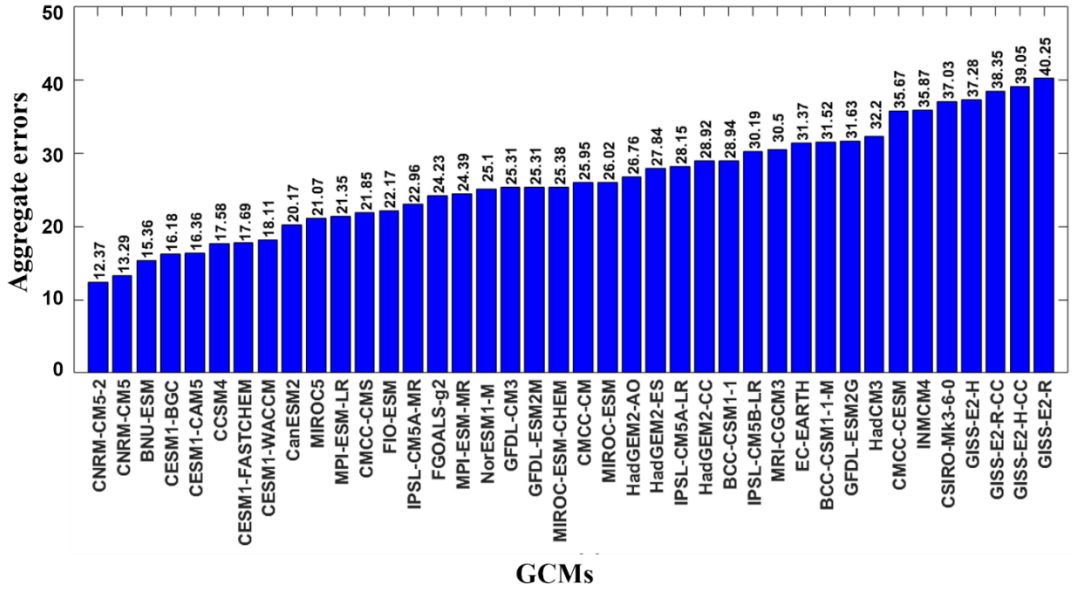

Figure 4.1 The aggregate errors of all performance metrics of 40 GCMs

Figure 4.2 shows the aggregate error of GCMs for different categories. CNRM-CM5 has the best performance for ocean, while it is second for land and temperature. Although CESM1-BGC is the best GCM for evaluating the precipitation category, its performance for the land and sea categories is fourth and fifth, respectively. There is only CNRM-CM5-2 which can perform best in more than two categories. It performs best for land and temperature. In addition, it ranks third for sea and rainfall categories.

None of the GCMs has the best performance for eacg category. The average of the multi-model ensemble is a possible approach to improve the simulation performance. Several studies had used multi-model ensembles to study climate in different regions of the world. For example, Schaller et al. (2011) created multi-model ensembles for global precipitation and temperature projections using the top five GCMs out of 24 CMIP3 GCMs. For the study of the Asian monsoon area, Bae et al. (2015) used multi-model ensembles of three GCMs out of nine CMIP3 GCMs. Wang et al. (2016) created multi-model ensembles for simulating temperature in southeastern Australia using the seven best GCMs from 28 CMIP5 GCMs. Khan et al. (2018) in their study on Pakistan used six best GCMs out of 31 CMIP5 GCMs to create multi-model ensembles for precipitation, temperature, and minimum and maximum temperature. In

another study on Pakistan, Ahmed et al. (2018) used the top three ranked GCMs out of 20 CMIP5 GCMs to create multi-model ensembles that simulated precipitation, while Ahmed et al. (2019) and Ahmed et al. (2020) created multi-model ensembles that simulated precipitation and minimum and maximum temperature by using the top four and 18 ranked GCMs out of 20 and 36 CMIP5 GCMs, respectively. In the Homsi et al. (2020) study on Syria, the four best-ranked GCMs out of 20 CMIP5 GCMs were selected to create multi-model ensembles for simulating precipitation.

Therefore, multi-model ensembles are evaluated to compare with single GCMs. Based on a review of the literature, there are no well-defined criteria for choosing the optimal number of GCMs for a multi-ensemble model. However, Ahmed et al. 2019 concluded that most studies select the best 3 to 10 GCMs to form the multi-ensemble model. These are multi-model ensembles of the top-six GCMs that perform best on all performance metrics in Figure 4.1 (hereafter referred to as 6-MODEL ENSEMBLE) and the 40 GCMs (hereafter referred to as 40-MODEL ENSEMBLE).

Figure 4.3 shows the relative error of 41 performance metrics for each CMIP5 model, 6-MODEL ENSEMBLE, and 40-MODEL ENSEMBLE. On the left side of the figure are the names of GCMs and the two multi-model ensembles, each with the highest to lowest total relative error listed from top to bottom, respectively. At the top of the figure are the names of all the performance metrics used in this part. The performance of these GCMs is represented by the color scale. A darker red means the GCM is performing well on that metric, while a darker green means the GCM is performing poorly on that metric. When the performance metrics are dark red, it means that the GCM's score on these metrics is very close to what was observed. The relative error results in Figure 4.3 obviously show that 6-MODEL ENSEMBLE has the best performance compared to the individual GCMs. While 40-MODEL ENSEMBLE performs better than 39 GCMs (except CNRM-CM5-2). Although the overall performance of CNRM-CM5-2 is lower than that of 6-MODEL ENSEMBLE, it is a good GCM for simulating temperature and precipitation over Southeast Asia. It still performs second-best and its aggregate error is only 8.78% higher than that of 6-MODEL ENSEMBLE. Since CNRM-CM5-2, 6-GCM-ENSEMBLE, and 40-MODEL ENSEMBL perform quite excellently in this past study, they are selected to present the evaluation results of each performance metric in detail in the next section

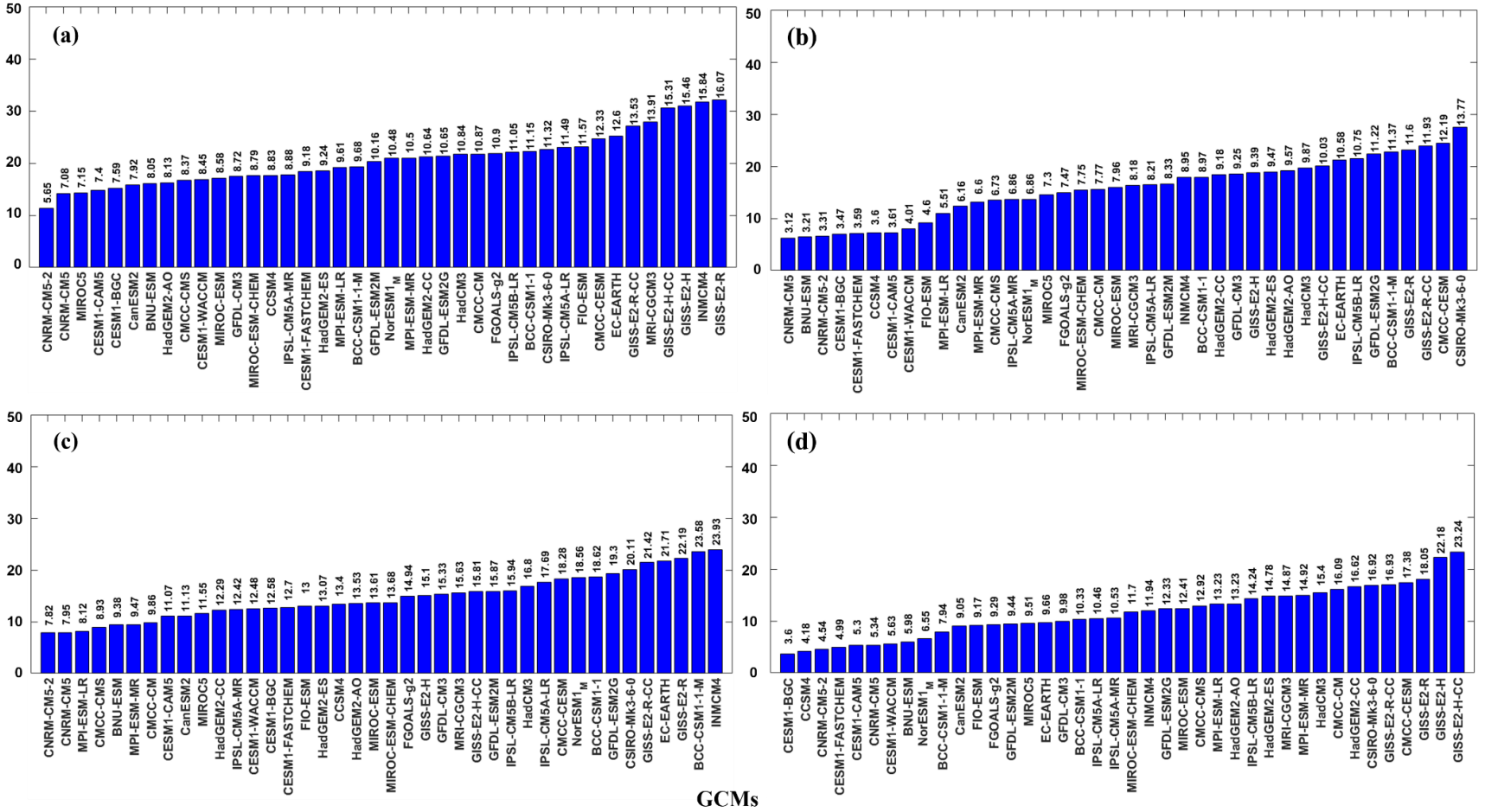

Figure 4.2 The aggregate errors by performance metrics considered (a) land only and (b) sea only (c) temperature, and (d) precipitation of 40 GCMs

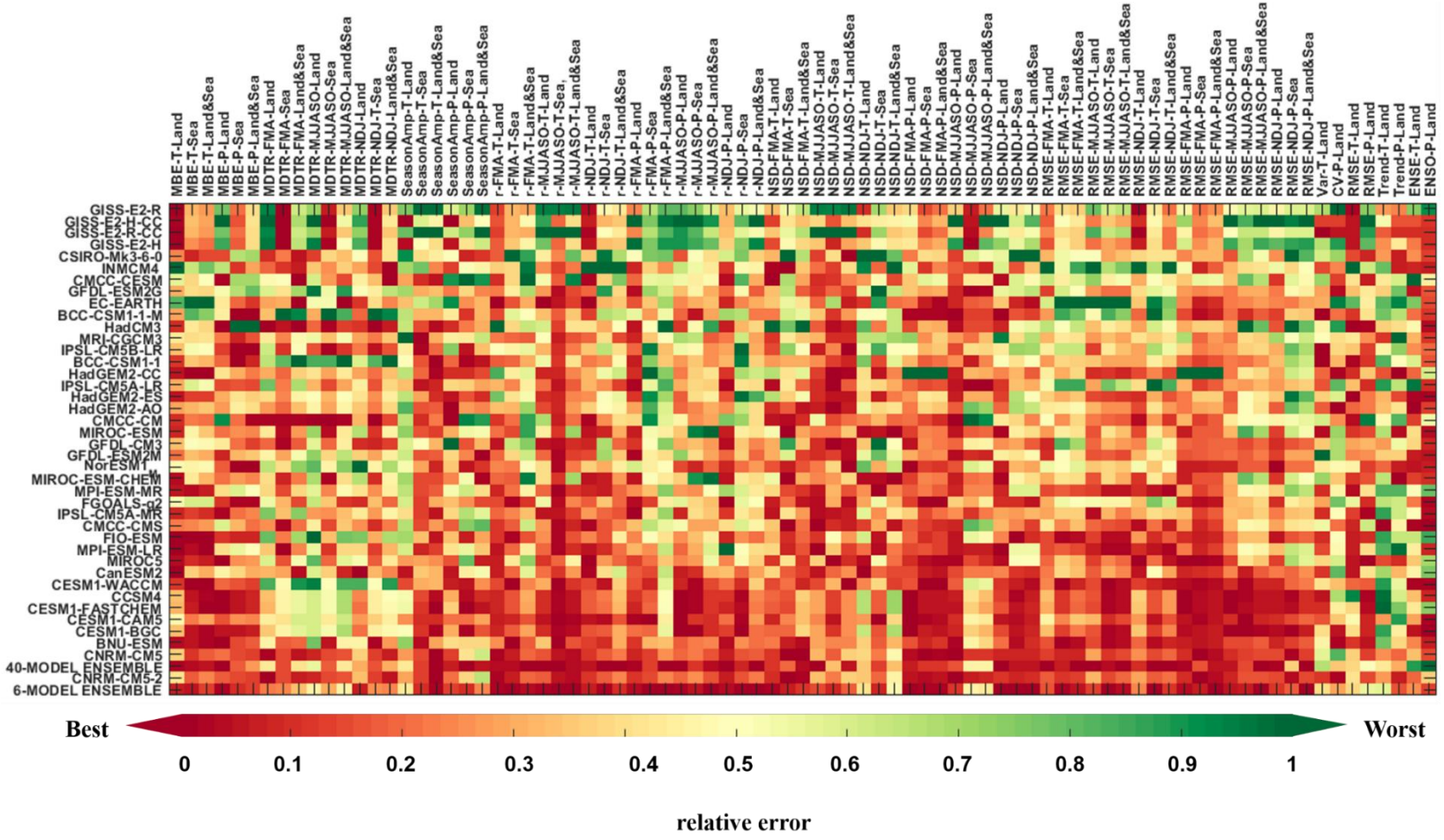

Figure 4.3 Relative error of 41 performance metrics (horizontal ordinate) for each CMIP5 model, 6-MODEL ENSEMBLE, and 40-MODEL ENSEMBLE (vertical ordinate).

4.1.2 Temperature and precipitation simulation for a short-term period of CNRM-CM5-2, 6-MODEL ENSEMBLE, and 40-MODEL ENSEMBLE.

4.1.2.1 Mean bias error (MBE)

The 40-year average temperature of mean reference data in the region Southeast Asia ranges from 16.61°C to 28.04 °C. In order to investigate the temperature simulation characteristics of GCMs, MBE-T is used to represent the direction of temperature. It can indicate that the GCMs overestimate (warm bias) or underestimate (cold bias) the temperature compared to the mean reference data. Figure 4.4 shows the spatial distribution of the bias of mean annual temperature over Southeast Asia for mean reference data, CNRM-CM5-2, 6-MODEL ENSEMBLE, and 40-MODEL ENSEMBLE. The bias values range from -5.54°C to 2.26°C for CNRM-CM5-2, -4.28°C to 3.21°C for 6-MODEL ENSEMBLE, and -3.02 °C to 4.37 °C for 40-MODEL ENSEMBLE. The numbers in each sub-picture are the MBE-T values, all of which have a cold bias (negative direction). They are more consistent with the red areas than with the blue area in Figure 4.4, indicating it indicates that the temperature simulations of CNRM-CM5-2 and 6-MODEL-ENSEMBLE and 40-MODEL-ENSEMBLE are overall underestimated compared to the mean reference data. The mean values of MBE-T for CNRM-CM5-2, 6-MODEL ENSEMBLE, and 40-MODEL ENSEMBLE for the land only case are -1.02 °C, -0.72 °C, and -0.17 °C, respectively, while the values for the sea-only case are -0.36 °C, -0.15 °C, and -0.11 °C, respectively.

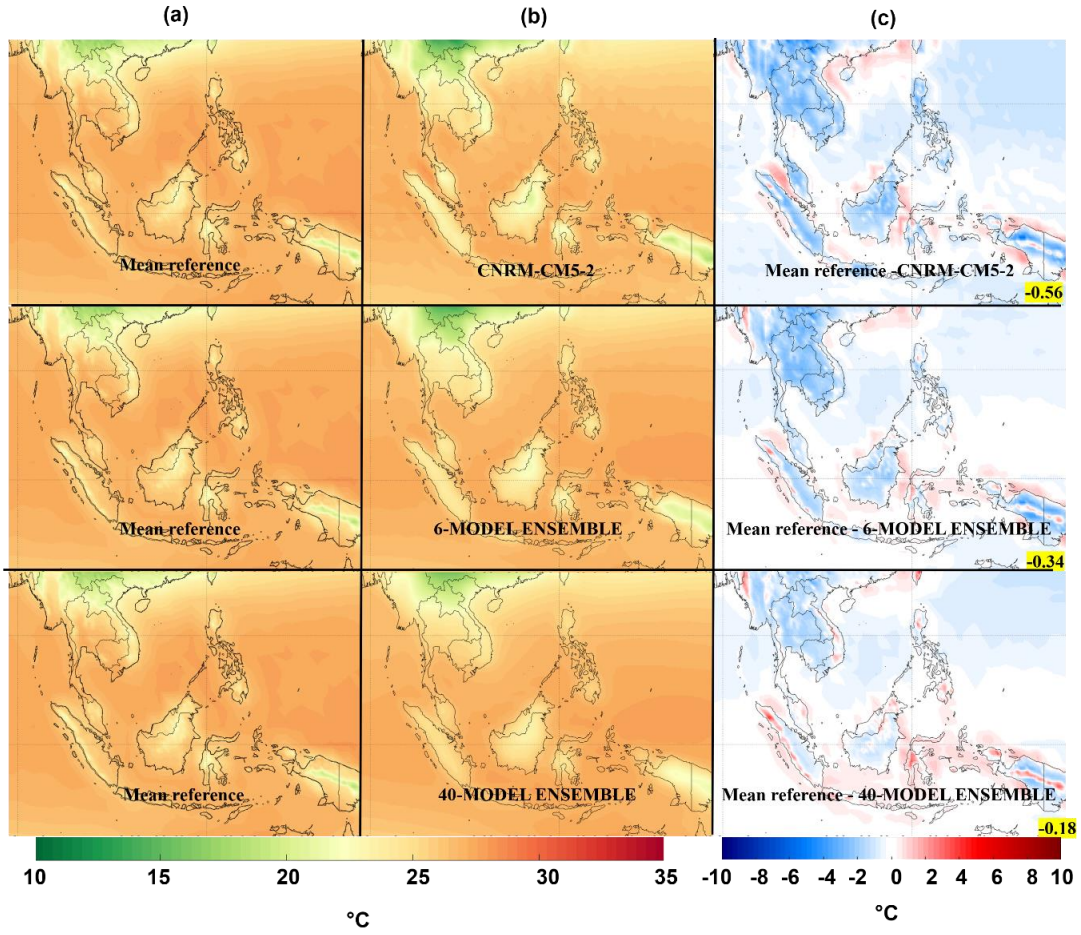

Figure 4.4 Spatial distribution of mean annual temperature for 1960-1999 of (a) mean reference data, (b) CNRM-CM5-2, 6-MODEL ENSEMBLE, and 40-MODEL, and (c) MBE thereof in °C. The numbers in the lower right of each dataset are the averaged MBE values for all pixels

The 40-year mean precipitation of mean reference data in the region Southeast Asia ranges from 874.51 mm to 5,699.00 mm. MBE-P is used to display the direction of the simulated precipitation. It gives the wettest or driest than the reference data. Figure 4.5 shows the spatial distribution of bias of the mean annual precipitation for mean reference data, CNRM-CM5-2, 6-MODEL ENSEMBLE, and 40-MODEL ENSEMBLE. The numbers in each sub-map are the MBE-P values of spatial annual precipitation. The blue area on the maps means that the precipitation is underestimated, while the red area overestimates precipitation. Figure 4.5 demonstrates most of the red area covers the sea, while the blue area covers the mainland. MBE-P values of CMRN-CM5-2 range from -2,087 mm to 3,808 mm while those of 6-MODEL ENSEMBLE

range from -2,102 mm to 2,883 mm and those of 40-MODEL ENSEMBLE range from -2,070 mm to 2,712 mm. However, the MBE-P values displayed in each sub-map of CMRN-CM5-2 and both multi-model ensembles show a positive direction which means overall precipitation simulations have higher than mean reference values. The mean values of MBE for CNRM-CM5-2, 6-MODEL ENSEMBLE, and 40-MODEL ENSEMBLE for land only case are 25.14 mm, 100.45 mm, and 144.10 mm, respectively, while the values for sea only case are 241.54 mm, -233.44 mm, and 363.46 mm, respectively.

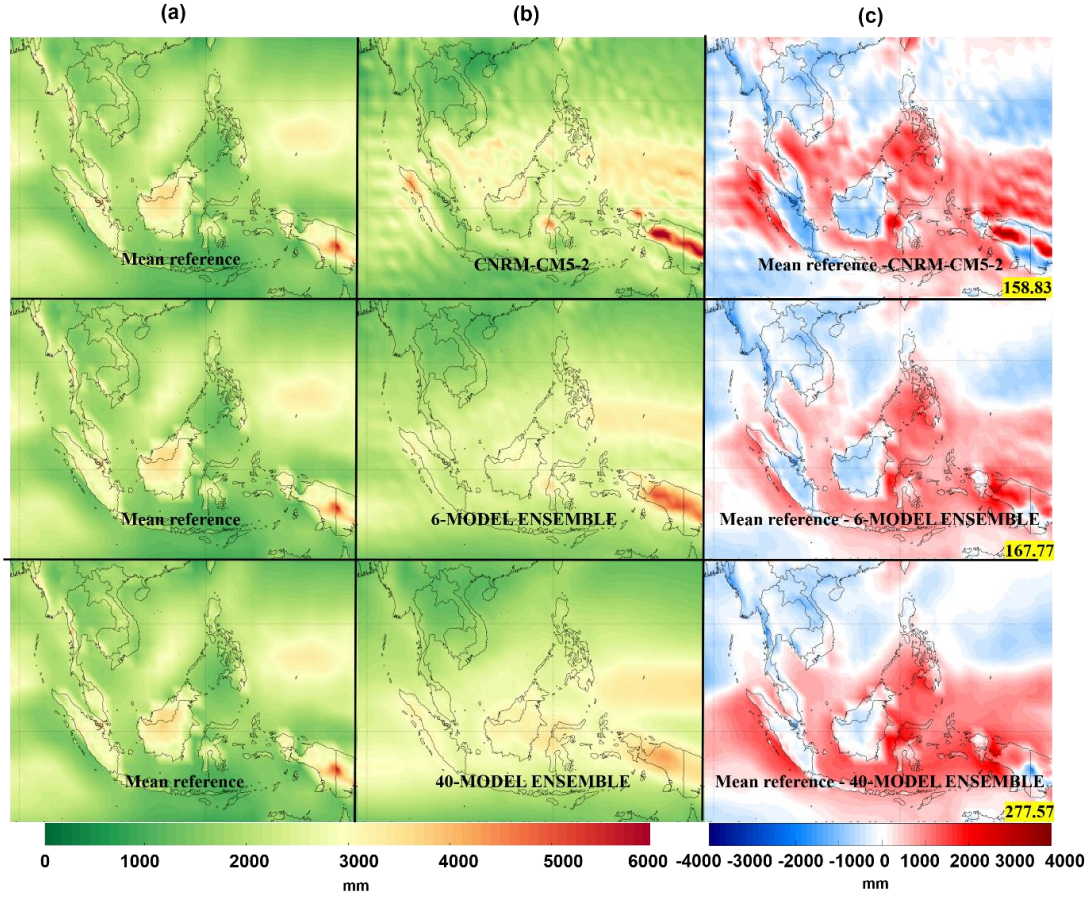

Figure 4.5 Same as Figure 4.4 but for precipitation

According to the literature review, there are many factors that cause the ocean area to be overestimated more than the land area. First, previous research has found that CMIP5 GCMs have difficulty simulating precipitation in the tropical west Pacific Ocean (Saha et al. 2014; Yang et al. 2018). Due to tropical convection, air rises and forms rain clouds, causing frequent rainfall and rapid decay. These rapid

occurrence and dissipation of rainfall may have caused the model to overestimate the quantity of precipitation compared to the recorded observational data (Yin et al. 2013). According to Pathak et al. 2019, these positive precipitation biases are primarily due to convective parameterizations of the atmospheric components. Meanwhile, Samanta et al. (2019) found that bias precipitation over the ocean is primarily influenced by convection and sea-surface-temperature interactions. These data support the idea that convection is the primary driving force behind the majority of precipitation in this area (Surussavadee, 2014). According to Surussavadee et al. (2014) and Maher et al. (2018), convective precipitation in the tropics is more difficult to simulate since cells of convective are small along with using a relatively short time for the precipitation formation over this area. Second, although GCMs are designed to simulate atmosphere and ocean processes, the GCMs structure clearly separates the elements of the climate system: the atmosphere, oceans, cryosphere, biosphere, and geosphere (Treut et al. 2007). Hence, the GCM's internal sub-models are also designed to focus on the different processes of the climate system (Gent 2012). The climate simulations on land and sea are simulated by different sub-models; as a result, the performance of GCMs simulating climate on land and sea is also different. Third, the biases might be due to the observation dataset part inputted in the ocean-component model.

It is difficult to collect precipitation observation data over the ocean due to the scattering of measurement devices and environmental issues (e.g., strong winds) (Sun al. 2018). As a result, precipitation simulations over the sea of the study area are highly inaccurate. Last, because several GCMs utilized the same sub-component versions among models (Pathak et al. 2019), the bias patterns of precipitation of GCMs are quite similar, as shown in Figure 4.5. Therefore, it is highly possible that each GCMs may use the same SST data from the same source, resulting in most sea area of the same overestimate.

In summary, the bias patterns of precipitation in Figure 4.5 over the sea (~12°S to15°N) are much higher than those over land area due to 1). tropical convection, 2). sub-models to simulate ocean-atmosphere interactions, 3). difficulty in obtaining observational data in sea area and 4). sharing the same SST data, resulting in the same overestimate over the sea's area.

4.1.2.2 Mean diurnal temperature range (MDTR)

MDTR is used to present the daily change range between the maximum and minimum temperature. It indicates the temperature trend of each season by considering the variances rate. Figure 4.6 shows the spatial pattern of the mean diurnal temperature range in Southeast Asia for summer, rainy, and winter of mean reference, CNRM-CM5-2, 6-MODEL ENSEMBLE, and 40-MODEL ENSEMBLE. In the case of land & sea, MDTRs of mean reference, CNRM-CM5-2, 6-MODEL ENSEMBLE, and 40-MODEL ENSEMBLE in summer ranges from 0.86 °C to 21.15 °C, from 0.55 to 20.14 °C, from 0.56 °C to 17.12 °C, and from 0.59 °C to 15.43 °C, respectively, while that in rainy ranges from 0.78 °C to 14.84 °C, from 0.52 °C to 13.24 °C, from 0.55 °C to 10.58 °C, and from 0.55 °C to 9.60 °C, respectively, and that in winter ranges from 0.89 °C to 14.97 °C, from 0.63°C to 16.55°C, from 0.57°C to 14.41°C, and from 0.59°C to 12.83°C. In the case of land & sea, the mean values of MDTR for mean reference, CNRM-CM5-2, 6-MODEL ENSEMBLE, and 40-MODEL ENSEMBLE in summer are 3.10°C, 3.02 °C, 2.69°C, and 2.61 °C, while those in rainy are 2.64°C, 4.34°C, 2.07°C, and 2.12°C and that in winter are 2.69°C, 2.77°C, 2.42°C, and 2.37°C. Overall of CNRM-CM5-2 of both land & sea case can perform MDTR value close to mean reference more than both multi-model ensembles for all seasons. MDTR of CNRM-CM5-2 is only 2.64% and 8.64% lower than that of the mean reference in summer and rainy, respectively; meanwhile, that is only 2.89 % higher than the mean reference in winter. Whereas MDTR in all seasons of 6-MODEL ENSEMBLE and 40-MODEL ENSEMBLE jumps up to 10% and 20% that of the mean reference. In the case of land only, the mean values of MDTR for mean reference, CNRM-CM5-2, 6-MODEL ENSEMBLE, and 40-MODEL ENSEMBLE in summer are 9.42°C, 9.61 °C, 8.38°C, and 7.64 °C, while those in rainy are 7.54°C, 7.04°C, 5.91°C, and 5.64°C and that in winter are 7.58°C, 8.55°C, 7.36°C, and 6.71°C. In the case of the sea only, the mean values MDTR for mean reference, CNRM-CM5-2, 6-MODEL ENSEMBLE, and 40-MODEL ENSEMBLE in summer are 1.48°C, 1.33°C, 1.23°C, and 1.32°C, while that in rainy are 1.44°C, 1.25°C, 1.09°C, and 1.21°C and that in winter are 1.39°C, 1.29 °C, 1.16°C, and 1.26°C.

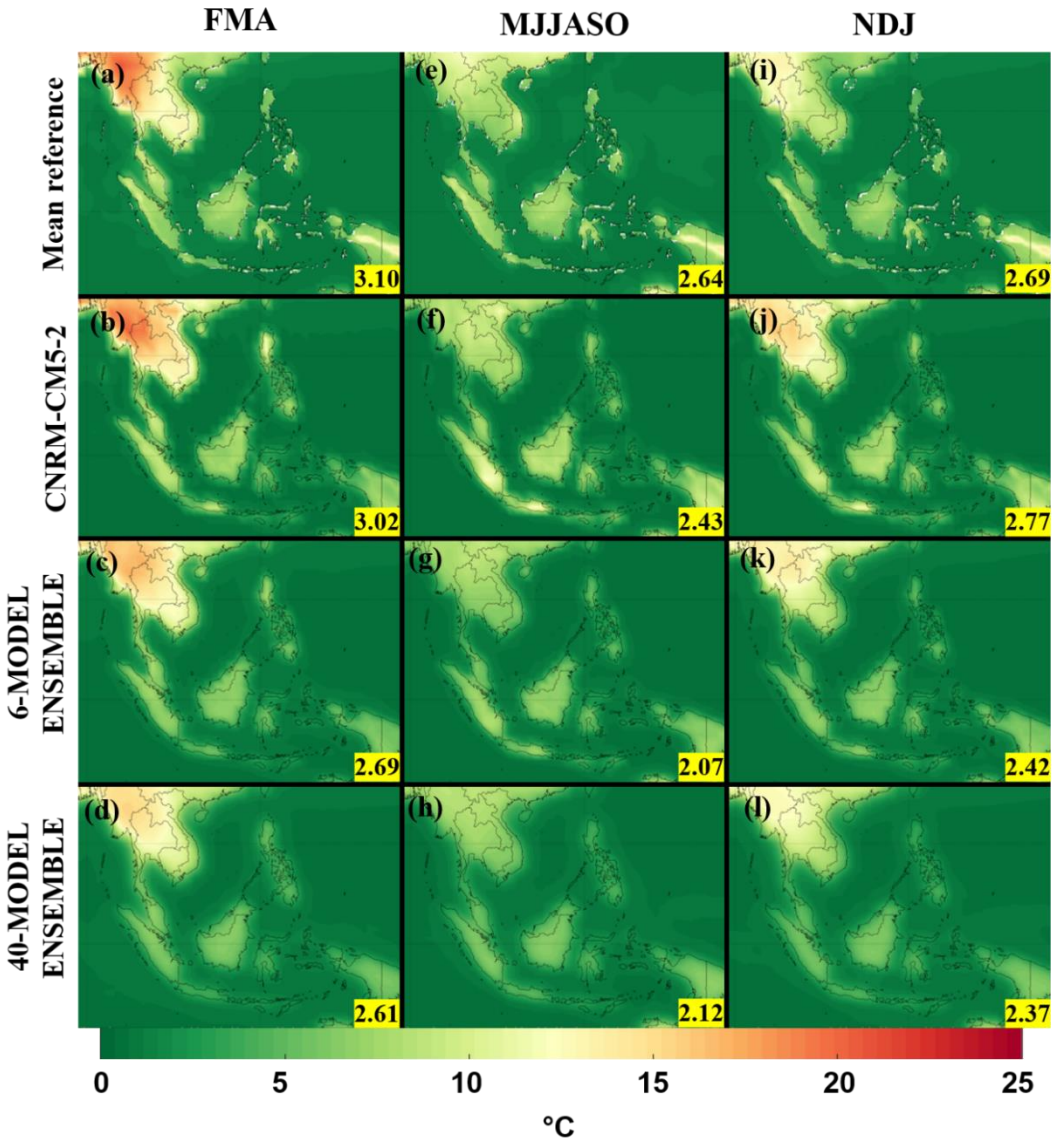

Figure 4.6 Spatial distribution of the mean diurnal temperature range for summer (left column) from (a) mean reference, (b) CNRM-CM5-2, (c) 6-MODEL ENSEMBLE, and (d) 40-MODEL ENSEMBLE, while (e) – (h) are same as (a) – (d), but that for rainy (middle column), as well as (i) – (l) are same as (a) – (d), but that for winter (right column). Numbers at the bottom-right of each dataset are the averaged MDTR values for all pixels.

4.1.2.3 Mean seasonal cycle amplitude (SeasonAmp)

Figure 4.7 shows the spatial distribution of the mean seasonal cycle amplitude of temperature (SeasonAmp-T) and precipitation (SeasonAmp-P) of mean reference, CNRM-CM5-2, 6-MODEL ENSEMBLE, and 40-MODEL

ENSEMBLE. The SeasonAmp-T and SeasonAmp-P gradient in the spatial pattern of CNRM-CM5-2, 6-MODEL ENSEMBLE, and 40-MODEL ENSEMBLE demonstrate well agreement with mean reference.

In the case of temperature, SeasonAmp-T is a metric that shows the intensity of changing temperature computing by the difference of the highest and lowest temperature month. All models show similar south-north gradient results. There are the most different temperatures throughout the northern mainland; on the other hand, they show a smooth gradient with a low SeasonAmp-T value in the maritime area, as well as the island areas. SeasonAmp-T of mean reference, CNRM-CM5-2, 6-MODEL ENSEMBLE, and 40-MODEL ENSEMBLE range from -2.23 °C to 12.72 °C, from -4.04 °C to 16.01 °C, from -3.67 °C to 15.76 °C, and from -3.03 °C to 15.09 °C, respectively (Figure 4.7). The mean values of SeasonAmp-T for land and sea pixel for the mean reference, CNRM-CM5-2, 6-MODEL ENSEMBLE, and 40-MODEL ENSEMBLE are 2.20 °C, 2.22 °C, 2.23 °C, and 2.19 °C. 40-MODEL ENSEMBLE has the best performance, where the mean value of SeasonAmp-T is only 0.01 °C less than that of the mean reference. Hence, 40-MODEL ENSEMBLE is the best performance model to simulate the difference in the months with the highest and lowest temperature. The mean values of SeasonAmp-T for land pixel for the mean reference, CNRM-CM5-2, 6-MODEL ENSEMBLE, and 40-MODEL ENSEMBLE are 3.03°C, 4.46°C, 4.82°C, and 4.83°C, while that for sea pixel are 1.44°C, 1.65°C, 1.68°C, and 1.66°C. When SeasonAmp-T of the model for land only and sea only cases are considered, they are not much different; however, SeasonAmp-T of CNRM-CM5-2 perform better than that of multi-model ensembles.

In the case of precipitation, SeasonAmp-P shows the intensity of changing precipitation computing by the difference of the highest and lowest precipitation month. This metric in this study is calculated as a percentage of mean annual precipitation. The spatial pattern showing SeasonAmp-P of the mean reference and all models demonstrate low to high value from the south-north gradient. SeasonAmp-P of mean reference, CNRM-CM5-2, 6-MODEL ENSEMBLE, and 40-MODEL ENSEMBLE range from -26.66 % to 26.44 %, from -20.33 % to 20.79 %, from -18.37 % to 22.89 %, and from -15.48 % to 22.95 %, respectively. Overall, all models have high SeasonAmp-P values over the northern part of Southeast Asia.

However, SeasonAmp-P over the northwest and southeast area of both multi-model ensembles is more similar to mean reference than CNRM-CM5-2. The mean values of SeasonAmp-P for 6-MODEL ENSEMBLE and 40-MODEL ENSEMBLE are only 0.59% and 0.13 % less than that of the mean reference, respectively, while that for CNRM-CM5-2 is 1.57% less than the mean reference. 40-MODEL ENSEMBLE is the best performance model to simulate the difference in the months with the highest and lowest precipitation. The mean values of SeasonAmp-P for land pixel for the mean reference, CNRM-CM5-2, 6-MODEL ENSEMBLE, and 40-MODEL ENSEMBLE are 3.92%, 5.32%, 7.27%, and 6.95%, while those for sea pixel are 3.35%, 2.34%,3.15 %, and 3.53%. Although the best model for SeasonAmp-P for land only case is CNRM-CM5-2, that for sea only case is 40-MODEL ENSEMBLE.

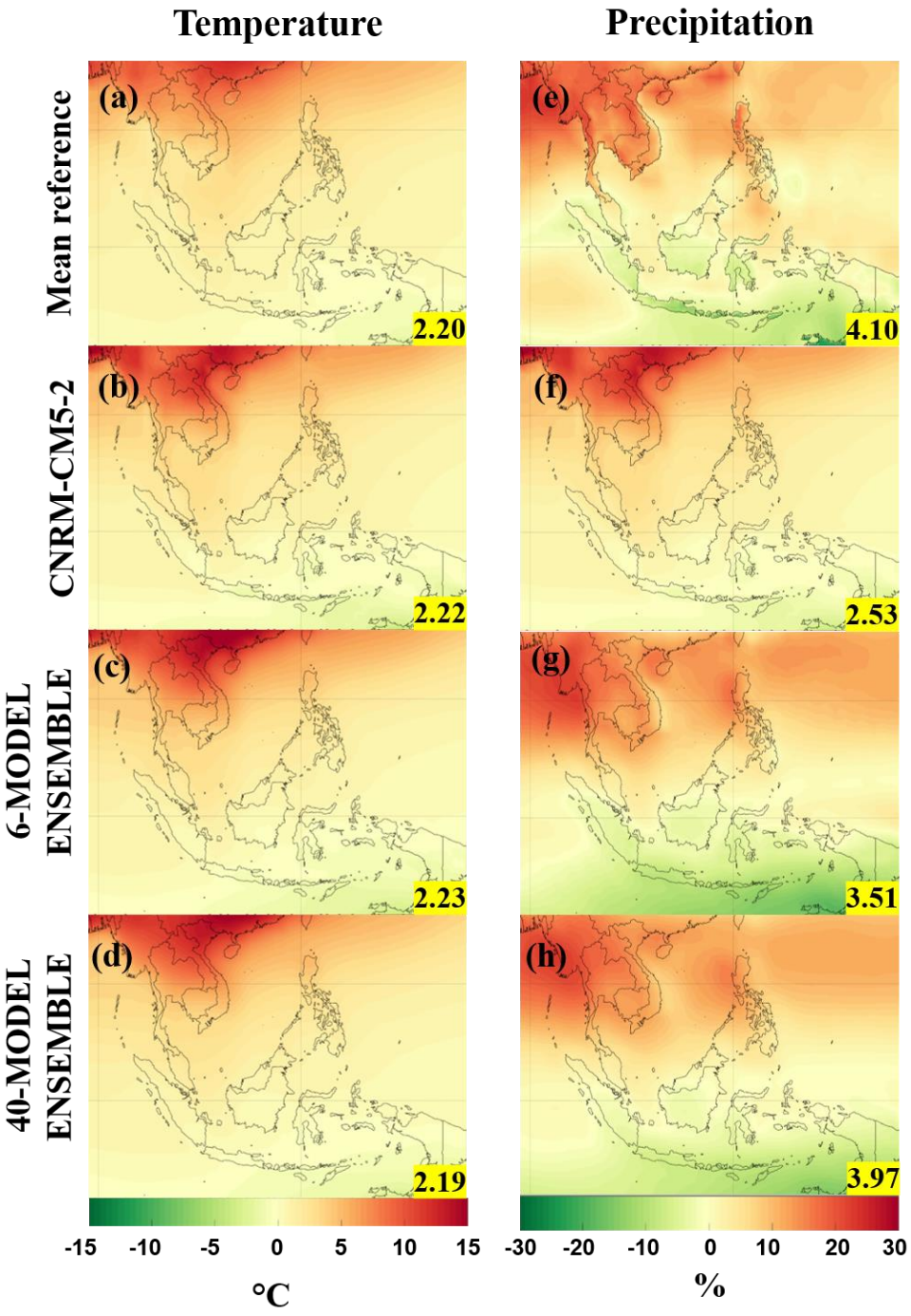

Figure 4.7 Spatial distribution of the mean seasonal cycle amplitude of temperature (left column) from (a) mean reference, (b) CNRM-CM5-2, (c) 6-MODEL ENSEMBLE, and (d) 40-MODEL ENSEMBLE, and the mean seasonal cycle amplitude of precipitation (right column) from (e) mean reference, (f) CNRM-CM5-2, (g) 6-MODEL ENSEMBLE, and (h) 40-MODEL. Numbers at the bottom-right of each dataset are the averaged SeansonAmp values for all pixels

4.1.2.4 Correlation coefficient (r)

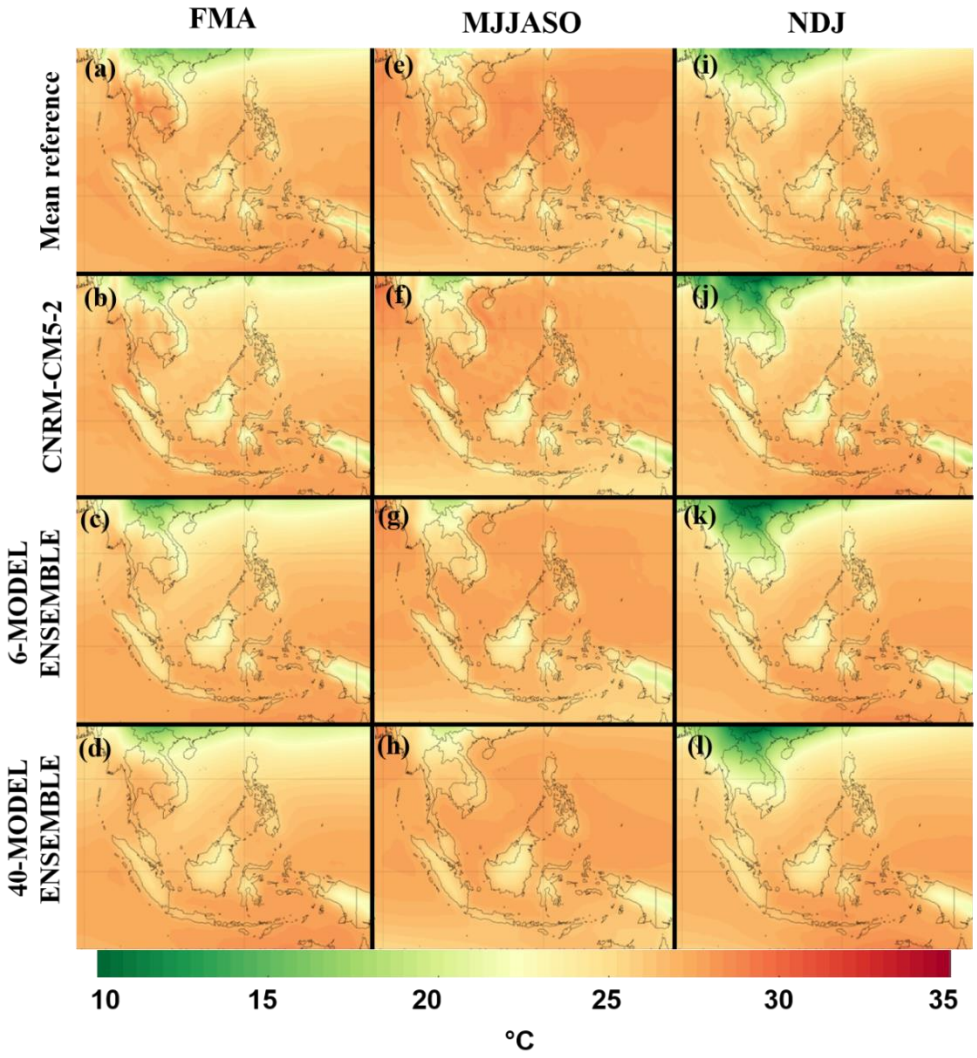

Figure 4.8 Spatial distribution of the mean seasonal temperature for mean reference, CNRM-CM5-2, 6-MODEL ENSEMBLE, and 40-MODEL ENSEMBLE in summer (left column), in rainy (middle column), and in winter (right column)

Figure 4.8 shows the mean seasonal temperature for the period 1960-1999 of mean reference, CNRM-CM5-2, 6-MODEL ENSEMBLE, and 40-MODEL ENSEMBLE order by summer (FMA), rainy (MJJASO), and winter (NDJ). They show cold temperatures over the northern part of the mainland. In addition, the mean reference shows the seasonal temperature over the mainland higher than that of all models.

Table 4.1 shows r, RMSE, and NSD results of mean seasonal temperature and precipitation for years 1960 – 1999 for both land & sea case for CNRM-CM5-2, 6-MODEL ENSEMBLE, and 40-MODEL ENSEMBLE compared to the mean reference. Asterisk (*) above number in Table 4.1 is the best value for metrics evaluations. To evaluate temperature simulation by r, the r-T rating of all simulation for all seasons is a very good level, their correlations range from 0.91 to 0.97. Although all simulations can perform well in terms r-T metric, both multi-model ensembles are very close to 1 more than CNRM-CM5-2, particularly 6-MODEL ENSEMBLE. Furthermore, 6-MODEL ENSEMBLE is the best performance model of all seasons. In the case of land only, CNRM-CM5-2, 6-MODEL ENSEMBLE, and 40-MODEL ENSEMBLE are highly correlated to the mean reference, with r-T of 0.9993, 0.9993, and 0.9992 in summer, of 0.9990, 0.9993, and 0.9997 in rainy, and 0.9968, 0.9976, and 0.9979 in winter. In the case of sea only, the mean values of r-T for CNRM-CM5-2, 6-MODEL ENSEMBLE, and 40-MODEL ENSEMBLE are 0.9989, 0.993, and 0.9991 in summer, 0.9992, 0.9997, and 0.9996 in rainy, and 0.9989, 0.9994, and 0.9994 in winter. Their cases reveal that all simulations are very close to 1.

Table 4.1 r, RMSE, and NSD between observations and model simulations of mean annual temperature and precipitation for years 1960 – 1999. They are evaluated for both land & sea case for summer (FMA), rainy (MJJASO), and winter (NDJ)

Models	Metrics	Temperature			Precipitation		
		Summer	Rainy	Winter	Summer	Rainy	Winter
CNRM-CM5-2	r	0.93	0.91	0.96	0.85	0.73	0.88
	RMSE(°C)	0.86	0.90	1.59	46.04	60.44	48.76
	NSD	0.94*	1.28	1.20	1.10	0.95*	0.90
6-MODEL ENSEMBLE	r	0.95*	0.92*	0.97*	0.92*	0.84*	0.90*
	RMSE(°C)	0.75	0.60	0.96	37.36*	46.61*	37.98*
	NSD	1.09	1.16	1.22	1.07*	0.75	0.97*
40-MODEL ENSEMBLE	r	0.95*	0.91	0.97*	0.91	0.81	0.90*
	RMSE(°C)	0.67*	0.54*	0.78*	47.72	47.25	38.97
	NSD	1.10	1.07*	1.17*	1.23	0.74	1.05

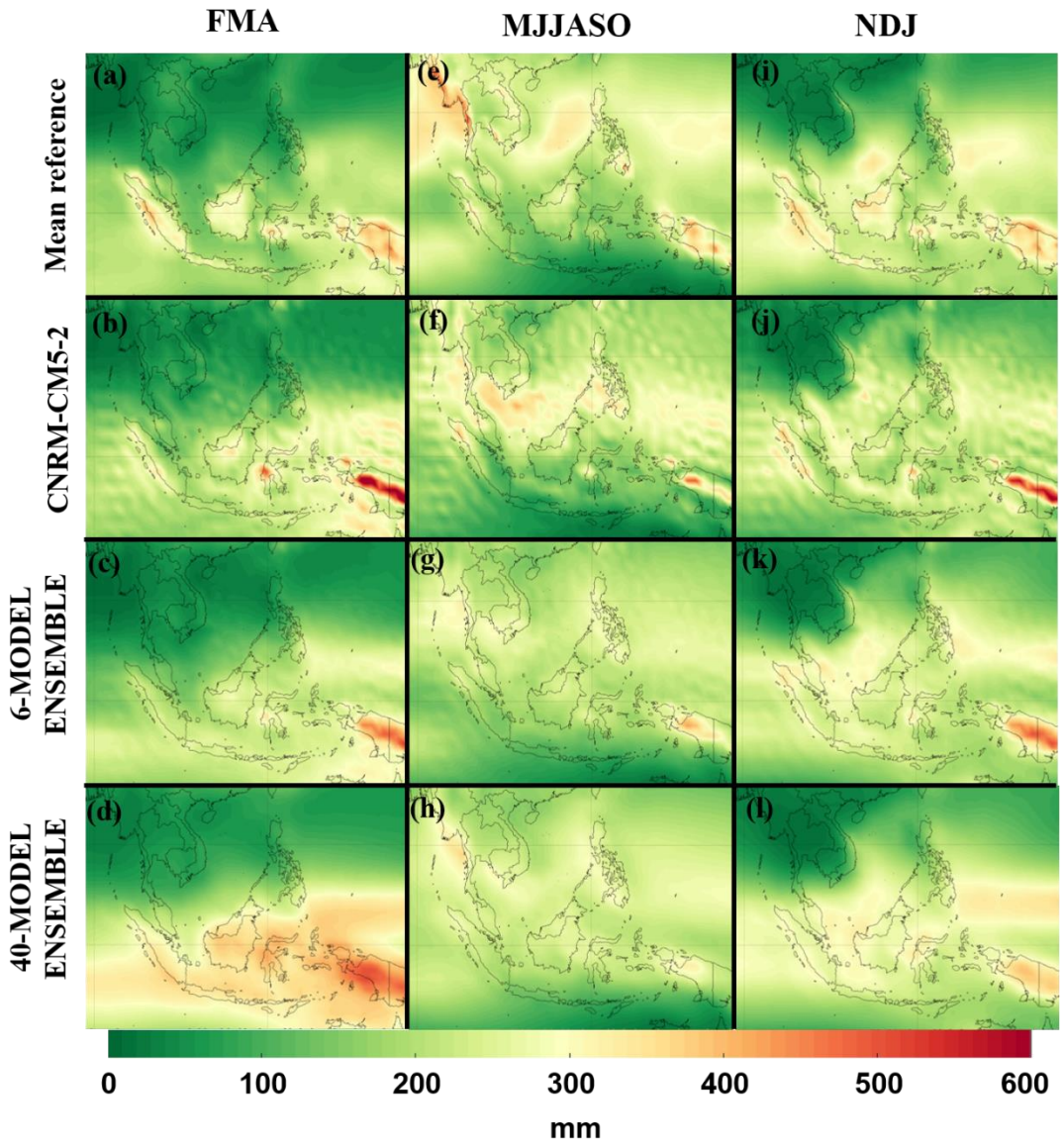

Figure 4.9 Same as Figure 4.8 but for precipitation

Figure 4.9 shows the mean seasonal precipitation for the period 1960-1999 for mean reference, CNRM-CM5-2, 6-MODEL ENSEMBLE, and 40-MODEL ENSEMBLE order by summer (FMA), rainy (MJJASO), and winter (NDJ). They show that low precipitation over the northern part of Southeast Asia in summer and winter while the southern part of that has high precipitation, especially Indonesia and Papua New Guinea. To evaluate precipitation simulation by r, the r-P rating of all simulation for all season is good to very good. Their correlations for all seasons range from 0.73 to 0.91. 6-MODEL ENSEMBLE is the only model that shows the best correlation for

all seasons, with r-T of 0.92 in summer, 0.84 in rainy, and 0.90 in winter, respectively. While 40-MODEL ENSEMBLE also performs best in winter, with r-P of 0.90. However, the mean values of r-T for CNRM-CM5-2, 6-MODEL ENSEMBLE, and 40-MODEL ENSEMBLE show weaker than that in summer and winter. In the case of land only, CNRM-CM5-2, 6-MODEL ENSEMBLE, and 40-MODEL ENSEMBLE are highly correlated to the mean reference, with r-P of 0.96, 0.98, and 0.98 in summer, of 0.94, 0.96, and 0.97 in rainy, and 0.98, 0.97, and 0.98 in winter. In the case of sea only, the mean values of r-T for CNRM-CM5-2, 6-MODEL ENSEMBLE, and 40-MODEL ENSEMBLE are 0.89, 0.91, and 0.89 in summer, 0.83, 0.89, and 0.75 in rainy, and 0.89, 0.90, and 0.85 in winter.

4.1.2.5 Root mean squared error (RMSE)

RMSE shows the different errors in terms of magnitude between models and means reference. The best RMSE value is closer to 0. To evaluate temperature simulation using RMSE, the mean values of RMSE-T for land & sea case for CNRM-CM5-2, 6-MODEL ENSEMBLE, and 40-MODEL ENSEMBLE for all seasons range from 0.54 °C to 1.13 °C. Their RMSE-T of almost season (except CNRM-CM5-2 in winter) have less than 1°C. 40-MODEL ENSEMBLE for all seasons shows very high accuracy with RMSE-T value closer to 0 than CNRM-CM5-2 and 6-MODEL ENSEMBLE. In addition, the RMSE-T for all models shows the weakest performance in the winter; in contrast, they perform best in the rainy. In the case of land only, all of models can perform RMSE-T less than 1 °C, which they for all seasons range from 0.37 °C to 0.95 °C. 40-MODEL ENSEMBLE has the best performance for all season, with RMSE-T of 0.41°C, 0.37°C, and 0.68 °C in summer, rainy, and winter, respectively. In addition, all models also can perform well in rainy; on the other hand, their performance also perform poorly in winter. In the case of sea only, all of models can perform RMSE-T less than 0.7°C, which they for all seasons range from 0.35 °C to 0.63 °C. 6-MODEL ENSEMBLE perform best for all season, with RMSE-T of 0.45, 0.35, and 0.36 in summer, rainy, and winter, respectively.

To evaluate precipitation simulation using RMSE, the mean values of RMSE-P for CNRM-CM5-2, 6-MODEL ENSEMBLE, and 40-MODEL ENSEMBLE for all seasons of land & sea case range from 37.36 mm to 60.44 mm. 6-

MODEL ENSEMBLE is a model that performs best for all season, its RMSE-P is 37.36 mm, 46.61 mm, and 37.98 mm in summer, rainy, and winter, respectively. While the mean values of RMSE-P for CNRM-CM5-2 and 40-MODEL ENSEMBLE are 18.85% and 21.71% higher than the 6-MODEL ENSEMBLE in summer, respectively. Meanwhile, the mean values of RMSE-P of CNRM-CM5-2 in rainy and winter are 21.51% and 20.51% higher than the 6-MODEL ENSEMBLE, respectively. Although having lower accuracy, RMSE-P of 40-MODEL ENSEMBLE is only 1.37 % and 2.54% higher than that of 6-MODEL ENSEMBLE in rainy and winter, respectively. In the case of land only, all models can perform RMSE-P less than 30 mm, which their RMSE-P for all seasons ranges from 20.78 mm to 29.60 mm. 40-MODEL ENSEMBLE also performs best in all seasons with RMSE-P of 20.78 mm, 26.70 mm, and 27.09 mm in summer, rainy, and winter, respectively. Besides, all models also can perform well in summer; on the other hand, they also perform poorly in rainy. In the case of the sea only, all models can perform RMSE-P less than 60 mm, which for all seasons range from 37.95 mm to 59.12 mm. The best performance of RMSE-P in summer and winter is CNRM-CM5-2, its RMSE-P is 0.37 mm and 40.65 mm, respectively, while that in rainy is 6-MODEL ENSEMBLE, its value is 46.74 mm.

4.1.2.6 Normalized standard deviation (NSD)

NSD represents individual pixels for CNRM-CM5-2, 6-MODEL ENSEMBLE, and 40-MODEL ENSEMBLE that distribute from its mean value. NSD of all models that are normalized by SD results of mean reference is shown in Table 4.1. The best value of NSD is closest to 1 which means low fluctuation. In the case of temperature, NSD-T for land & sea case for CNRM-CM5-2, 6-MODEL ENSEMBLE, and 40-MODEL ENSEMBLE for three seasons range from 0.94 to 1.28. Most of them show more than 1 which indicates that the distribution values of the three models are higher than the mean reference. The best performance of NSD-T in summer is CNRM-CM5-2, its NSD-T is 0.95. Whereas the 40-MODEL ENSEMBLE shows the best performance to simulate variability for rainy and winter by 1.07 and 1.17, respectively. Although 6-MODEL ENSEMBLE cannot perform best for all seasons, it can perform second-best in rainy. In the case of land only, NSD-T values of CNRM-CM5-2, 6-MODEL ENSEMBLE, and 40-MODEL ENSEMBLE for three

seasons range from 0.95 to 1.26. There is a larger NSD-T range more than land & sea study cases. CNRM-CM 2-5performs best in winter. While -40MODEL ENSEMBLE performs well for all seasons, especially in summer and rainy season. However, all models also show the largest NSD-T in winter. It means that the temperature simulation in winter has a higher fluctuation than that in another season. In the case of sea only, NSD-T of CNRM-CM5-2, 6-MODEL ENSEMBLE, and 40-MODEL ENSEMBLE for three seasons range from 0.98 to 1.17. CNRM-CM5-2 is the best performing model in summer, while 6-MODEL ENSEMBLE and 40-MODEL ENSEMBLE perform best in winter and rainy, respectively. On the other hand, the highest fluctuation of CNRM-CM5-2 and 6-MODEL ENSEMBLE is winter, while that of 40-MODELENSEMBLE is summer.

To evaluate the simulation precipitation using NSD, the mean NSD-P of CNRM-CM5-2, 6-MODEL ENSEMBLE, and 40-MODEL ENSEMBLE for three seasons range from 0.74 to 1.23. Although 6-MODEL ENSEMBLE is not best performing in temperature case, it performs best in precipitation case, its NSD-P is closest to 1 in summer and winter. While CNRM-CM5-2 performs best in rainy, its NSD-P is only 0.5 mm lower than 1. The overall performance of 40-MODEL ENSEMBLE is rather good because it performs second-best in rainy and winter, its NSD-P is 0.74 and 1.05, respectively. In the case of land only, CNRM-CM5-2 has the best performances in rainy, with a perfect NSD-P of 1. Moreover, it also performs best in winter. While 6-MODEL ENSEMBLE has the best performances in summer, its NSD-P is 0.99% higher than that of the mean reference. In the case of sea only, NSD-P values of CNRM-CM5-2, 6-MODEL ENSEMBLE, and 40-MODEL ENSEMBLE for three seasons range from 0.75 to 1.30. All models perform less than 1 in rainy and winter which means variability of models less than that of the mean reference. The small NSD-P of CNRM-CM5-2 is 4.16% less than the mean reference in rainy, while that of 6-MODEL ENSEMBLE and 40-MODEL ENSEMBLE is 9.09 % higher than that in summer and 2.04 % less than that in winter, respectively.

4.1.3 Temperature and precipitation simulation for a long-term period of CNRM-CM5-2, 6-MODEL ENSEMBLE, and 40-MODEL ENSEMBLE.

4.1.3.1 Variance (Var)

Table 4.2 shows the value of the results of Var, CV, and RMSE performance metrics for evaluating temperature and precipitation for land only for the year 1901-1999. The annual variability of temperature for 99-years evaluated by the standard deviation of mean reference is 0.31 °C, while that of CNRM-CM5-2 is 0.34 °C. Whereas the standard deviations of 6-MODEL ENSEMBLE and 40-MODEL ENSEMBLE are 0.22°C and 0.16°C, respectively. Overall, CNRM-CM5-2 is the best model that shows the mean variability of temperature for 99-years in Southeast Asia close to the mean reference. Its standard deviation is only 8.82% higher than that of the mean reference. As the simulation of temperature for 99-years by the standard deviation of 6-MODEL ENSEMBLE and 40-MODEL ENSEMBLE are lower than men reference about 40.90% and 93.75%, respectively.

Table 4.2 Var, CV, and RMSE between observations and model simulations of mean annual temperature and precipitation for years 1991 – 1999

Models	Temperature			Precipitation		
	Var (°C)	RMSE (°C)	Trend (°C /century $^{-1}$)	CV (%)	RMSE (mm)	Trend (%/century $^{-1}$)
Mean reference	0.31	-	0.16	0.13	-	5.26
CNRM-CM5-2	0.34*	1.56	0.35*	0.14*	246.03*	4.17*
6-MODEL ENSEMBLE	0.22	1.46	0.55	0.05	590.37	3.70
40-MODEL ENSEMBLE	0.16	1.44*	0.46	0.02	548.92	2.16

4.1.3.2 Coefficient of variation (CV)

The annual variability of temperature for 99-years evaluated by the coefficient of variation of mean reference is 0.13, while that of CNRM-CM5-2 are

0.14 °C. Whereas standard deviations of 6-MODEL ENSEMBLE and 40-MODEL ENSEMBLE are 0.05 °C and 0.02°C, respectively. Overall, CNRM-CM5-2 is the best model that shows the mean variability of temperature for the long-term in Southeast Asia close to the mean reference. Its CV is only 7.14% higher than that of mean reference. While both multi-model ensembles simulate CV value that is very different with quite lower than mean reference.

4.1.3.3 Root mean squared error (RMSE)

In the case of temperature, the long-term RMSE averaged of 40-MODEL ENSEMBLE is the most accurate model, with an RMSE of 1.44 °C. While the RMSE values of 40-MODEL ENSEMBLE and 6-MODEL ENSEMBLE are 1.56 °C and 1.46 °C. Their values are not much different, especially the RMSE value of both multi-model ensembles. It is a bit different about 0.02 °C. While the RMSE value of the CNRM-CM5-2 is 0.12 ° C and 0.10 ° C higher than that of 40-MODEL ENSEMBLE and 6-MODEL ENSEMBLE, respectively.

On the other hand, the evaluation of the mean precipitation for the 20th century by RMSE shows that CNRM-CM5-2 is the most accurate model, its RMSE is 246.03 mm. There is lower than RMSE of both multi-model ensembles. RMSE of CNRM-CM5-2 is 344.34 mm and 302.89 mm lower than that of 6-MODEL ENSEMBLE and 40-MODEL ENSEMBLE, respectively. These RMSE results reveal that the CNRM-CM5-2 can be able to significantly reduce the magnitude of error more than that of both multi-model ensembles.

4.1.3.4 Linear trend (Trend)

Figure 4.10 shows the 20th-century trend for temperature and precipitation of annual averaged for of mean reference, CNRM-CM5-2, 6-MODEL ENSEMBLE, and 40-MODEL ENSEMBLE. Trend-T and Trend-P are used to evaluate the overall temperature and precipitation trend as well as preliminary variability in Southeast Asia. In the case of temperature, the trend of mean reference has a positive temperature trend, its trend is 0.16 °C /century -1. CNRM-CM5-2, 6-MODEL ENSEMBLE, and 40-MODEL ENSEMBLE showed a positive temperature trend of 0.34 °C /century -1, 0.55 °C /century -1, and 0.45 °C /century -1. Even though CNRM-

CM5-2 performs best for evaluating the rate of temperature change for the 1901–1999 period, there is a much different rate of temperature change from the mean reference.

In the case of precipitation, the trend of mean reference has a positive temperature trend, its trend is 5.26 %/century -1. CNRM-CM5-2, 6-MODEL ENSEMBLE, and 40-MODEL ENSEMBLE showed a positive temperature trend of 4.17 % /century -1, 3.70 % /century -1, and 2.16 % /century -1. CNRM-CM5-2 still performs best in Trend-P for evaluating the rate of precipitation change for the 1901–1999 period.

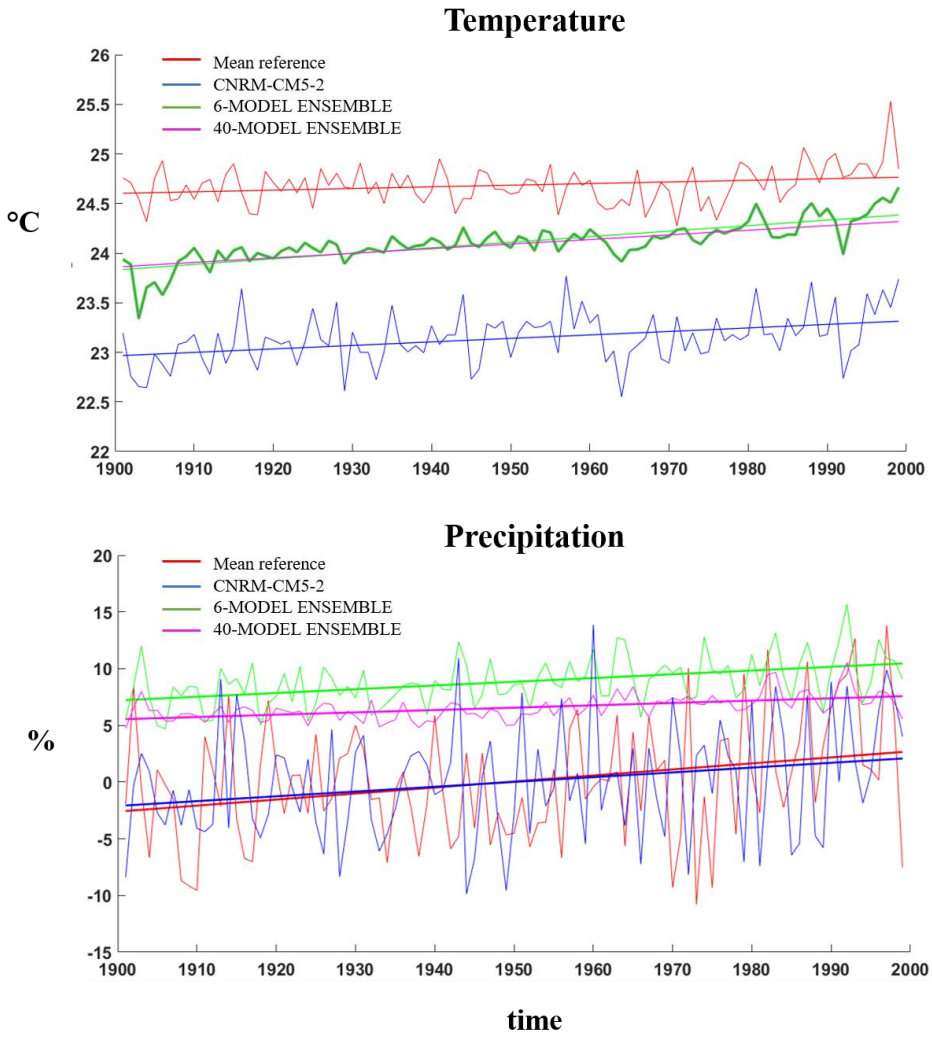

Figure 4.10 Annual averaged temperature and precipitation trend in Southeast Asia for years 1901-1999 of mean reference, CNRM-CM5-2, 6-MODEL ENSEMBLE, and 40-MODEL ENSEMBLE.

4.1.3.5 Correlation coefficient of ENSO (ENSO)

Figure 4.11 shows a correlation coefficient of winter temperature with Niño 3.4 index (ENSO-T), and that of winter precipitation with Niño 3.4 index (ENSO-P) for the 20th century of mean reference, CNRM-CM5-2, 6-MODEL ENSEMBLE, and 40-MODEL ENSEMBLE. In the spatial pattern of the temperature case, the CNRM-CM 2-5can exhibit the correlation of sea surface temperature anomalies in the Niño 3.4 region closest to the mean reference; even though, ENSO-T of that show higher than the mean reference over the north-west part of the mainland. Whereas 6-MODEL ENSEMBLE and 40-MODEL ENSEMBLE in spatial pattern show differently when compared with the mean reference. ENSO-T values of 6-MODEL ENSEMBLE over the island in the maritime area has higher than that of mean reference, while ENSO-T values of 40-MODEL ENSEMBLE over the study area has higher than that of mean reference. When the magnitude of ENSO-T is considered, ENSO-T averaged of CNRM-CM5-2 are slightly lower than in mean reference, its ENSO-T is only 0.09 less than mean reference. In contrast, ENSO-T averaged of -6MODEL ENSEMBLE and -40MODEL ENSEMBLE are 0.12and 0.41 higher than that of mean reference, respectively.

In the spatial pattern of the precipitation case, the CNRM-CM-5 2shows the correlation of sea surface temperature anomalies in the Niño 3.4 region closest to the mean reference. 6-MODEL ENSEMBLE shows ENSO-P value lower than that of mean reference over mainland; furthermore, its ENSO-P shows higher than that of mean reference over islands of maritime. -40MODEL ENSEMBLE is the worst performance model for evaluating the model by ENSO-P and it shows ENSO-P higher than that of mean reference over the study area. When the magnitude of ENSO-P is considered, ENSO-T averaged of CNRM-CM5-2 are lower than in mean reference, its ENSO-T is only 0.09 less than mean reference. While ENSO-P averaged of 6-MODEL ENSEMBLE and 40-MODEL ENSEMBLE is 0.10 and 0.59 higher than mean reference, respectively. Therefore, CNRM-CM 2-5is the best-performing model for ENSO-T and ENSO-P metrics because it performs well for evaluating the correlation in terms of spatial pattern and magnitude of the mean correlation coefficient.

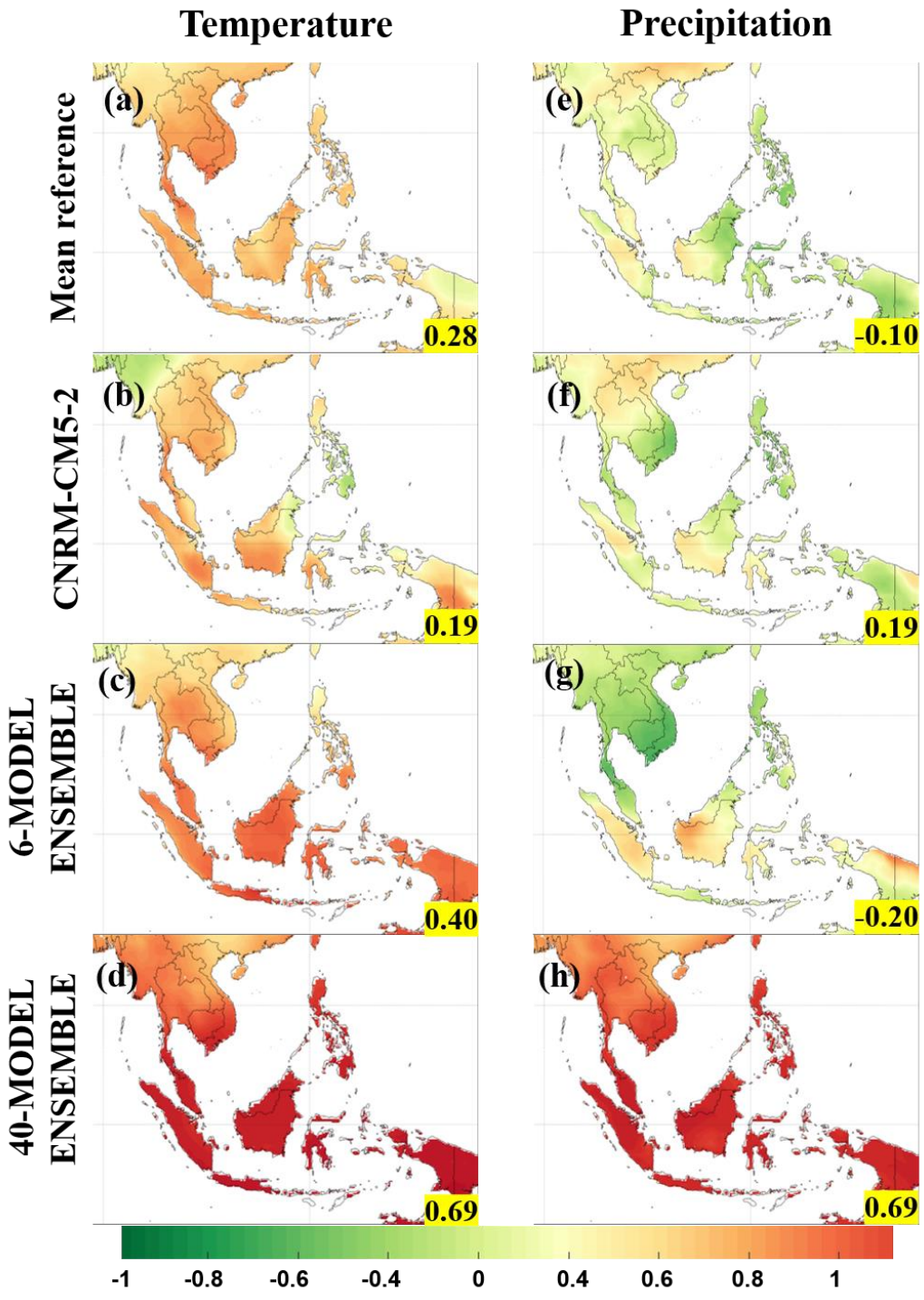

Figure 4.11 Spatial distribution of correlation coefficient of winter temperature with Niño 3.4 index (left column), and that of winter precipitation with Niño 3.4 index (right column) for 20th century of mean reference, CNRM-CM5-2, 6-MODEL ENSEMBLE, and 40-MODEL ENSEMBLE. Numbers at the bottom-right of each dataset are the averaged of ENSO values by all pixels.

4.1.4 CNRM-CM5-2, 6-MODEL ENSEMBLE, and 40-MODEL ENSEMBLE ranking by different categories.

When the performances of CNRM-CM5-2, 6-MODEL ENSEMBLE, and 40-MODEL ENSEMBLE are considered by different categories, Figure 4.12 shows relative errors for all performance metrics for land only, sea only cases, the temperature only, and precipitation only categories, respectively. The CNRM-CM5-2, 6-MODEL ENSEMBLE, and 40-MODEL ENSEMBLE are listed on the left of each sub-figure, while the total relative error values are listed on the right of the sub-figure. The 6-MODEL ENSEMBLE showing the lowest total relative error value is listed at the bottom of all sub-figures. Hence, Figure 4.12 shows that 6-MODEL ENSEMBLE is the best performance model for all categories, where their total relative errors are 4.95, 2.32, 7.69, and 3.68 for land only, sea only, the temperature only, and precipitation only, respectively.

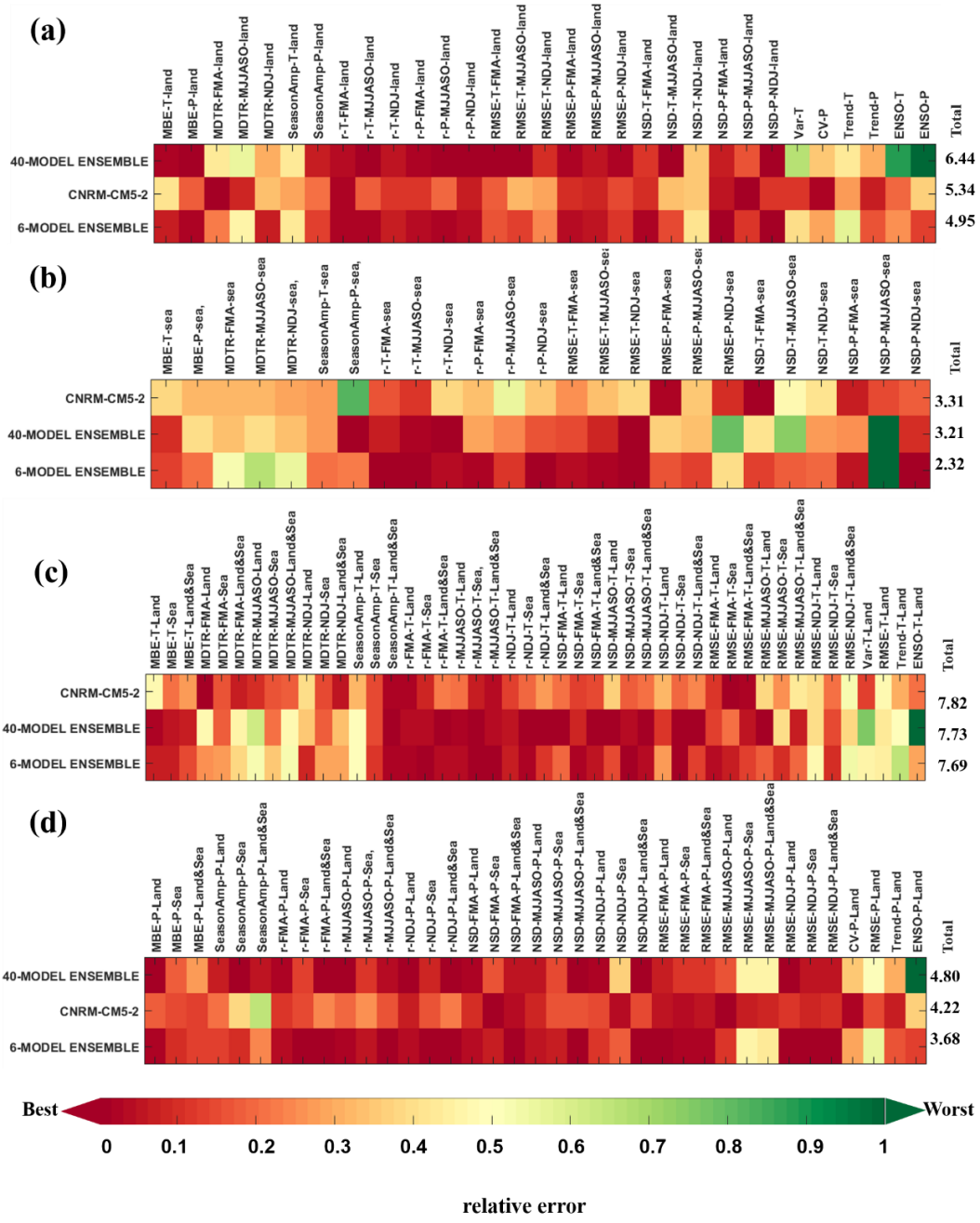

Figure 4.12 Relative error of performance metrics considered (a) land only and (b) sea only (c) temperature, and (d) precipitation for CNRM-CM5-2, 6-MODEL ENSEMBLE, and 40-MODEL ENSEMBLE (vertical ordinate).

4.2 Evaluation of CMIP6 GCMs in Thailand

4.2.1 Temperature simulation for a near-term period of 13 CMIP6 GCMs and 13-MODEL ENSEMBLE.

4.2.1.1 Mean (MA)

The first performance metric for evaluating GCMs is MA. It is used to illustrate the difference in spatial temperature by comparing model outputs and mean reference data. For finding the best GCM, there is the overall temperature closer to mean reference data. Figure 4.13 shows the spatial annual temperature for mean reference data, 13-MODEL ENSEMBLE, and the individual 13 GCMs. Numbers in each sub-image are an average of spatial annual temperature of each GCM. Spatially, all GCMs have the temperature gradient in the same direction with a low temperature in the north of Thailand (especially over high mountains) and a high temperature in the south of Thailand. The mean temperature of 13 CMIP6 GCMs range from 26.22 °C to 29.06 °C. The simulation result evaluated by MA shows that GFDL-CM4 is very similar to mean reference data; the difference is only 0.07 °C, whereas the mean temperature of MIROC6 performs worst in terms both of magnitude and shape that is very different from the mean reference data. The temperature simulation of MIROC6 is 2.77 °C higher than the mean reference data.

MA was used to assess CMIP5 GCMs over Lower Mekong Basin (Ruan et al. 2019) and eastern Tibetan Plateau (Su et al. 2013) during 2 periods (i.e., 1961 - 2004 and 1961-2005. GCM from NOAA-GFDL in this study shows the best performance in MA, but it was not good to perform in Ruan et al. (2019) and Su et al. (2013). Since GFDL-CM3 of their performance was ranked in the worst-performing model group. GFDL-CM3 was ranked 23 out of 34 models and 20 out of 24 models in Ruan et al. (2019) and Su et al. (2013), respectively (Table 4.3). Thus, the ranking results of both studies demonstrate that GFDL-CM3 is not an adequate ability to simulate the mean annual temperature over the tropical and subtropical zone.

The performance comparisons of temperature simulation between GFDL-CM3 in CMIP5 of Ruan et al. (2019) and Su et al. (2013) and GFDL-CM4 in CMIP6 of this study, we find that is very different, although the study area of

Ruan et al. (2019) is a part of this study. MA shows that the performance of GFDL-CM4 in this study can simulate better than the previous version in CMIP5, especially for simulation over the tropical zone. The ability of GFDL-CM4 is a significant increase that may be caused by installing a new version of the physical climate model along with spatial resolution higher than double in GFDL-CM3 (res. 2.5° × 2°) (Held et al 2019). We believe that these updates were a key factor because GFDL-CM4 can express higher efficiency than the previous version. Hence, the assessment for a similar area of this study and Ruan et al. (2019) reveals different results between GFDL-CM3 and GFDL-CM4

When considering the ranking of GCM from MIROC institution (the worst performance in MA), we find that the model ranking results of Ruan et al. (2019) and Su et al. (2013) are different to this study because MIROC5 of Ruan et al. (2019) and Su et al. (2013) was ranked 7 out of 34 models and 8 out of 24 models, respectively (Table 4.4). Thus, MIROC5 in CMIP5 was the well-performing model group for temperature simulation. On the other hand, MIROC6 performance which is the latest version from the MIROC institution under the CMIP6 project shows the worst performance in this study. Although MIROC6 has already determined new physical parameterizations in sub-modules (Tatebe et al. 2019), it has the lowest ranking score in this work. In addition, the horizontal resolution of MIROC6 is not higher than the previous version in CMIP5. Tatebe et al. (2019) reported that increasing the horizontal resolution of the model means that also increases computational cost; however, many GCMs in CMIP6 were developed in this part (Held et al. 2019; Séférian et al. 2019; Boucher et al. 2020; Grise and Davis 2020).

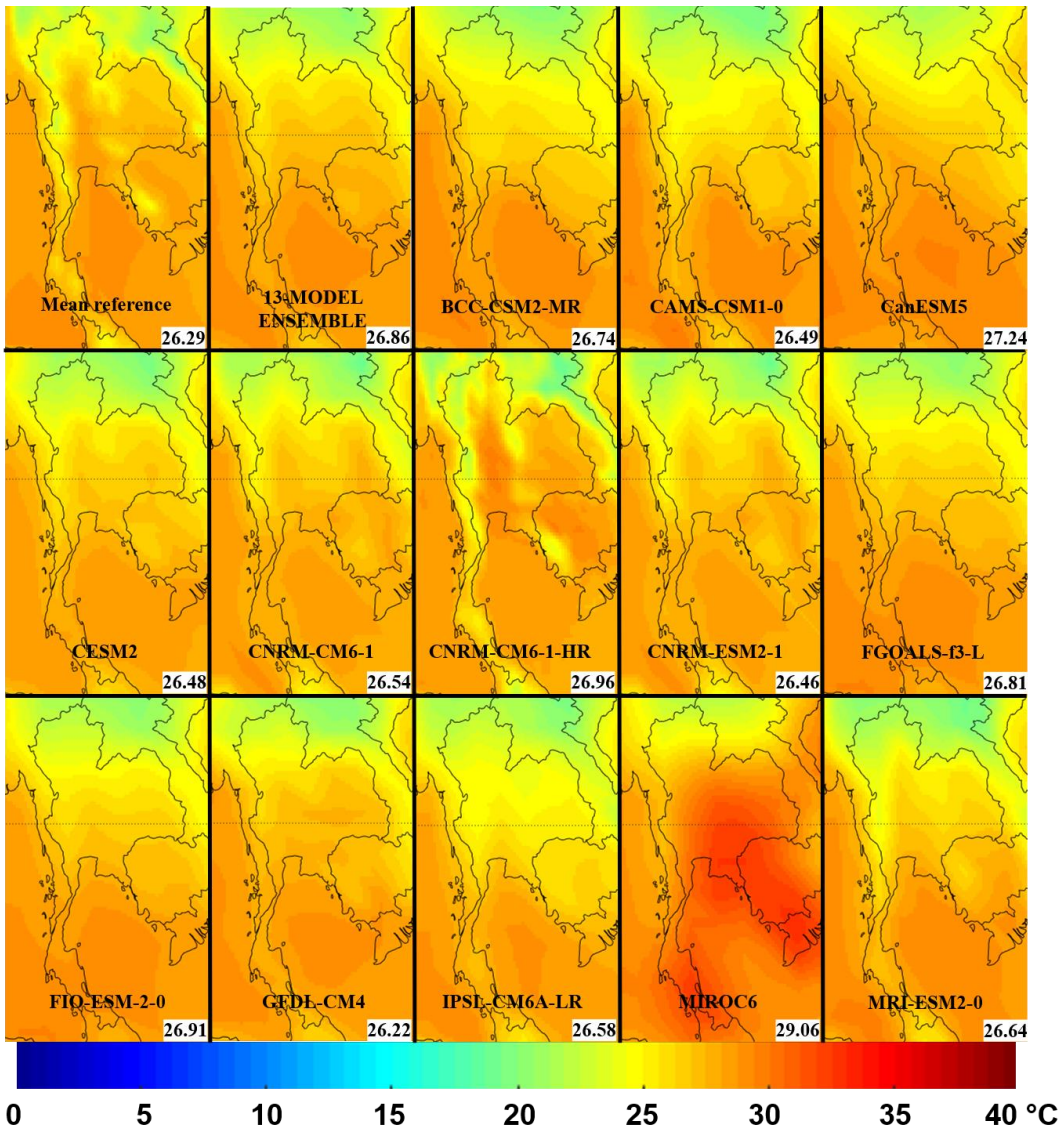

Figure 4.13 Mean annual temperature (MA) (°C) for years 2000-2014 of mean observations, 13-MODEL ENSEMBLE, and 13 GCMs. Numbers at the bottom-right of each dataset are the averaged MA values for all pixels.

Table 4.3 Ranking measures of best performance assessment of Former GCMs

Metrics	Model with the best performance	Former studies				
	CMIP6 & Institution	Reference	Variable	Year	Area	CMIP & Rank
MA	GFDL-CM4 (NOAA GFDL)	Ruan et al. 2019	annual temperature	1961-2004	Lower Mekong Basin	GFDL-CM3(23/34)
		Su et al. 2013	annual temperature	1961-2005	eastern Tibetan Plateau	GFDL-CM3(20/24)
MBE	GFDL-CM4 (NOAA GFDL)	Rupp et al. 2013	annual temperature	1960-1999	Pacific Northwest USA	GFDL-CM3(20/41)
		Miao et al. 2014	annual temperature	1901-2005	northern Eurasia	GFDL-CM3(3/24)
		Xuan et al. 2017	annual maximum temperature	1971-2000	Zhejiang Province in China	GFDL-CM3(18/18)
			annual minimum temperature	1971-2000	Zhejiang Province in China	GFDL-CM3(17/18)
		Miao et al. 2014	monthly temperature	1901-2005	northeastern Argentina	GFDL-CM3(15/25)
		Su et al. 2013	annual temperature	1901-2005	eastern Tibetan Plateau	GFDL-CM3(20/24)
SeaSonAmp	CNRM-CM6-1-HR (CNRM-CERFACS)	Rupp et al. 2013	annual temperature	1960-1999	Pacific Northwest USA	CNRM-CM5(11/41) CNRM-CM5-2 (13/41)
r	CNRM-CM6-1 CNRM-CM6-1-HR CNRM-ESM2-1 (CNRM-CERFACS)	Ruan et al. 2019	annual temperature	1961-2004	Lower Mekong Basin	CNRM-CM5 (23/34)
		Zhou and Yu 2006	annual temperature	1880-1999	Global Northern Hemispheric China	CNRM-CM3*(9/19) CNRM-CM3*(9/19) CNRM-CM3*(3/19)
		Xu et al. 2017	annual temperature	1979–2005	Tibetan Plateau	CNRM-CM5 (1/14)

Table 4.3 Ranking measures of best performance assessment of Former GCMs (Continued)

Metrics	Model with the best performance	Former studies				
	CMIP6 & Institution	Reference	Variable	Year	Area	CMIP & Rank
RMSE	CNRM-ESM21 (CNRM-CERFACS)	Miao et al. 2014	monthly temperature	1901-2005	northeastern Argentina	CNRM-CM5-2 (10/25)
		Ruan et al. 2019	annual temperature	1961-2004	Lower Mekong Basin	CNRM-CM5 (6/34)
		Xuan et al. 2017	annual maximum temperature	1971-2000	Zhejiang Province in China	CNRM-CM5 (11/18)
			annual minimum temperature	1971-2000	Zhejiang Province in China	CNRM-CM5 (5/18)
		Grose et al. 2014	annual temperature	1980–1999	Pacific Ocean region	CNRM-CM5-1 (8/27)

Table 4.4 Ranking measures of worst performance assessment of Former GCMs

Metrics	Model with the best performance	Former studies				
	CMIP6 & Institution	Reference	Variable	Year	Area	CMIP & Rank
MA	MIROC6 (MIROC)	Ruan et al. 2019	annual temperature	1961-2004	Lower Mekong Basin	MIROC5 (7/34)
		Su et al. 2013	annual temperature	1961-2005	eastern Tibetan Plateau	MIROC5 (8/24)
MBE	MIROC6 (MIROC)	Rupp et al. 2013	annual temperature	1960-1999	Pacific Northwest USA	MIROC5 (22/41)
		Miao et al. 2014	annual temperature	1901-2005	northern Eurasia	MIROC5 (15/24)
		Xuan et al. 2017	annual maximum temperature	1971-2000	Zhejiang Province in China	MIROC5 (1/18)
			annual minimum temperature	1971-2000	Zhejiang Province in China	MIROC5 (10/18)

Table 4.4 Ranking measures of worst performance assessment of Former GCMs (Continued)

Metrics	Model with the best performance	Former studies				
	CMIP6 & Institution	Reference	Variable	Year	Area	CMIP & Rank
		Miao et al. 2014	monthly temperature	1901-2005	northeastern Argentina	MIROC5 (15/25)
		Su et al. 2013	annual temperature	1961-2005	eastern Tibetan Plateau	MIROC5 (8/24)
SeaSonAmp	FGOALS-f3-L (LASG-CESS)	Rupp et al. 2013	annual temperature	1960-1999	Pacific Northwest USA	FGOALS-s2 (41/41)
r	MIROC6 (MIROC)	Zhou and Yu 2006	annual temperature	1960-1999	Global Northern Hemispheric China	MIROC3.2*(10/19) MIROC3.2*(6/19) MIROC3.2*(6/19)
		Ruan et al. 2019	annual temperature	1961-2004	Lower Mekong Basin	MIROC5 (5/34)
		Xu et al. 2017	annual temperature	1979–2005	Tibetan Plateau	MIROC4h (6/14)
		Su et al. 2013	annual temperature	1961-2005	eastern Tibetan Plateau	MIROC5 (14/24)
RMSE	MIROC6 (MIROC)	Xuan et al. 2017	annual maximum temperature	1971-2000	Zhejiang Province in China	MIROC5 (2/18)
			annual minimum temperature	1971-2000	Zhejiang Province in China	MIROC5 (9/18)
		Miao et al. 2014	monthly temperature	1901-2005	northeastern Argentina	MIROC5 (8/25)
		Ruan et al. 2019	annual temperature	1961-2004	Lower Mekong Basin	MIROC5 (30/34)
		Su et al. 2013	annual temperature	1961-2005	eastern Tibetan Plateau	MIROC5 (9/24)
		Grose et al. 2014	annual temperature	1980–1999	Pacific Ocean region	MIRCO5 (13/27)

4.2.1.2 Mean bias error (MBE)

MBE is used to indicate the direction of temperature that models are overestimating (warm bias) or underestimate (cold bias). Figure 4.14 shows the spatial distribution of bias of the mean annual temperature over the study area for mean reference data, 13-MODEL ENSEMBLE, and the individual 13 GCMs. Numbers in each sub-image are a bias of spatial annual temperature of each simulation. The MBE value of 13 CMIP6 GCMs range from -0.07°C to 2.78°C and most of CMIP6 GCMs show higher overestimate of mean reference values, except for GFDL-CM4 that underestimates temperature with the mean bias at -0.07°C (or mean bias of -3.10 %); moreover, GFDL-CM4 is a GCM that has the lowest bias in this study when compares to the other GCMs. Almost all models show which the MBE value is range ±1 °C. Whereas, MIROC6 is the only GCM that shows MBE above 2 ° C, and it is the highest MBE value for this study. MIROC6 shows a positive direction (warm bias) that it covers over the study area with a mean bias of 31.50 %.

MBE is a statistic metric that is used to assess the temperature simulation of GCMs over several regions by previous studies, e.g, Pacific Northwest USA (Rupp et al. 2013), Northern Eurasia (Miao et al. 2014), Zhejiang Province in China (Xuan et al. 2017), northeastern Argentina (Lovino et al. 2018), eastern Tibetan Plateau (Su et al. 2013) (Table 4.3). The GCMs ranking by MBE, Miao et al. (2014) found that GFDL-CM3 in CMIP5 was a good performance for simulation; it was ranked 3 out of 24 models, while Kumar et al. (2013) and Lovino et al. (2018) found that it was moderate performance. In addition, Xuan et al. (2017) and Su et al. (2013) reported that GFDL-CM3 is a poor performing model for temperature variable simulation and it was also ranked group of worst performance models. These previous studies revealed interesting points that GFDL-CM3 could well simulate the temperature over the Temperate zone as well as the Polar zone. On the other hand, the performance of GFDL-CM3 is extremely decreased when it simulates over the tropical and subtropical zone. GFDL-CM3 in CMIP5 has a limit for simulating and the simulation result might be up for each area study.

NOAA GFDL who generating the GFDL-CM group has interested in the development of GFDL-CM4 for better simulation of temperature over

the Tropical zone (Held et al. 2019). Hence, GFDL-CM4 participating in the CMIP6 project can increase the performance for simulating the temperature over Thailand.

While previous models by MIROC institution (the worst performance in MBE), their performances were also found to differ from each region (Table 4.4). Rupp et al. (2013); Miao et al. (2014); Xuan et al. (2017); Ruan et al. (2019) and Su et al. (2013) reported that MIROC5 was good to moderate ranked by MBE. It had a very excellent ranking by Xuan et al. (2017) and Su et al. (2013).

We remarked that the study areas of well performance group in previous studies (GFDL-CM3 in Miao et al. (2014) and MIROC5 in Xuan et al. (2017) and Su et al. (2013)) was also located near to the development institution of both of GFDL-CM3 and MIROC5 which they are the institution of the United States and Japan, respectively. It might be that the physical parameters of these models were set to test the temperature simulation over the main development institution area.

Although CMIP6 models have improved their climate simulations compared to previous generations, they still have persistent biases and uncertainties, especially a warm bias over tropical regions (Kim et al. 2020). Arias et al. (2020) discovered that CMIP6 GCMs have limitations when simulating air surface temperatures in areas with complex topography. Looking at the temperature bias in Figure 4.14, almost all CMIP6 GCMs show a similar spatial pattern of their biases. The majority of the values for the bias in the study area were negative, although there were a few areas with a positive bias, with most of these positive biases being in the higher topography than the neighboring regions. In addition, values are influenced by the latitude of an area (Park et al. 2019). Temperaute are known to differ by latitude, with lower latitudes being warmer and higher latitudes being cooler. Thus, these factors explain why most GCMs simulate temperature in the same direction, as does a model with systematic bias. Hence, the overestimates and underestimates are also likely due to model deficiencies related to topographic parameters and geographic location factors.

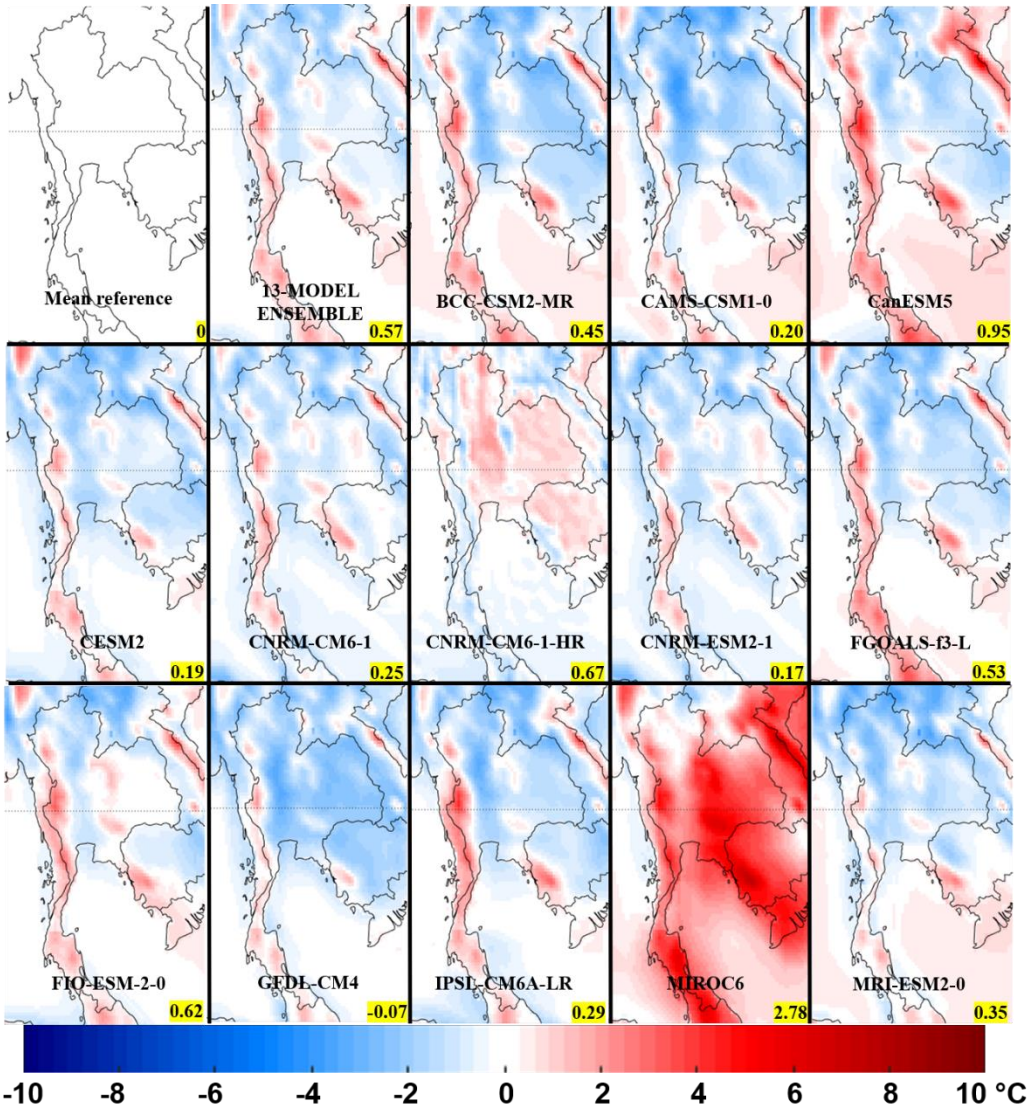

Figure 4.14 Spatial distribution of bias of the mean annual temperature (MBE in °C) for years 2000-2014 of 13-MODEL ENSEMBLE and 13 GCMs. Numbers at the bottom-right of each dataset are the averaged MBE values for all pixels.

4.2.1.3 Mean seasonal cycle amplitude (SeasonAmp)

Season-Amp is used to display the severity of temperature changes in each area of the study domain. Figure 4.15 shows the temperature gradient in the spatial pattern of all simulation that they range from -5°C to 15°C. Numbers in each sub-image are the changes in values of spatial annual temperature of each simulation. Out of the 13 GCMs, all show that the northern region of Thailand has more temperature changes than those in the southern region; these results are consistent with the reality of Thailand's climate (Tan and Pereira, 2010). This study finds that CNRM-CM6-1-HR is best able to simulate the mean temperature change as close to the mean reference data in terms of magnitude and it has a higher mean temperature change than the mean reference data only 0.1 ° C. Although CNRM-CM6-1-HR is the best GCM that can simulate the change of mean temperature in terms of magnitude (total of the area), it is not the best simulation in terms of shape. 13-GCM-ENSEMBLE is the best simulation that shows consistency with the mean reference data in terms of shape which clearly shows the northern region of the study area and the mean change value of this simulation has only 0.35 °C lower than the mean reference. FGOALS-f3-L generated by LAST-ACCESS institution is GCM that has the highest in the change value from the mean reference data, with the change value of 6.29°C; it has 2.45°C higher than the mean reference

The season-Amp metric is grouped in the highest confidence categories for CMIP5 ranking over Pacific Northwest USA by Rupp et al. (2013). They reported that multi-model simulation can simulate the severity of temperature change as close to the observed data, with temperature gradient as well as temperature change value of the multi-models within 1 °C. In addition, they found that CNRM-CM5 and CNRM-CM5-1 created by CNRM-CERFACS institutions were similarly ranked 11 and 13 out of 41 models, respectively. While FGOALS-s2 was found the worst performance for simulation the severity of temperature change. FGOALS-s2 was ranked 41 out of 41 models (lowest order) that their ranking has consistency with the ranking of this study because FGOALS-s2 of this study also ranks in the lowest order too. Although the latest model from the LASG-CESS institution participating CMIP6 has updated both the atmospheric model and oceanic model, FGOALS-f3-L

still perform worst to simulate the severity of temperature change when compares with the other GCMs, especially over the Thailand area (Guo et al. 2020).

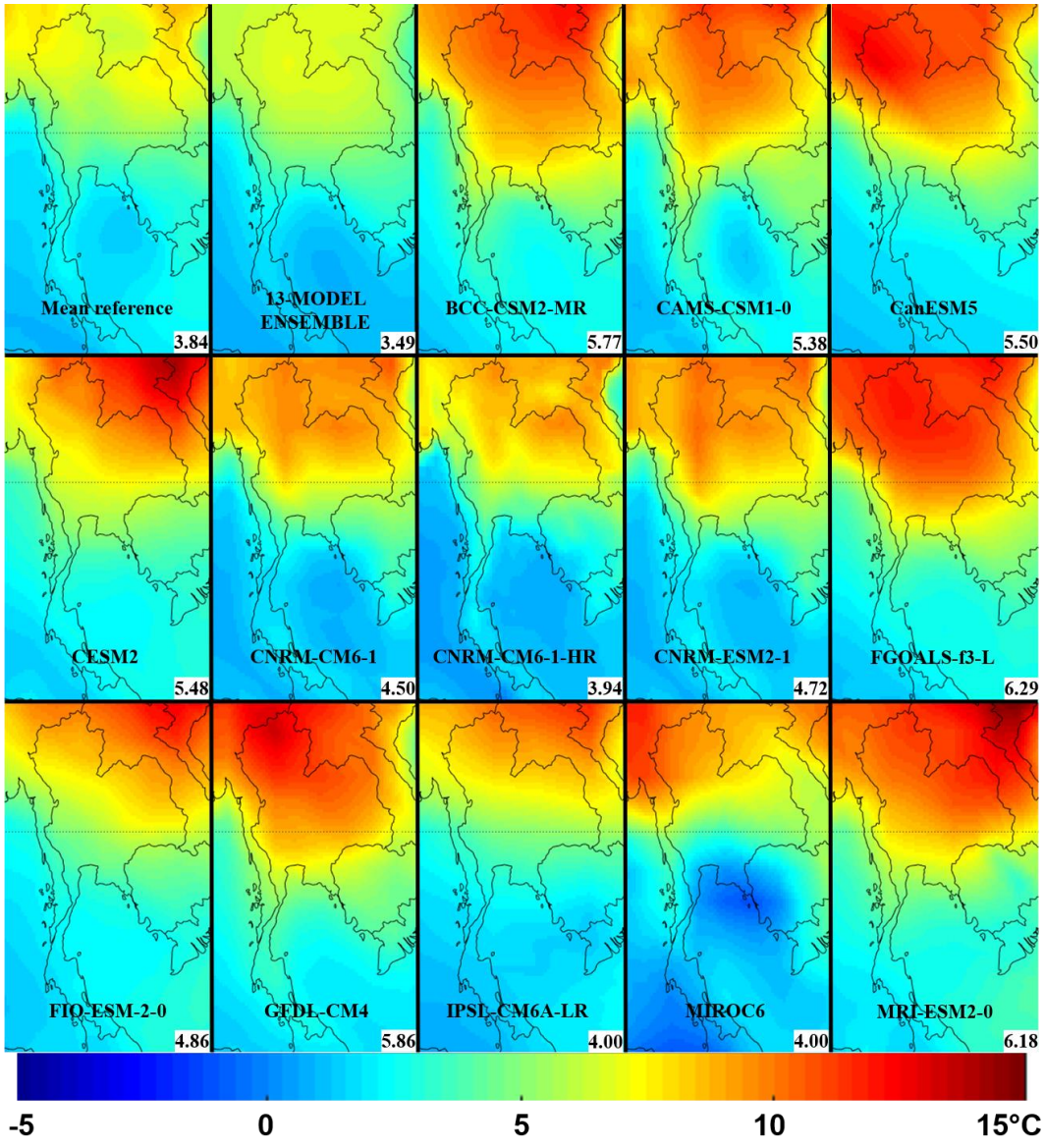

Figure 4.15 Comparisons of the mean seasonal cycle amplitudes of temperature (SeasonAmp) for years 2000-2014 of mean observations, 13-MODEL ENSEMBLE, and 13 GCMs. Numbers at the bottom-right of each dataset are the averaged SeansonAmp values for all pixels.

Table 4.5 r and RMSE between observations and model simulations of mean annual temperature for years 2000 2014. They are evaluated for land only, sea only, and both land & sea

Model		Land-only		Sea-only		land & sea	
		r	RMSE (°C)	r	RMSE (°C)	r	RMSE (°C)
1.	BCC-CSM2-MR	0.82	1.21	0.94	1.15	0.89	1.19
2.	CAMS-CSM1-0	0.87	1.15	0.92	1.09	0.91	1.13
3.	CanESM5	0.75**	1.51	0.83	1.34	0.84	1.44
4.	CESM2	0.91	0.90	0.94	0.62	0.94	0.80
5.	CNRM-CM6-1	0.94	0.75*	0.92	0.54	0.96*	0.67
6.	CNRM-CM6-1-HR	0.95*	1.07	0.87	0.76	0.95	0.95
7.	CNRM-ESM2-1	0.94	0.76	0.92	0.49*	0.96*	0.66*
8.	FGOALS-f3-L	0.85	1.16	0.89	1.10	0.91	1.13
9.	FIO-ESM-2-0	0.90	1.06	0.93	0.94	0.93	1.01
10.	GFDL-CM4	0.88	1.11	0.95	0.75	0.91	0.98
11.	IPSL-CM6A-LR	0.84	1.17	0.85	0.79	0.90	1.03
12.	MIROC6	0.82	3.63**	0.14**	2.45**	0.74**	3.19**
13.	MRI-ESM2-0	0.93	1.01	0.93	1.14	0.95	1.06
14.	13-MODEL ENSEMBLE	0.92	0.88	0.96*	0.95	0.95	0.91

* is the best value for each metrics' evaluations, while ** is the worst value for each metric's evaluations.

4.2.1.4 The correlation coefficient (r)

Table 4.5 shows r and RMSE values of mean temperature for the individual 13 GCMs and 13-MODEL ENSEMBLE that results of these metrics are computed for 3 study cases, including land-only, sea-only, and both land & sea.

r is used in this study for measuring the relationship level between model and reference data in each grid-cell. The correlation value in Table 4.5 shows that most GCMs have correlation values in the range of "good to very good", with correlation coefficients in the range of 0.70 to 0.95. Evaluation of CMIP6 GCMs by r found that three models from CNRM-CERFACS institution have the highest level of correlation between model and reference data. CNRM-CM6-1-HR is ranked as 1 for the land-only case, while CNRM-CM6-1 and CNRM-ESM2-1 are ranked as 1 for both land & sea case that presents the best correlation (r =0.96). For the sea-only case, 13-MODEL ENSEMBLE is a simulation that shows the best correlation level. However, only a model demonstrates correlation value as "unsatisfactory" for this study that is MIROC6, with the worst correlation (r =0.14).

Furthermore, the r metric was used to assess the performance of CMIP3 GCMs performance by Zhou and Yu (2006) and they found that CNRM-CM3 had a correlation value as "good to moderate". it was ranked 3 to simulate the temperature over the whole of China with a good correlation value, but it was ranked 9 out of 19 models over the Global and Northern Hemispheric, with a moderate correlation value (Table 4.3). Moreover, the r metric was used to assess the performance of CMIP5 GCMs performance over the Tibetan Plateau (Xu et al. 2017) and Lower Mekong Basin (Ruan et al. 2019). Xu et al. (2017) and Ruan et al. (2019) found that CNRM-CM5 created by CNRM-CERFACS institutions have correlations of 0.89 and 0.91, respectively that is in the range of "good". While Xu et al. (2017) showed that CNRM-CM5 performed best to simulate temperature and it was ranked 1. Although CNRM-CM5 by Ruan et al. (2019) had a high correlation value of 0.91, considering in terms of ranking found it was ranked 23 out of 34 models. Hence, in terms of ranking the performance of temperature simulation of the previous study above found that the performance of GCMs created by CNRM-CERFACS under both CMIP3 and CMIP5 projects might depend on the study area. Moreover, previous versions of CNRM performed well over subtropical and temperate zone but the Lower

Mekong Basin where it locates in the tropical zone and being a part of this study area was performing not well. In this study, CNRM-CM6-1, CNRM-CM6-1-HR, and CNRM-ESM2-1 in CMIP6 are listed as the three highest-ranked performance by r metric. Séférian et al. (2019) and Voldoire et al. (2019) reported that CNRM-family participating CMIP6 project had a more updated atmosphere and land surface components. This update of CNRM-family may up the simulation performance over Thailand.

A previous version of MIROC model under CMIP3 and CMIP5 in former studies showed quite a satisfactory ranking for Tibetan Plateau (Xu et al. 2017), Global, Northern Hemispheric, China (Zhou and Yu 2006), and eastern Tibetan Plateau (Su et al. 2013); moreover, MIROC5 in CMIP5 was outstanding ranking in Lower Mekong Basin (Ruan et al. 2019) and it was ranked 5 out of 34 models (Table 4.4).

For this study, the result of the r metric of MIROC6 performs worst for the sea-only case and both land &sea, along with second-worst for land. A major factor may be due to the design of MIROC6 that is still Atmosphere General Circulation Model (AGCMs), while MIROC5 in CMIP5 project is Coupled Atmosphere-Ocean General Circulation Model (AOGCMs). This difference may be the reason that climate simulation in MIROC5 is better than in MIROC6; however, AOGCMs have disadvantages that are using datasets and time to calculate more than AGCMs (Tatebe et al. 2019). Hence, MIROC6 may be a poorer performance from the previous version when compare with other GCMs.

4.2.1.5 Root mean squared error (RMSE)

RMSE is used to compare between GCMS and reference data for showing the magnitude of the different error of each grid-cell. RMSE value closer to 0 indicates that the model has a very accurate simulation. The evaluation of GCMs by RMSE for 3 study reveals that 12 of 13 CMIP6 GCMs show the magnitude of overall error less than 2 ° C. Two GCMs with the lowest error were CNRM-ESM2-1 and CNRM-CM6-1 which the magnitudes of the error are less than 1 °C. CNRM-ESM2-1 performs best for sea-only case and both land & sea case, with RMSE of 0.49 °C and 0.66 °C, respectively, while CNRM-CM6-1 performs best for the land-

only case, with RMSE of 0.75 °C (Table. 5). In contrast, GCMs that shows magnitudes of the highest error is MIROC6, with RMSE higher than 2°C.

GCMs ranking of Ruan et al. (2019) and Grose et al. (2014) by RMSE showed that CNRM-CM5 can perform on great over Lower Mekong Basin and Pacific Ocean region, with were ranked 6 out of 34 models and 8 out of 27 models, respectively, whereas Lovino et al. (2018) and Xuan et al. (2017) found that GCMs from CNRM-CERFACS institution performed well to moderate for temperature simulation. The evaluation of GCMs by RMSE by these former studies showed that the CNRM-CM family of models was found to be the GCM with good performance groups for simulating temperature over the tropical zone and moderate performance groups over the subtropical zone. Moreover, this study is confirmed that the 3 newly of GCMs generated by CNRM institution under the CMIP6 project have more development because they can be as ranking as 1 by SeasonAmp, r, and RMSE.

This study confirms that three GCMs generated by the CNRM institution under the CMIP6 project have high development because their ranking can climb up to1 when evaluate by SeasonAmp, r, and RMSE.

MIROC5 performed quite poorly for simulating over Lower Mekong Basin that it was ranked 30 out of 34 models, reported by Ruan et al. (2019). However, MIROC5 can perform satisfactorily that was ranked moderate ranking over northeastern Argentina (Lovino et al. 2018) and eastern Tibetan Plateau (Su et al. 2013), while MIROC5 by Xuan et al. (2017) perform second best for annual maximum temperature over Zhejiang Province in China. Therefore, the evaluation of GCMs with RMSE of previous studies and in this study can indicate that the MIROC6 may not be suitable for simulating temperature over the Tropical zone.

The different performance of GCMs may depend on spatial resolution; besides, the performance of GCMs may depend on the areas where GCMs developer interest and lead to determine parametrizations of components of the climate system. These are just some of the remarkable point that found in this study; however, to find the reason to make the better or worse performance of GCMs, they still need to study more.

4.2.2 CMIP6 GCMs ranking by different categories.

Figure 4.16 (a)-(c) show relative errors for all performance metrics of land-only cases, sea-only cases, and both land & sea cases, respectively. The GCMs and 13-MODEL ENSEMBLE are listed on the left of each sub-figure, while the total relative error is listed on the right of the sub-figure. The color scale shows relative error values that indicate the performance of GCMs; if darker blue indicates that GCM performs well for that metrics, whereas darker orange indicates that GCM performs poorly for that metrics. Therefore, the total relative error is the sum of relative errors from all metrics; hence, the less total relative error value means that the simulation of GCM is very closer to observations.

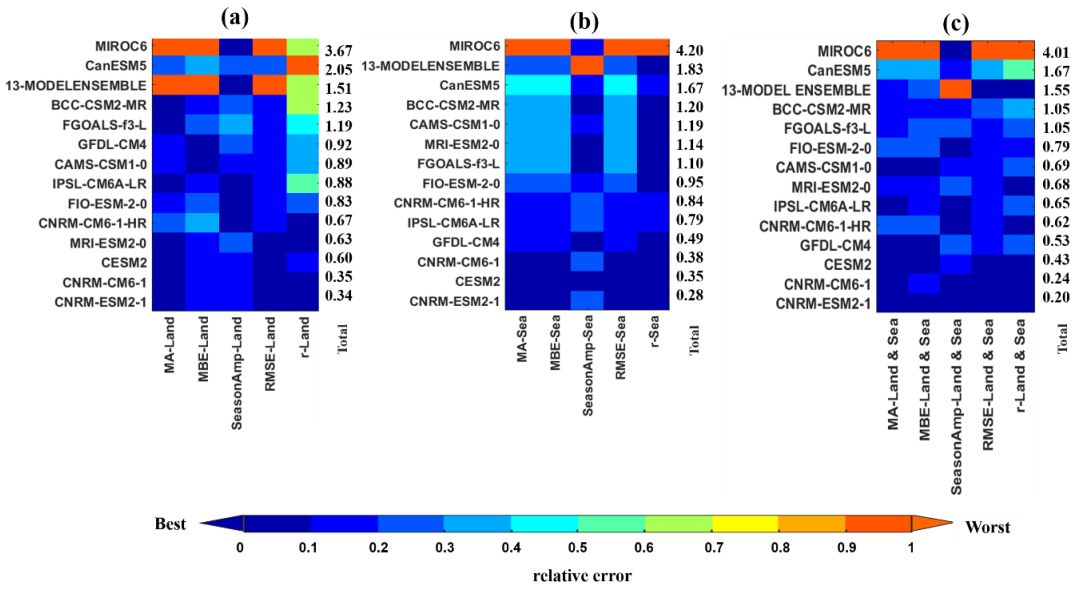

Figure 4.16 Relative error metrics of temperature variable for all performance metrics (horizontal ordinate) for each CMIPs models and model ensemble mean (vertical ordinate) for (a) land-only, (b) sea- only, and (c) both land & sea. The last column is the total score of relative error over 5 performance metrics

The GCMs are in order of highest to lowest total relative error from top to bottom, respectively. The evaluation of GCMs by 5 performance metrics shows that CNRM-ESM2-1 is the best GCM for evaluating all study cases, where their total relative errors are 0.34, 0.28, and 0.20 for land-only, sea-only, and both land & sea

cases. Besides, Figure 4.16 shows that the CNRM group performs satisfactorily for simulating temperature over Thailand because they are a high ranked for all study cases. The result of the CNRM group of this study is consistent with the CNRM-CM5 evaluation results over Northwest USA of Rupp et al. 2013 and CNRM-CM5-2 over Southeast Asia Kamworapan and Surussawadee (2019). On the other hand, MIROC6 performs worst for all study cases.

The physical core of both CNRM-ESM2-1 and CNRM-CM6-1 are similar but CNRM-ESM2-1 add more Earth system component, including carbon cycle of land and sea, aerosol, and atmosphere chemistry; moreover, CNRM-ESM2-1 is an improvement in Interaction Soil-Biosphere Atmosphere (ISBA) (Séférian et al. 2019). These additions could be a key reason that CNRM-ESM2-1 has better performance than CNRM-CM6-1 and CNRM-CM6-1-HR as well as other models to simulate temperature over Thailand.

CHAPTER 5
CONCLUSION

The first part evaluates the performance of 40 CMIP5 GCMs for simulating temperature and precipitation over Southeast Asia for the 1960-1999 (short-term period) and 1901-1999 (for a long-term period). Ground-based products (UD v.3.01 and CRU TS3.10.01) and reanalysis products (NCEP and ERA40) are used to evaluate the CMIP5 GCMs. GCMs ranking in this study is calculated by the sum of relative errors from nineteen performance metrics. Overall, model ranking by total relative error shows that CNRM-CN5-2 is the best performance model for simulating temperature and precipitation over Southeast Asia with the minimum total error and followed by CNRM-CM5, BNU-ESM, CESM-CAM5, and CCSM4, respectively. Since the multi-model ensemble approach could reduce the deficiency and improve performance, the top 6 GCMs (6-MODEL ENSEMBLE) and all of 40 GCMs (40-MODEL ENSEMBLE) are averaged to compare with individual GCMs.

When the performances of CNRM-CM5-2, 6-MODEL ENSEMBLE, and 40-MODEL ENSEMBLE are ranked by all performance metrics, 6-MODEL ENSEMBLE is the best performance model, while CNRM-CM5-2 and 40-MODEL ENSEMBLE is the second-best model and third-best model, respectively. In addition, the performance of CNRM-CM5-2, 6-MODEL ENSEMBLE, and 40-MODEL ENSEMBLE is considered by different categories. 6-MODEL ENSEMBLE is the only model that performs best for all categories (land only, sea only, the temperature only, and precipitation only categories). When the mean reference, CNRM-CM5-2, 6-MODEL ENSEMBLE, and 40-MODEL ENSEMBLE are detailed compared by each performance metric. CNRM-CM5-2 performs best for MBE-P, MDTR for all seasons, NSD-T-FMA, Var, CV, RMSE-P, Trend-T, Trend-P, ENSO-T, ENSO-P. While 6-MODEL ENSEMBLE performs best for r-T for all seasons, r-P for all seasons, RMSE-P for all seasons, NSD-P-FMA, NSD-P-NDJ. 40-MODEL ENSEMBLE performs best for MBE-T, SeasonAmp-T, SeasonAmp-P, r-T-MJJASO, r-T-NDJ, r-P-NDJ, RMSE-T for all seasons, NSD-T-MJJASO, NSD-T-NDJ, RMSE-T.

6-MODEL ENSEMBLE and CNRM-CM5-2 are the two best models to simulate the temperature and precipitation over Southeast Asia. This result proves the effectiveness of both by performance metrics that covers the spatial field, the measure of temporal variability, and representation of the common model of variability temporal and spatial pattern. Moreover, they can perform well to study the separately different categories like the temperature only, precipitation only, land only, and sea only categories. However, choosing between 6-MODEL ENSEMBLE and CNRM-CM5-2 are dependent on the conditions about time and computational resource because 6-MODEL ENSEMBLE requires more time and space 6 times more than CNRM-CM5-2.

The second part evaluates the performance of 13 CMIP6 GCMs for simulating temperature over Thailand for the 15 years of 2000-2014 (near-term). Ground-based products (UD v 5.01 and CRU TS v. 4.02) and reanalysis products (MERRA and ERA-interim) are used to evaluate the CMIP6 GCMs. GCMs ranking in this study is calculated by the sum of relative errors from five performance metrics. Most CMIP6 GCMs (except MIROC6) are able to simulate temperature over Thailand. However, CMIP6 GCMs (except GFDL-CM3) tend to overestimate (positive direction). The gap between the highest and lowest temperature of GCMs were higher compared to those of reference data, especially in the north part of Thailand. 12 out of 13 models (except MIROC6) provide the high accuracy results compared to reference data. RMSE values show that almost all GCMs have similar performance, except MIROC6. The evaluation of 13 CMIP6 GCMs by 5 performance metrics indicated that GFDL-CM4 and CNRM group participating under the CMIP6 project are the best performances. In particular, GFDL-CM4 is first ranked by MA and MBE, while the CNRM group is first ranked by SeasonAmp, r, and RMSE. On the other hand, MIROC6 performs worst for almost all performance (except for SeasonAmp, MIROC6 is third-ranked out of 13 models). In summary, model ranking by total relative error shows that CNRM-ESM2-1 is the best performance model and followed by CNRM-CM6-1, CESM2, GFDL-CM4, and CNRM-CM6-1-HR, respectively, where MIROC6 is the worst performance model.

Hence, the second part reveals that CNRM-ESM2-1 are the best models to simulate the temperature over Thailand. This result confirms that GCM from the

CNRM center (the best GCM at the regional level) is also the best GCM to simulate temperature at the country level. In addition, it proves additional Earth system component of the CNRM-ESM2-1 in CMIP6 has higher performance than other GCMs. Although performance metrics using this part are not complex evaluation, this result is still the best choice to study temperature in Thailand.

The results of this dissertation are beneficial to climate scientists who study climate in regionalization. Input datasets from the best GCMs of this study could be downscaled with finer spatial resolution over the Southeast Asia and Thailand area for simulating the other climate variables (i.e., example, temperature, precipitation, wind), and projections of future climate. In addition, the evaluation of GCM in this study provides the important supportive information to select suitable GCM using the future scenarios of that GCM for climate projection in the future over Southeast Asia and Thailand.

For future work, this study could be extended to 1) cover other areas in Southeast Asia, 2) include other latest CMI6 GCMs releases, and 3) the future scenario of the best CMIP6 GCM will be used for climate projection over Thailand. Because Thailand is just a part of Southeast Asia, it cannot confirm that GCM performing the best evaluated by this study will also perform well in other areas in Southeast Asia. Also, CMI6 GCMs are currently more releasing. Therefore, evaluations of other CMIP6 GCMs (new GCMs) in other countries are necessary to examine the result that if the best GCM at the regional level can also perform best at the country-level.

REFERENCES

Agyekum, J., Annor, T., Lamptey, B., Quansah, E., and Agyeman, R.Y.K. (2018) "Evaluation of CMIP5 global climate models over the Volta Basin: precipitation." *Adv. Clim. Chang. Res.*, 2018,1–24.

Ahmadalipour, A., Rana, A., Moradkhani, H. and Sharma, A. (2017). "Multi-criteria evaluation of CMIP5 GCMs for climate change impact analysis." *Theor. Appl. Climatol.*, 128, 71–87.

Almazroui, M., Saeed, F., Saeed, S., Islam, M., Ismail, M., Kluste, N.A.B., and Siddiqui, M. (2020). "Projected Change in Temperature and Precipitation over Africa from CMIP6." *Environ. Earth Sci*, 4, 455-475.

Ahmed, K., Sachindra, D. A., Shahid, S., Demirel, M. C., and Chung, E. S. (2018). "Selection of multi-model ensemble of GCMs for the simulation of precipitation based on spatial assessment metrics." Hydrol. Earth Syst. Sci. Discuss., 1-35.

Ahmed, K., Sachindra, D. A., Shahid, S., Demirel, M. C., and Chung, E. S. (2019). "Selection of multi-model ensemble of general circulation models for the simulation of precipitation and maximum and minimum temperature based on spatial assessment metrics." Hydrol. Earth Syst. Sci., 23, 4803-4824.

Ahmed, K., Sachindra, D. A., Shahid, S., Iqbal, Z., Nawaz, N., and Khan, N. (2020). "Multi-model ensemble predictions of precipitation and temperature using machine learning algorithms." Atmos. Res., 236, 1–20.

Arias, P. A., Ortega, G., Villegas, L. D., and Martínez, J. A., (2021). "Colombian climatology in CMIP5/CMIP6 models: persistent biases and improvements." Revista Facultad De Ingeniería Universidad De Antioquia, 100, 75-96.

Bae, D. H., Koike, T., Awan, J. A., Lee, M. H., and Sohn, K. H. (2015). "Climate change impact assessment on water resources and susceptible zones identification in the Asian monsoon region." Water Resour Manage., 29, 5377–5393.

Balsamo, G., Albergel, C., Beljaars, A., Boussetta, S., Brun, E., Cloke, H., Dee, D., Dutra, E., Muñoz-Sabater, J., Pappenberger, F.,de Rosnay, P., Stockdale,T., and Vitart, F. (2015). "ERA-Interim/Land: a global land surface reanalysis data set." *Hydrol. Earth Syst. Sci.,* 19, 389-407.

Bannister, D., Herzog, M., Graf, H-F., Hosking, J.S., and Short, C.A. (2017) "An Assessment of Recent and Future Temperature Change over the Sichuan Basin, China, Using CMIP5 Climate Models." *J. Clim.,* 30, 6701–6722.

Bao, Y., Song, Z., and Qiao, F. (2020). "FIO-ESM version 2.0: Model description and evaluation." *J. Geophys. Res.*, 125, e2019JC016036.

Bauer, B., McKenzie, S., Menalled, F., Mangold, J., and Peders, G. (2016). "Climate Science 101 for Montana." *Montana State University Extension* ,11,1-4.

Bentsen, M., Bethke, I., Debernard, J.B., Iversen, T.; Kirkevåg, A., Seland, Ø.; Drange, H., Roelandt, C., Seierstad, I.A., Hoose, C., and Kristjánsson, J. E. (2012). "The Norwegian earth system model, NorESM1-M. Part 1: Description and basic evaluation." *Geosci. Model Dev. Discuss.,* 5, 2843–2931.

Berrisford, P., Kallberg, P., Kobayashi, S., Dee, D., Uppala, S., Simmons, A. J., Poli, P., and Sato, H. (2011). "Atmospheric conservation properties in ERA-Interim." *Q. J. R. Meteorol. Soc.,* 137, 1381–1399.

Bitz, C. M., and Marshall, S .J. (2012). "Cryosphere Models :Ocean and Land in the Encyclopedia of Sustainability Science and Technology." *Climate Change Modeling and Methodology*, 31-62.

Bock, L., Lauer, A., Schlund, M., Barreiro, M., Bellouin, N., Jones, C., Meehl, G. A., Predoi, V., Roberts, M. J., and Eyring, V. (2020). "Quantifying progress across different CMIP phases with the ESMValTool." *J. Geophys. Res. Atmos.*, 125, e2019JD032321.

Bosilovich, M., Akella, S., Coy, L., Cullather, R., Draper, C., Gelaro, R., Kovach, R., Liu, Q., Molod, A., Norris, P., Wargan, K., Chao, W., Reichle, R., Takacs, L., Vikhliaev, Y., Bloom, S., Collow, A., Firth, S., Labow, G., Partyka, G., Pawson, S., Reale, O., Schubert, S. D., and Suarez, M. (2015). *Merra-2: Initial*

evaluation of the climate. Technical Report Series on Global Modeling and Data Assimilation NASA/TM2015-104606/Vol. 43. NASA: GSFCG. <https://gmao.gsfc.nasa.gov/pubs/docs/Bosilovich803.pdf.> (Apr. 5,2020).

Boucher, O., Servonnat, J., Albright, A. L., Aumont, O., Balkanski, Y., Bastrikov, V., Bekki, S., Bonnet, R., Bony, S., Bopp, L., Braconnot, P., Brockmann, P., Cadule, P., Caubel, A., Cheruy, F., Cozic, A., Cugnet, D., D'Andrea, F., Davini, P., de Lavergne, C., Denvil, S., Deshayes, J., Devilliers, M., Ducharne, A., Dufresne, J.-L., Dupont, E., Éthé, C., Fairhead, L., Falletti, L., Foujols, M.-A., Gardoll, S., Gastineau, G., Ghattas, J., Grandpeix, J.-Y., Guenet, B., Guez, L., Guilyardi, E., Guimberteau, M., Hauglustaine, D., Hourdin, F., Idelkadi, A., Joussaume, S., Kageyama, M., Khodri, M., Krinner, G., Lebas, N., Levavasseur, G., Lévy, C., Li, L., Lott, F., Lurton, T., Luyssaert, S., Madec, G., Madeleine, J.-B., Maignan, F., Marchand, M., Marti, O., Mellul, L., Meurdesoif, Y., Mignot, J., Musat, I., Ottlé, C., Peylin, P., Planton, Y., Polcher, J., Rio, C., Rousset, C., Sepulchre, P., Sima, A., Swingedouw, D., Thiéblemont, R., Traoré, A.-K., Vancoppenolle, M., Vial, J., Vialard, J., Viovy, N., and Vuichard, N. (2020). “Presentation and evaluation of the IPSL-CM6A-LR climate model.” *J. Adv. Model. Earth Syst.*, 12, e2019MS002010.

Centre for Environmental Data Analysis. (2010). "CRU TS v. 3.10.01." <http://data.ceda.ac.uk//badc/cru/data/cru_ts/> (Jun. 5, 2014).

Centre for Environmental Data Analysis. (2018). "CRU TS v. 3.10.01." <http://data.ceda.ac.uk//badc/cru/data/cru_ts/> (April. 16, 2020).

Chhin, R., and Yoden, S. (2018). “Ranking CMIP5 GCMs for model ensemble selection on regional scale: case study of the Indochina Region.” J. Geophys. Res. Atmos., 123, 8949-8974.

Collins, M., Tett, S. F. B., and Cooper, C. (2001) “The internal climate variability of HadCM3, a version of the Hadley Centre coupled model without flux adjustments.” *Clim. Dyn.*, 17, 61–81.

Crespo, L.R., Keenlyside, N., and Koseki, S. (2019). "The role of sea surface temperature in the atmospheric seasonal cycle of the equatorial Atlantic." *Clim. Dyn,* 52, 5927-5946.

Cubasch, U., Wuebbles, D., Chen, D., Facchini, M.C., Frame, D., Mahowald, N., and Winther, J.-G. (2013). *Introduction. In: Climate Change 2013: The Physical Science Basis. Contribution of Working Group I to the Fifth Assessment Report of the Intergovernmental Panel on Climate Change* [Stocker, T.F., D. Qin, G.-K. Plattner, M. Tignor, S.K. Allen, J. Boschung, A. Nauels, Y. Xia, V. Bex and P.M. Midgley (eds.)]. Cambridge University Press, Cambridge, United Kingdom and New York, NY, USA.

Danabasoglu, G., Lamarque, J.-F., Bacmeister, J., Bailey, D. A., DuVivier, A. K., Edwards, J., Emmons, L. K., Fasullo, J., Garcia, R., Gettelman, A., Hannay, C., Holland, M. M., Large, W. G., Lauritzen, P. H., Lawrence, D. M., Lenaerts, J. T. M., Lindsay, K., Lipscomb, W. H., Mills, M. J., Neale, R., Oleson, K. W., Otto-Bliesner, B., Phillips, A. S., Sacks, W., Tilmes, S., van Kampenhout, L., Vertenstein, M., Bertini, A., Dennis, J., Deser, C., Fischer, C., Fox-Kemper, B., Kay, J. E., Kinnison, D., Kushner, P. J., Larson, V. E., Long, M. C., Mickelson, S., Moore, J. K., Nienhouse, E., Polvani, L., Rasch, P. J., and Strand, W. G. (2020). "The Community Earth System Model Version 2 (CESM2)." *J. Adv. Model. Earth Syst.*, 12(2), e2019MS001916.

Dasgupta, S., and Meisner, C. (2009). "Climate change and sea level rise :A review of the scientific evidence." *Environment Department of the World Bank*, 118**,**1-28.

De Bono, A., Peduzzi, P., Kluser, S., and Giuliani, G. (2004). "Impacts of summer 2003 heat wave in Europe. " *UNEP/DEWA/GRID-EuropeEnvironment Alert Bulletin*, 2**,** 1 –4.

Decker, M., Brunke, M.A., Wang, Z., Sakaguchi, K2, Zeng. X.B., and Bosilovich, M.G. (2012) "Evaluation of the reanalysis products from GSFC, NCEP, and ECMWF using flux tower observations." *J. Clim.*, 25(6), 1916–1944.

Dee, D. P., Uppala, S.M., Simmons, A.J., Berrisford,P., Poli, P., Kobayashi, S., Andrae, U., Balmaseda, M.A., Balsamo, G., Bauer, P., Bechtold, P., Beljaars,M.C.M., Van de Berg, L., Bidlot, J., Bormann,N. Delsol, C., Dragani, R., Fuentes,M ., Geer, A.J., Haimberger, L., Healy, S.B., Hersbach, H ., Hólm, E.V., Isaksen, L., Kållberg, P., Köhler, M., Matricardi, M., McNally, A. P., Monge-Sanz, B.M., Morcrette, J. J., Park, B. K., Peubey, C., Rosnay, P. De., Tavolato, C., Thépaut, J. N., and Vitart, F., (2011). "The ERA-Interim reanalysis: Configuration and performance of the data assimilation system." *Q. J. R. Meteorol. Soc.*, 137, 553-597.

Dufresne, J.-L., Foujols, M.-A., Denvil, S., Caubel, A., Marti, O., Aumont, O., Balkanski, Y., Bekki, S., Bellenger, H., Benshila, R., Bony, S., Bopp, L., Braconnot, P. =,Brockmann, P., Cadule, P., Cheruy, F., Codron, F., Cozic, A., Cugnet, D., de Noblet, N., Duvel, J.-P., Ethé., C., Fairhead, L., Fichefet, T., Flavoni, S., Friedlingstein, P., Grandpeix, J-Y., Guez, L., Guilyardi, L., Hauglustaine, D., Hourdin, F., Idelkadi, A., Ghattas, J., Joussaume, S., Kageyama, M., Krinner, G., Labetoulle, S., Lahellec, A., Lefevbre, M.-P., Lefevre, F., Levy, C., Li, Z.X., Lloyd, J., Lott, F., Madec, G., Mancip, M., Marchand, M., Masson, S., Meurdesoif, Y., Mignot, J., Musat, I., Parouty, S., Polcher, J., Rio, C., Schulz, M., Swingedouw, D., Szopa, S., Talandier, C., Terray, P., Viovy, N., and Vuichard, N. (2013). "Climate change projections using the IPSL-CM5 earth system model-From CMIP3 to CMIP5." *Clim. Dyn.*, 40(9), 2123-2165.

Dunlea, E., and Elfring, C. (2012). *A national strategy for advancing climate modeling (No. DOE/SC0005113).* National Research Council.

Dunne, J. P., John, J. G., Adcroft, A. J., Griffies, S. M., Hallberg, R. W., Shevliakova, E., Stouffer, R. J., Cooke, W., Dunne, K. A., Harrison, M. J., Krasting, J. P., Malyshev, S. L., Milly, P. C. D., Phillipps, P. J., Sentman, L. A., Samuels, B. L., Spelman, M. J., Winton, M., Wittenberg, A. T., and Zadeh, N. (2012) "GFDL's ESM2 global coupled climate-carbon Earth System Models Part I: Physical formulation and baseline simulation characteristics." *J. Clim*, 25(19), 6646-6665.

Edwards, P. N. (2011). “History of climate modeling.” *Wires. Clim. change.*, 2(1), 128-139.

Endo, N., Matsumoto, J., and Lwin, T. (2009). “Trends in precipitation extremes over Southeast Asia.” *Sola*, 5, 168-171.

ESGF the Earth System Grid Federation, 2015. https://www.wcrp-climate.org/wgcm-cmip/. Accessed 10 May 2015.

ESGF the Earth System Grid Federation, 2017. https://esgf-node.llnl.gov/search/cmip6/. Accessed 22 March 2020.

European Centre for Medium-Range Weather Forecasts. (2004). "ERA-40" <https://apps.ecmwf.int/datasets/data/era40-daily/levtype=sfc/> (Jun. 8, 2014).

European Centre for Medium-Range Weather Forecasts. (2019)."ERA-interim" <https://apps.ecmwf.int/datasets/data/interim-full-daily/levtype%3Dsfc/> (April. 15, 2020).

Fogli, P. G., and Iovino, D. (2014). “CMCC–CESM–NEMO: toward the new CMCC earth system model.” *CMCC research paper*, (248).

Flato, G., Gillett, N., Arora, V., Cannon, A. and Anstey, J. (2019). *Modelling Future Climate Change; Chapter 3 in Canada’s Changing Climate Report*, (ed.) E. Bush and D.S. Lemmen; Government of Canada, Ottawa, Ontario, p. 74-111.

Frenken, K. (2011). *Irrigation in Southern and Eastern Asia in Figures: Aquastat Survey, 2011*. Food and Agricultural Organization FAO: Rome, Italy, p. 512.

Gao, L., Bernhardt, M., and Schulz, K. (2012). “Elevation correction of ERA-Interim temperature data in complex terrain.” *Hydrol. Earth Syst. Sci.*, 16, 4661–4673.

Gelaro, R., McCarty, W., Suárez, M. J., Todling, R., Molod, A., Takacs, L., Randles, C.A., Darmenov, A., Bosilovich, M.G., Reichle, R., Wargan, K., Coy L., Cullather, R., Draper, C., Akella, S., Buchard, V., Conaty, A., da Silva, A.M., Gu, W., Kim, G.-K., Koster, R., Lucchesi, R., Merkova, D., Nielsen, J.E., Partyka, G., Pawson, S., Putman, W., Rienecker, M., Schubert, S.D.,

Sienkiewicz, M., and Zhao, B. (2017). “The modern-era retrospective analysis for research and applications, version 2 (MERRA-2).” *J. Clim*, 30(14), 5419-5454.

Gent, R. P. (2012). *Coupled Climate and Earth System Models’ in Rasch, P. (ed.) Climate change modeling methodology*. New York, NY: Springer.

Gettelman, A., and R.B. Rood (2016). *Demystifying Climate Models: A Users Guide to Earth Systems Models*, Springer, Berlin, Heidelberg, 274 pp.

Gilewski, P., and Nawalany, M. (2018). “Inter-Comparison of Rain-Gauge, Radar, and Satellite (IMERG GPM) Precipitation Estimates Performance for Rainfall-Runoff Modeling in a Mountainous Catchment in Poland.” *Water*, 10(11), 1665.

Giorgetta, M. A., Roeckner, E., Mauritsen, T., Bader, B. S. J., Crueger, T., Esch, M., Rast, S., Schmidt, L. K. H., Kinne, S., Mobis, B., and Krismer, T. (2013). *The atmospheric general circulation model ECHAM6-model description*. Tech. rep., Max Planck Institute for Meteorology, Hamburg.

Gleckler, P. J., Taylor, K. E., and Doutriaux, C. (2008). “Performance metrics for climatemodels.” *J. Geophys. Res. Atmos.*, 113, D06104.

Global Impact Investment Network. (2018). *The landscape for impact investing in Southeast Asia*.

Griffies, S. M., Winton, M., Donner, L. J., Horowitz, L. W., Downes, S. M., Farneti, R., Gnanadesikan, A., Hurlin, W. J., Lee, H.-C., Liang, Z., Palter, J. B., Samuels, B. L., Wittenberg, A. T., Wyman, B. L., Yin, J., and Zadeh, N. (2011) “The GFDL CM3 Coupled Climate Model: Characteristics of the Ocean and Sea Ice Simulations.” *J. Clim*, 24, 3520–3544.

Grise, K.M., and Davis, S.M. (2020). “Hadley cell expansion in CMIP6 models.” *Atmospheric Chem. Phys*, 20(9), 5249–5268.

Grose, M.R., Brown, J.N., Narsey, S., Brown, J.R., Murphy, B.F., Langlais, C., Gupta A.S., Moise, A.F., and Irving, D.B. (2014). “Assessment of the CMIP5 global

climate model simulations of the western tropical Pacific climate system and comparison to CMIP3." *Int. J. Climatol.*, 34(12),3382–3399.

Guo, Y., Yu, Y., Lin, P., Liu, H., He, B., Bao, Q., Zhao, S., and Wang, X. (2020). "Overview of the CMIP6 Historical Experiment Datasets with the Climate System Model CAS FGOALS-f3-L." *Adv. Atmos. Sci.*, 37, 1057–1066.

Haarsma, R. J., Roberts, M. J., Vidale, T. L., Senior, C. A., Bellucci, A., Bao, Q., Chang, P., Corti, S., Fuckar, N. S., Guemas, Virginie, von Hardenberg, J., Hazeleger, W., Kodama, C., Koenigk, T., Leung, L. R., Lu, J., Luo, J.-J., Mao, J., Mizielinski, M. S., Mizuta, R., Nobre, P., Satoh, M., Scoccimarro, E., Semmler, Tido , Small, J. and von Storch, J.-S. (2016). "High resolution model intercomparison project (HighResMIP v1.0) for CMIP6." *Geosci. Model Dev.*, 9,4185–4208.

Handmer, J., Honda, Y., Kundzewicz, Z.W., Arnell, N., Benito, G., Hatfield, J., Mohamed, I.F., Peduzzi, P., Wu, S., Sherstyukov, B., Takahashi, K., and Yan, Z. (2012). *Changes in impacts of climate extremes: human systems and ecosystems. In: Managing the Risks of Extreme Events and Disasters to Advance Climate Change Adaptation* [Field, C.B., V. Barros, T.F. Stocker, D. Qin, D.J. Dokken, K.L. Ebi, M.D. Mastrandrea, K.J. Mach, G.-K. Plattner, S.K. Allen, M. Tignor, and P.M. Midgley (eds.)]. A Special Report of Working Groups I and II of the Intergovernmental Panel on Climate Change (IPCC). Cambridge University Press, Cambridge, UK, and New York, NY, USA, pp. 231-290.

Haraguchi, M., and Lall, U. (2015). "Flood risks and impacts: A case study of Thailand's floods in 2011 and research questions for supply chain decision making." *Int. J. Disaster Risk Reduct.*,14, 256–272.

Harris. I., Jones, P.D., Osborn, T.J., and Lister, D.H. (2014) "Updated high-resolution grids of monthly climatic observations - the cru ts3.10 dataset." *Int. J. Climatol*, 34, 623–642.

Harris, I., Osborn, T.J., Jones, P., and Lister, D. (2020) “Version 4 of the CRU TS monthly high-resolution gridded multivariate climate dataset.” *Scientific data*, 7, 1-18.

Hazeleger, W., Wang, X., Severijns, C., S¸tef˘anescu, S., Bintanja, R., Sterl, A., Wyser, K., Semmler, T., Yang, S., van den Hurk, B., van Noije, T., van der Linden, E., and van der Wiel, K. (2011) “EC-Earth V2.2: description and validation of a new seamless earth system prediction model.” *Clim. Dyn.*, 1–19.

He, B., Bao, Q., Wang, X., Zhou, L., Wu, X., Liu, Y., Wu, G., Chen, K., He, S., Hu, W., Li, J., Li, J., Nian, G., Wang, L., Yang, J., Zhang, M., and Zhang, X. (2019). “CAS FGOALS-f3-L model datasets for CMIP6 historical atmospheric model intercomparison project simulation.” *Adv. Atmos. Sci.*, 36(8), 771–778.

Hebeler F (2020) RMSE. MATLAB Central File Exchange. <https://www.mathworks.com/matlabcentral/ Fileexchange/21383-rmse>. (Jan.16,2020)

Held, I. M., Guo, H., Adcroft, A., Dunne, J. P., Horowitz, L. W., Krasting, J., Shevliakova, E., Winton, M., Zhao, M., Bushuk, M., Wittenberg, A. T., Wyman, B., Xiang, B., Zhang, R., Anderson, W., Balaji, V., Donner, L., Dunne, K., Durachta, J., Gauthier, P. P. G., Ginoux, P., Golaz, J.-C., Griffies, S. M., Hallberg, R., Harris, L., Harrison, M., Hurlin, W., John, J., Lin, P., Lin, S.-J., Malyshev, S., Menzel, R., Milly, P. C. D., Ming, Y., Naik, V., Paynter, D., Paulot, F., Rammaswamy, V., Reichl, B., Robinson, T., Rosati, A., Seman, C., Silvers, L. G., Underwood, S., and Zadeh, N. (2019). “Structure and Performance of GFDL’s CM4.0 Climate Model.” *J. Adv. Model. Earth Syst.*, 11, 3691–3727.

Hoegh-Guldberg, O., Jacob, D., Taylor, M., Bindi, M., Brown, S., Camilloni, I., Diedhiou, A., Djalante, R., Ebi, K.L., Engelbrecht, F., Guiot, J., Hijioka, Y., Mehrotra, S., Payne, A., Seneviratne, S.I., Thomas, A., Warren, R., and Zhou, G. (2018). *Impacts of 1.5oC Global Warming on Natural and Human Systems. In: Global Warming of 1.5°C. An IPCC Special Report on the impacts of*

global warming of 1.5°C above pre-industrial levels and related global greenhouse gas emission pathways, in the context of strengthening the global response to the threat of climate change, sustainable development, and efforts to eradicate poverty [Masson-Delmotte, V., P. Zhai, H.-O. Portner, D. Roberts, J. Skea, P.R. Shukla, A. Pirani, W. Moufouma-Okia, C. Pean, R. Pidcock, S. Connors, J.B.R. Matthews, Y. Chen, X. Zhou, M.I. Gomis, E. Lonnoy, T. Maycock, M. Tignor, and T. Waterfield (eds.)]. In Press.

Homsi, R., Shiru, M. S., Shahid, S., Ismail, T., Harun, S. B., Al-Ansari, N., Chau, K. W., and Yaseen, Z. M. (2020). "Precipitation projection using a CMIP5 GCM ensemble model: a regional investigation of Syria." Eng. Appl. Comput. Fluid. Mech., 14, 90–106.

Homsi, R., Shiru, M. S., Shahid, S., Ismail, T., Harun, S. B., Al-Ansari, N., Chau, K. W., and Yaseen, Z. M. (2020). "Precipitation projection using a CMIP5 GCM ensemble model: a regional investigation of Syria." Eng. Appl. Comput. Fluid. Mech., 14, 90–106.

Houghton, D . D. (2002). *Introduction to Climate Change : Lecture Notes for Meteorologists* .WMO Technical Publication :World Meteorological Organization, Geneva, 926,1-143.

Hourdin, F., Musat, I., Bony, S., Braconnot, P., Codron, F., Dufresne, J.L., Fairhead, L., Filiberti, M.A., Friedlingstein, P., Grandpeix, J.Y., Krinner, G., Levan, P., Li, Z.X., and Lott, F. (2006). "The LMDZ4 general circulation model: climate performance and sensitivity to parametrized physics with emphasis on tropical convection." *Clim. Dyn.*, 27(7–8),787–813.

Huang, F., Xu, Z., and Guo, W. (2019). "Evaluating vector winds in the Asian-Australian monsoon region simulated by 37 CMIP5 models." *Clim. Dyn.*, 53, 491-507.

Hurrell, J. W., Holland, M. M., Gent, P. R., Ghan, S., Kay, J. E., Kushner, P. J., Lamarque, J. F., Large, W. G., Lawrence, D., Lindsay, K., Lipscomb, W. H., Long, M. C., Mahowald, N., Marsh, D. R., Neale, R. B., Rasch, P., Vavrus, S., Vertenstein, M., Bader, D., Collins, W. D., Hack, J. J., Kiehl, J., and Marshall,

S. (2013). “The community earth system model: a framework for collaborative research.” *Bull. Am. Meteorol. Soc.*, *94*(9), 1339-1360.

IPCC. (2007). *Climate Change 2007 : The Physical Science Basis . Contribution of Working Group I to the Fourth Assessment Report of the Intergovernmental Panel on Climate Change*]Solomon, S ., D .Qin, M .Manning, Z .Chen, M . Marquis, K .B .Averyt, M .Tignor and H .L .Miller)eds . [(.Cambridge University Press, Cambridge, United Kingdom and New York, NY, USA, 996pp.

IPCC. (2012) *Glossary of terms . In : Managing the Risks of Extreme Events and Disasters to Advance Climate Change Adaptation*]Field, C .B ., V .Barros, T.F .Stocker, D .Qin, D.J .Dokken, K.L .Ebi, M.D .Mastrandrea, K.J .Mach, G- .K .Plattner, S .K .Allen, M .Tignor, and P .M .Midgley)eds . (.A Special Report of Working Groups I and II of the Intergovernmental Panel on Climate Change)IPCC .(Cambridge University Press, Cambridge, UK, and New York, NY, USA, pp .555-564.

IPCC. (2013). *Climate Change 2013: The Physical Science Basis. Contribution of Working Group I to the Fifth Assessment Report of the Intergovernmental Panel on Climate Change* [Stocker, T.F., D. Qin, G.-K. Plattner, M. Tignor, S.K. Allen, J. Boschung, A. Nauels, Y. Xia, V. Bex and P.M. Midgley (eds.)]. Cambridge University Press, Cambridge, United Kingdom and New York, NY, USA, 1535 pp.

IPCC. (2014) *Climate Change 2014 : Impacts, Adaptation, and Vulnerability . Summaries, Frequently Asked Questions, and Cross -Chapter Boxes . A Contribution of Working Group II to the Fifth Assessment Report of the Intergovernmental Panel on Climate Change* e]Field, C.B., V.R .Barros, D.J . Dokken, K.J .Mach, M.D .Mastrandrea, T.E .Bilir, M .Chatterjee, K.L .Ebi, Y .O .Estrada, R .C .Genova, B .Girma, E .S .Kissel, A .N .Levy, S . MacCracken, P.R., Mastrandrea, and L .L .White)eds . [(.World Meteorological Organization, Geneva, Switzerland, 190pp.

Ji, D., Wang, L., Feng, J., Wu, Q., Cheng, H., Zhang, Q., Yang, J., Dong, W., Dai, Y., Gong, D., Zhang, R.-H., Wang, X., Liu, J., Moore, J. C., Chen, D., and Zhou, M. (2014) "Description and basic evaluation of Beijing Normal University Earth System Model (BNU-ESM) version 1." *Geosci. Model Dev.*, 7, 2039-2064

Jones, C. D., Hughes, J. K., Bellouin, N., Hardiman, S. C., Jones, G. S., Knight, J., Liddicoat, S., O'Connor, F. M., Andres, R. J., Bell, C., Boo, K. O., Bozzo, A., Butchart, N., Cadule, P., Corbin, K. D., DoutriauxBoucher, M., Friedlingstein, P., Gornall, J., Gray, L., Halloran, P. R., Hurtt, G., Ingram, W. J., Lamarque, J. F., Law, R. M., Meinshausen, M., Osprey, S., Palin, E. J., Chini, L. P., Raddatz, T., Sanderson, M. G., Sellar, A. A., Schurer, A., Valdes, P., Wood, N., Woodward, S., Yoshioka, M. and Zerroukat, M. (2011) The HadGEM2-ES implementation of CMIP5 centennial simulations." *Geosci. Model Dev.*, 4(3), 543–570.

Kalnay, E. (1996). "The NCEP/NCAR 40-year reanalysis project." *Bull. Am. Meteorol. Soc.*, 77(3), 437–470.

Kamworapan, S., and Surussavadee, C. (2019). "Evaluation of CMIP5 Global Climate Models for Simulating Climatological Temperature and Precipitation for Southeast Asia." *Adv. Meteorol*, 2019,1-18.

Karim, R., Tan, G., Ayugi, B., Babaousmail, H., and Liu, F. (2020). "Evaluation of historical CMIP6 model simulations of seasonal mean temperature over Pakistan during 1970–2014." Atmosphere, 11, 1005.

Khalid, S., Azad, S., and Rahman, Z. (2017). "Climate change: A review of the current trends and major environmental effects." *Science Technology and Development*, 36(3), 160-176.

Khan, N., Shahid, S., Ahmed, K., Ismail, T., Nawaz, N., and Son, M. (2018). "Performance assessment of general circulation model in simulating daily precipitation and temperature using multiple gridded datasets." Water, 10, 1793.

Kim, Y. H., Min, S. K., Zhang, X., Sillmann, J., and Sandstad, M. (2020). "Evaluation of the CMIP6 multi-model ensemble for climate extreme indices." Weather Clim. Extrem. 29, 100269.

Kumar, S ., Merwade, V ., Kinter III, J ., and .Niyogi, D .2012 . ("Evaluation of temperature and precipitation trends and long-term persistence in CMIP5 20th century climate simulations." *J. Clim*, 26, 4168-4185.

Lauer, A ., Zhang, C ., and Elison- Timm, O. (2013). "Downscaling of Climate Change in the Hawaii Region Using CMIP5 Results :On the Choice of the Forcing Fields." *J. Clim*, 26, 10006-10030.

Le Treut, H., Somerville, R., Cubasch, U., Ding, Y., Mauritzen, C., Mokssit, A., Peterson, T., and Prather, M. (2007). *Historical Overview of Climate Change. In: Climate Change 2007: The Physical Science Basis. Contribution of Working Group I to the Fourth Assessment Report of the Intergovernmental Panel on Climate Change* [Solomon, S., D. Qin, M. Manning, Z. Chen, M. Marquis, K.B. Averyt, M. Tignor and H.L. Miller (eds.)]. Cambridge University Press, Cambridge, United Kingdom and New York, NY.

Li, J., Liu, Z., Yao, Z., and Wang, R. (2019). "Comprehensive assessment of Coupled Model Intercomparison Project Phase 5 global climate models using observed temperature and precipitation over mainland Southeast Asia." *Int. J. Climatol*, 39, 4139-4153.

Lionello, P., and Scarascia, L. (2018). "The relation between climate change in the Mediterranean region and global warming." *Reg. Environ. Change*, 18(5), 1481-1493.

Lovino, M.A., Müller, O.V., Berbery, E.H., and Müller, G.V. (2018). "Evaluation of CMIP5 retrospective simulations of temperature and precipitation in northeastern Argentina." *Int. J. Climatol*, 38, e1158–e1175.

Maher, P., Vallis, G. K., Sherwood, S. C., Webb, M. J., and Sansom, P. G. (2018). "The impact of parameterized convection on climatological precipitation in atmospheric global climate models." Geophys. Res. Lett., 45, 3728–3736.

Martin, G. M., Milton, S. F., Senior, C. A., Brooks, M. E., Ineson, S., Reichler, T., and Kim, J. (2010). "Analysis and reduction of systematic errors through a seamless approach to modeling weather and climate." *J. Clim*, 23(22), 5933-5957.

Matsuura, K., and Willmott, C.J. (2012a). "Terrestrial Air Temperature: 1900–2010 Gridded Monthly Time Series (version 3.01)." <http://climate.geog.udel.edu/~climate/html_ pages/Global2011/README.GlobalTsT2011.html> (Jan. 8, 2016).

Mcmahon, T.A., Peel, M.C., and Karoly, D.J. (2015). "Assessment of precipitation and temperature data from CMIP3 global climate models for hydrologic simulation." *Hydrol. Earth Sys.t Sci.*, 19, 361–377.

Meehl, G. A., Covey, C., Delworth, T., Latif, M., McAvaney, B., Mitchell, J. F., Stouffer, R. J., and Taylor, K. E. (2007). "The WCRP CMIP3 multimodel dataset: A new era in climate change research." *Bull. Am. Meteorol. Soc.*, *88*(9), 1383-1394.

Meehl, G., Covey, C., Latif, M., McAvaney, B., Mitchell, J., and Stouffer, R. (2007). *IPCC standard output from coupled ocean-atmosphere GCMs.* Lawrence Livermore National Laboratory Program for Climate Model Diagnosis and Intercomparison, Livermore, California.

Miao, C., Duan, Q., Sun, Q., Huang, Y., Kong, D., Yang, T., Ye, A., Di, Z, and Gong, W. (2014) "Assessment of CMIP5 climate models and projected temperature changes over Northern Eurasia. Environ." *Environ. Res. Lett.*, 9, 055007.

Mishra, P., Pandey, C. M., Singh, U., Gupta, A., Sahu, C., and Keshri, A. (2019). "Descriptive statistics and normality tests for statistical data." *Ann. Card. Anaesth.*, 22(1), 67.

Moise, A., Wilson, L., Grose, M., Whetton, P., Watterson, I., and Bhend, J. (2015). "Evaluation of CMIP3 and CMIP5 models over the Australian region to inform confidence in projections." *Aust. Meteorol. Oceanogr. J.*, 65, 19-53.

Moriasi, D.N., Arnold, J.G., Van Liew, M.W., Binger, R.L., Harmel, R.D., and Veith, T.L. (2007). “Model evaluation guidelines for systematic quantification of accuracy in watershed simulations.” *Trans. ASABE*, 50. 885–900.

NASA/NOAA. (2020). “NASA, NOAA Analyses Reveal 2019 Second Warmest Year on Record.” < https://www.nasa.gov/press-release/nasa-noaa-analyses-reveal-2019-second-warmest-year-on-record> (accessed 7 January 2021).

Nastis, S. A., Michailidis, A., and Chatzitheodoridis, F. (2012). “Climate change and agricultural productivity.” *Afr. J. Agric. Res.*, 7(35), 4885-4893.

National Aeronautics and Space Administration Goddard Space Flight Center. (2016). "Modern-Era Retrospective analysis for Research and Applications, Version 2" <https://gmao.gsfc.nasa.gov/reanalysis/MERRA-2/> (Jun. 8, 2020).

Pathak, R., Sahany, S., Mishra, S. K., and Dash, S. K. (2019). “Precipitation biases in CMIP5 models over the South Asian region.” Sci. Rep., 9, 1-13.

Physical Sciences Laboratory. (2010). "University of Delaware Air Temperature & Precipitation" <https://psl.noaa.gov/data/gridded/data.UDel_AirT_Precip.html> (Jun. 8, 2014).

Physical Sciences Laboratory. (2017). "University of Delaware Air Temperature & Precipitation" <https://psl.noaa.gov/data/gridded/data.UDel_AirT_Precip.html> (April. 15, 2020).

Physical Sciences Laboratory. (2010). "NCEP/NCAR Reanalysis 1: Surface." <https://psl.noaa.gov/data/gridded/data.ncep.reanalysis.surface.html>

Qiao, F., Song, Z., Bao, Y., Song, Y., Shu, Q., Huang, C., and Zhao, W. (2013). “Development and evaluation of an Earth System Model with surface gravity waves.” *J. Geophys. Res.*, 118(9), 4514-4524.

Raddatz, T., Reick, C., Knorr, W., Kattge, J., Roeckner, E., Schnur, R., Schnitzler, K. G., Wetzel, P., and Jungclaus, J. (2007) “Will the tropical land biosphere

dominate the climate– carbon cycle feedback during the twenty-first century?." *Clim. Dyn.*, 29, 565–574.

Radić, V., and Clarke, G.K.C. (2011). "Evaluation of IPCC models' performance in simulating late-twentieth century climatologies and weather patterns over North America." *J. Clim,* 24, 5257–5274.

Raghavan, S .V., Vu, M .T., and Liong, S .Y. (2016). "Regional climate simulations over Vietnam using the WRF model." *Theor. Appl. Climatol.*, 126, 161–182.

Rahman, M. A., Kamal, S. M., and Billah, M. M. (2016). "Rainfall variability and linear trend models on north-west part of Bangladesh for the last 40 years." *Am. J. Appl. Math.*, 4(3), 158-162.

Randall, D.A., Wood, R.A., Bony, S., Colman, R., Fichefet,T., Fyfe, J., Kattsov, V., Pitman, A., Shukla, J., Srinivasan, J., Stouffer, R.J., Sumi, A., Taylor, K.E. (2007). *Climate models and their evaluation.* In: Solomon S, Qin D, Manning M, Chen Z, Marquis M, Averyt KB, Tignor M, Miller HL (eds) Climate change 2007: the physical science basis. Contribution of working group I to the fourth assessment report of the intergovernmental panel on climate change. Cambridge University Press, Cambridge, pp. 589-662.

Reid, P.C., Fischer, A., Lewis-Brown, E., Meredith, M.P., Sparrow, M2, Andersson, A.J., Antia, A., Bathmann, U., Beaugrand, G., and Brix, H. (2009). "Impacts of the Oceans on Climate Change." *Adv. Mar. Biol..*, 56, 1–150.

Rienecker, M. M., Suarez, M. J., Gelaro, R., Todling, R., Bacmeister, J., Liu, E., Bosilovich, M. G., Schubert, S. D., Takacs, L., Kim, G-K., Bloom, S., Chen, J., Collins, D., Conaty, A., da Silva, A., Gu, W., Joiner, J., Koster, R. D., Lucchesi, R., Molod, A., Owens, T., Pawson, S., Pegion, P., Redder, C. R., Reichle, R., Robertson, F. R., Ruddick, A. G., Sienkiewicz, M., and Woollen, J (2011) "MERRA: NASA's Modern-Era Retrospective Analysis for Research and Applications." *J. Clim*, 24, 3624–3648.

Rivera, J. A., and Arnould, G. (2020). “Evaluation of the ability of CMIP6 models to simulate precipitation over Southwestern South America: Climatic features and long-term trends (1901–2014).” Atmos. Res., 241, 104953.

Rong, X. Y., Li, J., Chen, H. M., Xin Y.F., Su J.Z., Hua L.J., and Zhang Z.Q. (2019). “Introduction of CAMS-CSM model and its participation in CMIP6.” *Climate Change Research*, 15, 540–544.

Rotstayn, L. D., Collier, M. A., Dix, M. R., Feng, Y., Gordon, H. B., O’Farrell, S. P., Smith, I. N., and Syktus, J. (2010) “Improved simulation of Australian climate and ENSO-related rainfall 4 variability in a global climate model with an interactive aerosol treatment.” *Int. J. Climatol*, 30, 1067–1088.

Rupp, D .E., Abatzoglou, J .T., Hegewisch, K .C., and Mote, P .W. (2013). “Evaluation of CMIP5 20th century climate simulations for the Pacific Northwest U.S.A.” *J. Geophys. Res. Atmos.*,118, 10884–10906.

Ruan, Y., Liu, Z., Wang, R., and Yao, Z. (2019). “Assessing the Performance of CMIP5 GCMs for Projection of Future Temperature Change over the Lower Mekong Basin.” *Atmosphere*, 10(2), 93.

Russ, J. C. (1994). *The Image Processing Handbook*, Second Edition, CRC Press, Boca Raton, ISBN 0-8493-2516-1. Used with permission.

Saha, A., Ghosh, S., Sahana, A. S., and Rao, E. P. (2014). “Failure of CMIP5 climate models in simulating post-1950 decreasing trend of Indian monsoon.” Geophys. Res. Lett., 41,

Sakamoto, T. K., Komuro, Y., Nishimura, T., Ishii, M., Tatebe, H., Shiogama, H., Hasegawa, A., Toyoda, T., Mori, M., Suzuki, T., Imada, Y., Nozawa, T., Takata, K., Mochizuki, K., Ogochi, K., Emori, S., Hasumi, H., and Kimoto, M. (2012) “MIROC4h-A New High-Resolution Atmosphere-Ocean Coupled General Circulation Model.” *J. Meteor. Soc. Japan. Ser. II*, 90(3), 325-359.

Sanderson, B. M., Wehner, M., and Knutti, R. (2017). “Skill and independence weighting for multi-model assessments.” *Geosci. Model Dev.*, 10(6), 2379-2395.

Samanta, D., Karnauskas, K. B., and Goodkin, N. F. (2019). “Tropical Pacific SST and ITCZ biases in climate models: Double trouble for future rainfall projections?.” Geophys. Res. Lett., 46, 2242–2252.

Schaller, N., Mahlstein, I., Cermak, J., and Knutti, R. (2011). “Analyzing precipitation projections: a comparison of different approaches to climate model evaluation.” J. Geophys. Res,116, D10118.

Schneider, S. H. (1992). *Introduction to Climate Modeling. In K. E. Trenberth, ed., Climate System Modeling.* Cambridge: Cambridge University Press, 3–26.

Séférian, R., Nabat, P., Michou, M., Saint-Martin, D., Voldoire, A., Colin, J., Decharme, B., Delire, C., Berthet, S., Chevallier, M., Sénési, S., Franchisteguy, L., Vial, J., Mallet, M., Joetzjer, E., Geoffroy, O., Guérémy, J.-F., Moine, M.-P., Msadek, R., Ribes, A., Rocher, M., Roehrig, R., Salas-y Mélia, D., Sanchez, E., Terray, L., Valcke, S., Waldman, R., Aumont, O., Bopp, L., Deshayes, J., Éthé, C., and Madec, G. (2019). “Evaluation of CNRM Earth-System model, CNRM-ESM2-1: role of Earth system processes in present-day and future climate.” *J. Adv. Model. Earth Syst.*, 11, 4182-.4227.

Seneviratne, S.I., Nicholls, N., Easterling, D., Goodess, C.M., Kanae, S., Kossin, J., Luo, Y., Marengo, J., McInnes, K., Rahimi, M., Reichstein, M., Sorteberg, A., Vera, C., and Zhang, X. (2012). *Changes in climate extremes and their impacts on the naturalphysical environment. In: Managing the Risks of Extreme Events and Disasters to Advance Climate Change Adaptation* [Field, C.B., V. Barros, T.F. Stocker, D. Qin, D.J. Dokken, K.L. Ebi, M.D. Mastrandrea, K.J. Mach, G.-K. Plattner, S.K. Allen, M. Tignor, and P.M. Midgley (eds.)]. A Special Report of Working Groups I and II of the Intergovernmental Panel on Climate Change (IPCC). Cambridge University Press, Cambridge, UK, and New York, NY, USA, pp. 109-230.

Shepardsona, D . P ., Niyogib, D ., Roychoudhuryc, A ., and Hirschd, A. (2011). “Conceptualizing climate change in the context of a climate system :implications for climate and environmental education .” *Environ. Educ. Res.*, 18(3), 323-352.

Siew, J.H., Tangang, F.T., and Juneng, L. (2014). “Evaluation of CMIP5 coupled atmosphere–ocean general circulation models and projection of the Southeast Asian winter monsoon in the 21st century.” *Int. J. Climatol*, 34, 2872–2884.

Stouffer, R.J., Eyring, V., Meehl, G.A., Bony, S., Senior, C., Stevens. B., and Taylor, K.E. (2017). “CMIP5 Scientific Gaps and Recommendations for CMIP6.” *Bull. Am. Meteorol. Soc.,* 98, 95–105.

Su, F., Duan, X., Chen, D., Hao, Z., and Cuo, L. (2013) “Evaluation of the global climate models in the CMIP5 over the Tibetan Plateau.” *J. Clim*, 26,3187–3208.

Sun, Q., Miao, C., Duan, Q., Ashouri, H., Sorooshian, S., and Hsu, K.-L. (2018). “A review of global precipitation data sets

Supharatid, S. (2015). “Assessment of CMIP3-CMIP5 Climate Models Precipitation Projection and Implication of Flood Vulnerability of Bangkok.” *Am. J. Clim. Change*, 4, 140-162.

Surussavadee, C. (2014). “Evaluation of high-resolution tropical weather forecasts using satellite passive millimeter-wave observations.” IEEE transactions on geoscience and remote sensing, 52, 2780 -2787.

Swart, N. C., Cole, J. N. S., Kharin, V. V., Lazare, M., Scinocca, J. F., Gillett, N. P., and Winter, B. (2019). “The Canadian Earth System Model version 5 (CanESM5.0.3).” *Geosci. Model Dev.*, 12(11), 4823-4873.

Symon, C. (2013). *Climate Change : Action, Trends and Implications for Business* . Cambridge Judge Business School and Cambridge Programme for Sustainability Leadership,1-20.

Tan, C.T., and Pereira, J.J. (2010) *Climate Change Adaptation: An Overview of Southeast Asia. Asian Journal of Environment and Disaster Management.* Research Publishing Services, Singapore, 2, pp. 371-395.

Tantrakarnapa, K. (2018). *Second Bienial Updated Report of Thailand, Office of Natural Resources and Environmental Policy and Planning*, Bangkok, Thailand, 1-108.

Tatebe, H., Ogura, T., Nitta, T., Komuro, Y., Ogochi, K., Takemura, T., Sudo, K., Sekiguchi, M., Abe, M., Saito, F., Chikira, M., Watanabe, S., Mori, M., Hirota, N., Kawatani, Y., Mochizuki, T., Yoshimura, K., Takata, K., O'ishi, R., Yamazaki, D., Suzuki, T., Kurogi, M., Kataoka, T., Watanabe, M., and Kimoto, M. (2019). "Description and basic evaluation of simulated mean state, internal variability, and climate sensitivity in MIROC6." Geosci. Model Dev., 12(7), 2727–2765.Taylor, K. E., Stouffer, R. J., and Meehl, G .A) .2012 .("An overview of CMIP5 and the experiment design." *Bull. Am. Meteorol. Soc., Soc.*, 93, 485-498.

Trenberth, K. E., (1996) *Coupled climate system modelling, Chapter 3 of: Climate Change, Developing Southern Hemisphere Perspectives* Editors: T. Giambelluca and A. Henderson-Sellers. John Wiley & Sons Ltd. 475pp, 63-88

Trenberth, K .E., Miller, K., Mearns L., and S .Rhodes. (2000). *Effects of Changing Climate on Weather and Human Activities . Understanding Global Change : Earth Science and Human Impacts Series, Global Change Instruction Program.* UCAR .University Science Books, 46 pp.

UNFCCC. (1992). *United Nations Framework Convention on Climate Change* .New York :United Nations, General Assembly.

UNISDR. (2010). *Synthesis report on ten ASEAN countries disaster risks assessment: ASEAN disaster risk management initiative*. UNISDR, Geneva.

Uppala, S. M. (2005). "The ERA-40 re-analysis." *Quarterly Journal of the Royal Meteorological Society*, 131, (612), 2961–3012.

Vigaud, N., Richard, Y., Rouault, M., and Fauchereau, N. (2009). "Moisture transport between the South Atlantic Ocean and southern Africa: Relationships with summer rainfall and associated dynamics." *Clim. Dyn.*, 32, 113–123.

Voldoire, A., Sanchez- Gomez,E., Salas y Me´lia, D., Decharme, B .Cassou, C., Se´ne´si, S .Valcke, S., Beau, I., Alias, A., Chevallier, M., De´que´, M., Deshayes, J., Douville, H., Fernandez, E., Madec, G., Maisonnave, E., Moine,

M.P., Planton, S., Saint-Martin, D., Szopa, S., Tyteca, R., Alkama, R., Belamari, S., Braun, A., Coquart, L., and Chauvin, F. (2013). "The CNRM-CM5 .1 global climate model: description and basic evaluation." *Clim. Dyn.*, 1–31.

Voldoire, A., Saint-Martin, D., Sénési, S., Decharme, B., Alias, A., Chevallier, M., Colin, J., Guérémy, J.-F., Michou, M., Moine, M.-P., Nabat, P., Roehrig, R., Salas y Mélia, D., Séférian, R., Valcke, S., Beau, I., Belamari, S., Berthet, S., Cassou, C., Cattiaux, J., Deshayes, J., Douville, H., Ethé, C., Franchistéguy, L., Geoffroy, O., Lévy, C., Madec, G., Meurdesoif, Y., Msadek, R., Ribes, A., Sanchez-Gomez, E., Terray, L., and Waldman, R. (2019). "Evaluation of CMIP6 DECK experiments with CNRM-CM6-1." *J. Adv. Model. Earth Syst.*, 11, 2177–2213.

Volodin, E., Dianskii, N., and Gusev, A. (2010) "Simulating present-day climate with the INMCM4.0 coupled model of the atmospheric and oceanic general circulations." *IZV Atmos.ocean phy+*, 46, 414–431.

Wang, B., Liu, D. L., Macadam, I., Alexander, L. V., Abramowitz, G., and Yu, Q. (2016). "Multi-model ensemble projections of future extreme temperature change using a statistical downscaling method in south eastern Australia." Clim. Change, 138, 85–98.

Wargan, K., Labow, G., Frith, S., Pawson, S., Livesey, N., and Partyka, G. (2017). "Evaluation of the ozone fields in NASA's MERRA-2 reanalysis." *J. Clim*, 30(8), 2961–2988.

Warrick, R. A., and Oerlemans, J. (1990). *Sea Level Rise, in Houghton, J. T., Jenkins, G. J., and Ephraums, J. J. (eds.), Climate Change: The IPCC Scientific Assessment*, Cambridge University Press, pp. 257-282.

Watanabe, S., Hajima, T., Sudo, K., Nagashima, T., Takemura, T., Okajima, H., Nozawa, T., Kawase, H., Abe, M., Yokohata, T., Ise, T., Sato, H., Kato, E., Takata, K., Emori, S., and Kawamiya, M. (2011) "MIROC-ESM: model

description and basic results of CMIP5-20c3m experiments." *Geosci. Model Dev. Discuss.*, 4, 1063–1128.

Watanabe, S., Hirabayashi, Y., Kotsuki, S., Hanasaki, N., Tanaka, K., Mateo, C., and Oki, T. (2014). "Application of performance metrics for climate models to project future river discharge in Chao Phraya River Basin." *Hydrol. Res. Lett.*, 8(1), 33–38.

Waugh, D.W., and Eyring, V. (2008). "Quantitative performance metrics for stratospheric-resolving chemistry-climate models." *Atmospheric Chem. Phys.*, 8,5699.

WCRP, Coupled Model Intercomparison Project (Phase 6). <https://esgf-node.llnl.gov/search/cmip6/> (Jan. 16, 2020)

White, M.P., Hilario, F.D., de Guzman, M.R.G., and Cinco, M.T.A. (2009). "A Review of Climate Change Model Predictions and Scenario Selection for impacts on Asian Aquaculture."

Wilkinson, C. (2000). *"Status of Coral Reefs of the World :2000 ".* Global Coral Reef Monitoring Network and Reef and Rainforest Research Center, Townsville, Australia,1-363.

Willmott, C.J. and Matsuura, K. (1995). "Smart interpolation of annually averaged air temperature in the United States." *J. Appl. Meteorol.*, 34, 2577-2586.

Willmott, C.J., and Matsuura, K. (2018). "Terrestrial Air Temperature: 1900-2017 Gridded Monthly Time Series." <http://climate.geog.udel.edu/~climate/html_pages/Global2017/README.GlobalTsT2017.html > (Jan. 30, 2020).

Willmott, C.J. and Robeson, S.M. (1995). "Climatologically aided interpolation (CAI) of terrestrial air temperature." *Int. J. Climatol.*, 15(2), 221-229.

Willmott, C.J., Rowe, C.M. and Philpot, W.D. (1985). "Small-scale climate maps: a sensitivity analysis of some common assumptions associated with grid-point interpolation and contouring." *American Cartographer*, 12, 5-16.

Wu, T., Lu, Y., Fang, Y., Xin, X., Li, L., Li, W., Jie, W., Zhang, J., Liu, Y., Zhang, L., Zhang, F., Zhang, Y., Wu, F., Li, J., Chu, M., Wang, Z., Shi, X., Liu, X., Wei, M., Huang, A., Zhang, Y., and Liu, X. (2019). "The Beijing Climate Center climate system model (BCC-CSM): The main progress from CMIP5 to CMIP6." *Geosci. Model Dev.*, 12, 1573-1600.

Wu, T., Song, L., Li, W., Wang, Z., Zhang, H., Xin, X., Zhang, Y., Zhang, L., Li, J., Wu, F., Liu, Y., Zhang, F., Shi, X., Chu, M., Zhang, J., Fang, Y., Wang, F., Lu, Y., Liu, X., Wei, M., Liu, Q., Zhou, W., Dong, M., Zhao, Q., Ji, J., Li, L., and Zhou, M. (2014). "An overview of BCC climate system model development and application for climate change studies." *Journal of Meteorological Research*, 28, 34-56.

Xin, X., Wu, T., Zhang, J., Yao, J., and Fang, Y. (2020) "Comparison of CMIP6 and CMIP5 simulations of precipitation in China and the East Asian summer monsoon." *Int. J. Climatol*, 1- 18.

Xuan, W., Ma, C., Kang, L., Gu, H., Pan, S., and Xu, Y-P. (2017) "Evaluating historical simulations of CMIP5 GCMs for key climatic variables in Zhejiang Province, China." *J. Appl. Meteorol.*, 128, 207-222.

Xu, J., Gao, Y., Chen, D., Xiao, L., and Ou, T. (2017). "Evaluation of global climate models for downscaling applications centered over the Tibetan plateau." *Int. J. Climatol*, 37, 657–671.

Yan, G., Wen-Jie, D., Fu-Min, R., Zong-Ci, Z., and Jian-Bin, H. (2013). "Surface air temperature simulations over China with CMIP5 and CMIP3." *Adv. Clim. Chang.*, 4(3), 145-152.

Yang, X., Yong, B., Yu, Z., and Zhang, Y. (2021). "An evaluation of CMIP5 precipitation simulations using ground observations over ten river basins in China." Nord. Hydrol., 52, 676-698.

Yin, L., Fu, R., Shevliakova, E., and Dickinson, R. E. (2013). "How well can CMIP5 simulate precipitation and its controlling processes over tropical South America?." Clim. Dyn., 41, 3127-3143.

Yuen, B. and Kong, L. (2009). “Climate change and urban planning in Southeast Asia.” *Cities and Climate Change*, 2, 1-12.

Yukimoto, S., Kawai, H., Koshiro, T., Oshima, N., Yoshida, K., Urakawa, S., Tsujino, H., Deushi, M., Tanaka, T., Hosaka, M., Yabu, S., Yoshimura, H., Shindo, E., Mizuta, R., Obata, A., Adachi, Y., and Ishii, M. (2019). “The Meteorological Research Institute Earth System Model Version 2.0, MRI-ESM2.0: Description and Basic Evaluation of the Physical Component.” *J. Meteor. Soc. Japan. Ser. II.*, 97, 931–965.

Yukimoto, S., Yoshimura, H., Hosaka, M., Sakami, T., Tsujino, H., Hirabara, M., Tanaka, T. Y., Deushi, M., Obata, A., Nakano, H., Adachi, Y., Shindo, E., Yabu, S., Ose, T., and Kitoh, A. (2011). “Meteorological Research Institute Earth System Model Version 1 (MRI-ESM1)—Model Description—.” *J. Meteor. Soc. Japan*, Tech. Rep. of MRI, 64, 83 pp.

Zhang, Y. L. and Yu, Y.-Q. (2011) “Analysis of Decadal Climate Variability in the Tropical Pacific by Coupled GCM.” *Atmospheric Sci. Lett.*, 4, 204–208.

Zemp, M., Haeberli, W., Bajracharya, S., Chinn, T. J., Fountain, A.G., Hagen, J.O., Huggel, C., Kääb, A., Kaltenborn, B. P., Karki, M., Kaser, G., Kotlyakov, V.M., Lambrechts, C., Li Z. Q., Molnia, B. F., Mool, P., Nellemann, C., Novikov, V., Osipova, G.B., Rivera, A., Shrestha, B., Svoboda, F., Tsvetkov, D. G., and Yao, T. D. (2007). “Glaciers and ice caps. Part I :Global overview and outlook .Part II :Glacier changes around the world .Global Outlook for Ice and Snow.” *UNEP*, 33, 115–52.

Zhou, T., and Yu, R. (2006). “Twentieth-century surface air temperature over China and the globe simulated by coupled climate models.” *J. Clim*, 19(22),5843–5858.

Zhou, T. J., Wang, B., Yu, Y. Q., Liu, Y. M., Zheng, W. P., Li, L. J., Wu, B., Lin, P. F., Guo, Z., Man, W. M., Bao, Q., Duan, A. M., Liu, H. L., Chen, X. L., He, B., Li, J. D., Zou, L. W., Wang, X. C., Zhang, L. X., Sun, Y., and Zhang, W.

X., (2018). “The FGOALS climate system model as a modeling tool for supporting climate sciences: An overview.”, *EPP*, 2(4), 276– 291.

APPENDICES A

Table A4.1 MBE-T and MBE-P values for years 1960 - 1999. They are evaluated for land only, sea only, and both land & sea

Models	Temperature			Precipitation		
	Land-only	Sea-only	Land & Sea	Land-only	Sea-only	Land & Sea
BCC-CSM1-1	0.35	0.76	0.68	185.31	102.80	119.62
BCC-CSM1-1-M	0.88	1.73	1.56	-414.90	93.10	-10.44
BNU-ESM	-0.10	-0.11	-0.11	-0.15	248.42	197.76
CanESM2	0.05	0.79	0.64	-428.05	493.82	305.92
CCSM4	-1.05	0.12	-0.12	-7.30	154.51	121.53
CESM1-BGC	-1.03	0.12	-0.12	-54.42	150.69	108.88
CESM1-CAM5	-1.46	-0.48	-0.68	-159.05	367.80	260.42
CESM1-FASTCHEM	-0.98	0.15	-0.08	0.26	143.38	114.21
CESM1-WACCM	-0.35	-0.02	-0.09	-188.62	254.28	164.01
CMCC-CESM	1.77	0.83	1.02	15.52	813.02	650.47
CMCC-CM	0.30	0.48	0.45	-853.95	302.84	67.05
CMCC-CMS	0.71	0.53	0.57	-550.09	427.70	228.40
CNRM-CM5	-1.13	-0.25	-0.43	-196.79	250.35	159.21
CNRM-CM5-2	-1.27	-0.38	-0.56	-172.12	243.56	158.83
CSIRO-Mk3-6-0	0.74	0.18	0.29	136.40	783.69	651.76
EC-EARTH	-2.51	-2.13	-2.20	-408.78	287.23	145.36
FGOALS-g2	-1.62	-1.27	-1.34	-116.63	112.95	66.16
FIO-ESM	0.03	-0.01	0.00	-111.67	173.84	115.65
GFDL-CM3	-1.02	-1.09	-1.08	-397.78	303.08	160.23
GFDL-ESM2G	-0.94	-0.86	-0.88	497.73	790.98	731.21
GFDL-ESM2M	-0.62	-0.73	-0.71	85.27	425.70	356.31
GISS-E2-H	-0.05	0.56	0.43	805.27	276.37	384.18
GISS-E2-H-CC	0.06	0.73	0.59	942.06	260.10	399.10
GISS-E2-R	0.05	0.70	0.57	733.79	307.02	394.00
GISS-E2-R-CC	0.04	0.69	0.56	727.33	307.95	393.43
HadCM3	0.30	0.92	0.80	12.70	1137.82	908.49
HadGEM2-AO	0.89	0.67	0.72	-259.24	563.42	395.74
HadGEM2-CC	-0.18	-0.04	-0.07	-390.45	409.32	246.31
HadGEM2-ES	0.17	0.28	0.26	-281.73	526.03	361.39
INMCM4	-3.05	-1.36	-1.70	614.39	218.79	299.42
IPSL-CM5A-LR	-0.91	-1.23	-1.17	-135.46	253.42	174.15
IPSL-CM5A-MR	-0.24	-0.28	-0.27	25.69	312.68	254.19

Table A4.1 MBE-T and MBE-P values for years 1960 - 1999. They are evaluated for land only, sea only, and both land & sea (Continued)

Models	Temperature			Precipitation		
	Land-only	Sea-only	Land & Sea	Land-only	Sea-only	Land & Sea
IPSL-CM5B-LR	-1.02	-1.13	-1.11	-119.77	89.31	46.70
MIROC5	-0.11	-0.21	-0.19	-8.85	356.84	282.31
MIROC-ESM	-0.26	-0.97	-0.83	-191.94	366.33	252.54
MIROC-ESM-CHEM	-0.14	-0.92	-0.76	-205.36	376.29	257.74
MPI-ESM-LR	0.00	-0.07	-0.06	-369.83	679.09	465.29
MPI-ESM-MR	0.18	0.10	0.11	-375.73	705.60	485.20
MRI-CGCM3	-1.33	-0.83	-0.94	218.12	174.53	183.42
NorESM1_M	-1.43	-0.99	-1.08	-174.93	103.58	46.81
6-MODEL ENSEMBLE	-1.01	-0.16	-0.34	-98.30	235.89	167.77
40-MODEL ENSEMBLE	-0.41	-0.13	-0.18	-39.34	358.71	277.57

Table A4.2 DTR values for summer, rainy, and winter for years 1960 - 1999. They are evaluated for land only, sea only, and both land & sea.

Models	Summer			Rainy			Winter		
	Land-only	Sea-only	Land & Sea	Land-only	Sea-only	Land & Sea	Land-only	Sea-only	Land & Sea
Mean reference	9.42	1.48	3.10	7.54	1.39	2.64	7.58	1.44	2.69
BCC-CSM1-1	6.82	0.66	1.91	4.79	0.59	1.45	5.98	0.58	1.68
BCC-CSM1-1-M	7.96	0.46	1.99	6.38	0.43	1.64	7.04	0.40	1.75
BNU-ESM	7.50	1.67	2.86	4.96	1.33	2.07	6.29	1.40	2.40
CanESM2	8.05	1.77	3.05	5.52	1.74	2.51	7.55	1.78	2.95
CCSM4	7.99	1.01	2.43	5.46	0.88	1.82	6.91	0.97	2.18
CESM1-BGC	7.92	1.01	2.42	5.50	0.88	1.83	6.97	0.97	2.19
CESM1-CAM5	7.59	1.06	2.39	5.46	0.97	1.89	6.82	1.04	2.22
CESM1-FASTCHEM	8.06	1.01	2.45	5.49	0.88	1.82	6.97	0.97	2.19
CESM1-WACCM	6.11	1.00	2.04	4.46	0.91	1.64	5.28	0.90	1.80

Table A4.2 DTR values for summer, rainy, and winter for years 1960 - 1999. They are evaluated for land only, sea only, and both land & sea. (Continued)

Models	Summer			Rainy			Winter		
	Land-only	Sea-only	Land & Sea	Land-only	Sea-only	Land & Sea	Land-only	Sea-only	Land & Sea
CMCC-CESM	7.43	2.00	3.11	5.49	1.65	2.43	6.33	1.79	2.71
CMCC-CM	9.70	1.46	3.14	7.29	1.37	2.58	8.46	1.42	2.85
CMCC-CMS	8.25	1.46	2.84	5.94	1.25	2.21	6.86	1.32	2.45
CNRM-CM5	9.68	1.33	3.03	7.04	1.24	2.42	8.60	1.29	2.78
CNRM-CM5-2	9.61	1.33	3.02	7.04	1.25	2.43	8.55	1.29	2.77
CSIRO-Mk3-6-0	9.98	1.25	3.03	8.20	1.75	3.06	8.97	1.62	3.12
EC-EARTH	8.17	1.79	3.09	5.72	1.89	2.67	7.22	1.86	2.95
FGOALS-g2	7.23	1.82	2.92	5.39	1.72	2.47	7.26	1.79	2.91
FIO-ESM	6.27	1.26	2.28	4.28	1.06	1.72	5.51	1.11	2.00
GFDL-CM3	8.48	1.45	2.88	5.59	1.20	2.10	7.26	1.33	2.54
GFDL-ESM2G	7.01	1.05	2.27	4.39	0.87	1.59	6.16	0.97	2.02
GFDL-ESM2M	7.52	1.19	2.48	5.09	1.02	1.85	6.54	1.13	2.23
GISS-E2-H	5.61	1.49	2.33	4.43	1.40	2.02	5.28	1.48	2.26
GISS-E2-H-CC	5.49	1.48	2.30	4.29	1.39	1.98	5.19	1.48	2.24
GISS-E2-R	5.75	1.49	2.36	5.15	1.45	2.20	5.58	1.48	2.32
GISS-E2-R-CC	5.74	1.49	2.36	5.17	1.45	2.21	5.58	1.48	2.32
HadCM3	9.21	1.55	3.11	6.71	1.37	2.46	7.93	1.47	2.78
HadGEM2-AO	8.22	1.28	2.69	5.88	1.11	2.08	6.60	1.18	2.29
HadGEM2-CC	8.09	1.28	2.67	6.05	1.11	2.12	6.78	1.20	2.34
HadGEM2-ES	7.72	1.23	2.55	5.80	1.08	2.04	6.43	1.16	2.23
INMCM4	10.34	1.36	3.19	6.25	1.13	2.18	8.39	1.27	2.72

Table A4.2 DTR values for summer, rainy, and winter for years 1960 - 1999. They are evaluated for land only, sea only, and both land & sea. (Continued)

Models	Summer			Rainy			Winter		
	Land -only	Sea-only	Land & Sea	Land -only	Sea-only	Land & Sea	Land -only	Sea-only	Land & Sea
IPSL-CM5A-LR	6.37	1.25	2.30	6.31	1.25	2.28	6.33	1.25	2.29
IPSL-CM5A-MR	6.41	1.14	2.22	6.45	1.14	2.23	6.40	1.14	2.21
IPSL-CM5B-LR	6.91	1.36	2.49	6.79	1.36	2.47	6.96	1.36	2.50
MIROC5	7.03	1.32	2.48	4.89	1.20	1.95	6.14	1.24	2.24
MIROC-ESM	7.61	1.52	2.76	5.15	1.34	2.12	5.75	1.30	2.21
MIROC-ESM-CHEM	7.72	1.57	2.82	5.24	1.36	2.15	5.76	1.31	2.22
MPI-ESM-LR	7.92	1.50	2.81	5.62	1.27	2.16	6.52	1.29	2.35
MPI-ESM-MR	7.82	1.33	2.65	5.57	1.15	2.05	6.45	1.15	2.23
MRI-CGCM3	7.64	1.23	2.54	5.66	1.07	2.01	6.75	1.18	2.32
NorESM1_M	6.80	1.07	2.24	4.85	0.95	1.74	4.85	0.95	2.00
6-MODEL ENSEMBLE	8.38	1.23	2.69	5.91	1.09	2.07	7.36	1.16	2.42
40-MODEL ENSEMBLE	7.64	1.32	2.61	5.64	1.21	2.12	6.68	1.26	2.37

Table A4.3 SeasonAmp-T and SeasonAmp-P values for years 1960 - 1999. They are evaluated for land only, sea only, and both land & sea

Models	Temperature			Precipitation		
	Land-only	Sea-only	Land & Sea	Land-only	Sea-only	Land & Sea
Mean reference	3.76	1.80	2.20	6.47	3.50	4.10
BCC-CSM1-1	4.98	1.60	2.22	7.54	3.41	4.25
BCC-CSM1-1-M	5.35	2.18	2.62	8.80	3.90	4.87
BNU-ESM	5.53	1.86	2.58	8.63	4.68	5.05
CanESM2	3.93	1.38	1.77	6.09	2.12	2.84
CCSM4	5.06	1.62	2.16	8.17	3.35	3.83
CESM1-BGC	5.00	1.66	2.17	8.19	3.41	3.68
CESM1-CAM5	4.41	1.68	2.06	7.63	2.84	3.39
CESM1-FASTCHEM	5.10	1.65	2.18	8.52	3.44	3.95

Table A4.3 SeasonAmp-T and SeasonAmp-P values for years 1960 - 1999. They are evaluated for land only, sea only, and both land & sea (Continued)

Models	Temperature			Precipitation		
	Land-only	Sea-only	Land & Sea	Land-only	Sea-only	Land & Sea
CESM1-WACCM	4.16	1.45	1.77	6.94	3.33	3.46
CMCC-CESM	4.46	1.93	2.27	1.71	6.50	6.27
CMCC-CM	5.36	1.92	2.50	6.62	6.31	6.25
CMCC-CMS	5.39	1.98	2.56	7.54	5.76	6.08
CNRM-CM5	4.45	1.63	2.20	5.69	2.25	2.59
CNRM-CM5-2	4.46	1.65	2.22	5.32	2.34	2.53
CSIRO-Mk3-6-0	6.00	2.26	2.79	9.25	3.22	4.41
EC-EARTH	2.94	1.09	1.27	1.61	4.28	3.32
FGOALS-g2	5.22	1.97	2.60	8.28	2.71	3.74
FIO-ESM	5.47	1.41	2.14	8.28	3.28	4.80
GFDL-CM3	5.18	2.37	2.63	1.16	2.98	4.90
GFDL-ESM2G	5.45	2.16	2.64	7.71	2.34	3.50
GFDL-ESM2M	5.27	2.00	2.45	8.52	2.75	4.09
GISS-E2-H	3.65	1.22	1.66	6.10	2.23	2.58
GISS-E2-H-CC	3.78	1.12	1.59	6.38	2.48	2.90
GISS-E2-R	1.92	0.67	0.90	3.31	1.33	1.73
GISS-E2-R-CC	1.84	0.64	0.87	3.15	1.30	1.68
HadCM3	5.31	1.63	2.26	7.10	2.79	3.36
HadGEM2-AO	5.76	1.61	2.45	6.31	4.34	4.69
HadGEM2-CC	5.35	1.57	2.17	5.82	3.14	4.49
HadGEM2-ES	5.33	1.47	2.07	6.09	4.02	4.37
INMCM4	5.47	0.90	1.87	7.23	1.95	2.98
IPSL-CM5A-LR	4.60	1.74	2.32	8.55	2.35	3.40
IPSL-CM5A-MR	4.74	1.64	2.27	8.52	1.49	2.70
IPSL-CM5B-LR	4.86	1.85	2.46	10.48	3.69	4.92
MIROC5	4.44	2.14	2.54	5.54	5.86	4.30
MIROC-ESM	5.52	1.61	2.39	8.14	5.15	2.83
MIROC-ESM-CHEM	5.48	1.62	2.41	7.85	5.10	4.18
MPI-ESM-LR	5.23	1.91	2.38	8.74	5.15	4.96
MPI-ESM-MR	5.36	1.98	2.43	9.33	5.37	5.09
MRI-CGCM3	6.20	1.80	2.60	8.87	4.81	5.64
NorESM1_M	5.05	1.46	2.09	8.37	3.29	4.39
6-MODEL ENSEMBLE	4.82	1.68	2.23	7.27	3.15	3.51
40-MODEL ENSEMBLE	4.83	1.65	2.19	6.95	3.53	3.97

Table A4.4 r-T for years 1960 - 1999. They are evaluated for land only, sea only, and both land & sea.

Models	Summer			Rainy			Winter		
	Land -only	Sea-only	Land & Sea	Land -only	Sea-only	Land & Sea	Land -only	Sea-only	Land & Sea
BCC-CSM1-1	1.00	1.00	0.92	1.00	1.00	0.77	1.00	1.00	0.95
BCC-CSM1-1-M	1.00	1.00	0.90	1.00	1.00	0.80	1.00	1.00	0.94
BNU-ESM	1.00	1.00	0.94	1.00	1.00	0.87	1.00	1.00	0.96
CanESM2	1.00	1.00	0.90	1.00	1.00	0.83	1.00	1.00	0.94
CCSM4	1.00	1.00	0.93	1.00	1.00	0.91	1.00	1.00	0.96
CESM1-BGC	1.00	1.00	0.93	1.00	1.00	0.91	1.00	1.00	0.96
CESM1-CAM5	1.00	1.00	0.94	1.00	1.00	0.92	1.00	1.00	0.97
CESM1-FASTCHEM	1.00	1.00	0.93	1.00	1.00	0.91	1.00	1.00	0.96
CESM1-WACCM	1.00	1.00	0.93	1.00	1.00	0.88	1.00	1.00	0.95
CMCC-CESM	1.00	1.00	0.85	1.00	1.00	0.59	1.00	1.00	0.93
CMCC-CM	1.00	1.00	0.86	1.00	1.00	0.85	1.00	1.00	0.95
CMCC-CMS	1.00	1.00	0.89	1.00	1.00	0.89	1.00	1.00	0.96
CNRM-CM5	1.00	1.00	0.94	1.00	1.00	0.91	1.00	1.00	0.96
CNRM-CM5-2	1.00	1.00	0.93	1.00	1.00	0.91	1.00	1.00	0.96
CSIRO-Mk3-6-0	1.00	0.99	0.86	1.00	1.00	0.64	0.99	1.00	0.94
EC-EARTH	1.00	1.00	0.93	1.00	1.00	0.88	1.00	1.00	0.96
FGOALS-g2	1.00	1.00	0.95	1.00	1.00	0.84	1.00	1.00	0.96
FIO-ESM	1.00	1.00	0.94	1.00	1.00	0.86	0.99	1.00	0.95
GFDL-CM3	1.00	1.00	0.88	1.00	1.00	0.89	1.00	1.00	0.97
GFDL-ESM2G	1.00	1.00	0.88	1.00	1.00	0.87	1.00	1.00	0.95
GFDL-ESM2M	1.00	1.00	0.89	1.00	1.00	0.88	1.00	1.00	0.96
GISS-E2-H	1.00	1.00	0.91	1.00	1.00	0.78	1.00	1.00	0.96

Table A4.4 r-T for years 1960 - 1999. They are evaluated for land only, sea only, and both land & sea. (Continued)

Models	Summer			Rainy			Winter		
	Land -only	Sea-only	Land & Sea	Land -only	Sea-only	Land & Sea	Land -only	Sea-only	Land & Sea
GISS-E2-H-CC	1.00	1.00	0.90	1.00	1.00	0.78	1.00	1.00	0.96
GISS-E2-R	1.00	1.00	0.93	1.00	0.99	0.57	1.00	1.00	0.95
GISS-E2-R-CC	1.00	1.00	0.93	1.00	0.99	0.56	1.00	1.00	0.95
HadCM3	0.99	1.00	0.89	1.00	1.00	0.77	0.99	1.00	0.95
HadGEM2-AO	1.00	1.00	0.88	1.00	1.00	0.83	0.99	1.00	0.95
HadGEM2-CC	0.99	1.00	0.89	1.00	1.00	0.84	0.99	1.00	0.94
HadGEM2-ES	0.99	1.00	0.90	1.00	1.00	0.84	0.99	1.00	0.94
INMCM4	1.00	1.00	0.85	1.00	1.00	0.84	0.98	1.00	0.92
IPSL-CM5A-LR	1.00	1.00	0.91	1.00	1.00	0.86	0.99	1.00	0.97
IPSL-CM5A-MR	1.00	1.00	0.92	1.00	1.00	0.88	0.99	1.00	0.97
IPSL-CM5B-LR	1.00	1.00	0.90	1.00	1.00	0.84	0.99	1.00	0.95
MIROC5	1.00	1.00	0.88	1.00	1.00	0.76	1.00	1.00	0.97
MIROC-ESM	1.00	1.00	0.86	1.00	1.00	0.67	1.00	1.00	0.96
MIROC-ESM-CHEM	1.00	1.00	0.85	1.00	1.00	0.67	1.00	1.00	0.96
MPI-ESM-LR	1.00	1.00	0.91	1.00	1.00	0.89	1.00	1.00	0.96
MPI-ESM-MR	1.00	1.00	0.91	1.00	1.00	0.89	1.00	1.00	0.96
MRI-CGCM3	1.00	1.00	0.94	1.00	1.00	0.86	1.00	1.00	0.97
NorESM1_M	1.00	1.00	0.90	1.00	1.00	0.85	0.99	1.00	0.95
6-MODEL ENSEMBLE	1.00	1.00	0.95	1.00	1.00	0.92	1.00	1.00	0.97
40-MODEL ENSEMBLE	1.00	1.00	0.95	1.00	1.00	0.91	1.00	1.00	0.97

Table A4.5 r-P values for years 1960 - 1999. They are evaluated for land only, sea only, and both land & sea.

Models	Summer			Rainy			Winter		
	Land -only	Sea- only	Land & Sea	Land -only	Sea- only	Land & Sea	Land -only	Sea- only	Land & Sea
BCC-CSM1-1	0.97	0.79	0.83	0.93	0.79	0.67	0.95	0.72	0.75
BCC-CSM1-1-M	0.89	0.87	0.78	0.94	0.89	0.65	0.91	0.78	0.80
BNU-ESM	0.97	0.86	0.83	0.95	0.83	0.67	0.98	0.87	0.82
CanESM2	0.95	0.89	0.75	0.96	0.88	0.62	0.95	0.88	0.78
CCSM4	0.96	0.88	0.79	0.97	0.90	0.76	0.97	0.92	0.80
CESM1-BGC	0.95	0.88	0.77	0.97	0.91	0.77	0.97	0.92	0.82
CESM1-CAM5	0.98	0.91	0.80	0.97	0.87	0.77	0.96	0.92	0.78
CESM1-FASTCHEM	0.97	0.88	0.79	0.97	0.90	0.76	0.97	0.92	0.80
CESM1-WACCM	0.95	0.90	0.77	0.96	0.90	0.74	0.96	0.90	0.75
CMCC-CESM	0.95	0.82	0.77	0.90	0.76	0.51	0.98	0.75	0.77
CMCC-CM	0.92	0.76	0.77	0.91	0.82	0.64	0.90	0.77	0.73
CMCC-CMS	0.92	0.80	0.77	0.90	0.81	0.65	0.94	0.80	0.70
CNRM-CM5	0.97	0.89	0.85	0.94	0.83	0.74	0.98	0.89	0.83
CNRM-CM5-2	0.96	0.89	0.85	0.94	0.83	0.73	0.98	0.89	0.88
CSIRO-Mk3-6-0	0.89	0.78	0.71	0.95	0.74	0.56	0.92	0.76	0.75
EC-EARTH	0.95	0.85	0.73	0.94	0.81	0.61	0.97	0.87	0.77
FGOALS-g2	0.98	0.89	0.80	0.89	0.78	0.61	0.98	0.80	0.69
FIO-ESM	0.94	0.83	0.81	0.94	0.80	0.53	0.97	0.87	0.81
GFDL-CM3	0.96	0.83	0.72	0.93	0.80	0.65	0.98	0.85	0.80
GFDL-ESM2G	0.98	0.79	0.76	0.93	0.76	0.63	0.96	0.82	0.83
GFDL-ESM2M	0.98	0.84	0.81	0.87	0.78	0.65	0.96	0.85	0.82
GISS-E2-H	0.81	0.78	0.68	0.85	0.64	0.29	0.94	0.77	0.49

Table A4.5 r-P values for years 1960 - 1999. They are evaluated for land only, sea only, and both land & sea. (Continued)

Models	Summer			Rainy			Winter		
	Land -only	Sea- only	Land & Sea	Land -only	Sea- only	Land & Sea	Land -only	Sea- only	Land & Sea
GISS-E2-H-CC	0.80	0.78	0.66	0.84	0.59	0.21	0.95	0.75	0.46
GISS-E2-R	0.94	0.80	0.70	0.86	0.67	0.44	0.95	0.80	0.67
GISS-E2-R-CC	0.94	0.80	0.70	0.85	0.65	0.40	0.95	0.80	0.67
HadCM3	0.98	0.83	0.65	0.95	0.76	0.24	0.98	0.86	0.74
HadGEM2-AO	0.93	0.77	0.76	0.94	0.83	0.63	0.96	0.79	0.73
HadGEM2-CC	0.97	0.74	0.72	0.94	0.79	0.56	0.97	0.78	0.63
HadGEM2-ES	0.96	0.76	0.73	0.95	0.78	0.54	0.97	0.72	0.53
INMCM4	0.97	0.85	0.85	0.89	0.73	0.54	0.97	0.82	0.70
IPSL-CM5A-LR	0.98	0.82	0.69	0.93	0.78	0.59	0.98	0.83	0.73
IPSL-CM5A-MR	0.99	0.84	0.73	0.96	0.78	0.60	0.97	0.83	0.74
IPSL-CM5B-LR	0.95	0.75	0.83	0.90	0.75	0.67	0.95	0.71	0.77
MIROC5	0.96	0.88	0.83	0.94	0.82	0.47	0.96	0.82	0.74
MIROC-ESM	0.97	0.82	0.80	0.92	0.61	0.14	0.98	0.83	0.72
MIROC-ESM-CHEM	0.97	0.83	0.80	0.92	0.62	0.16	0.98	0.83	0.73
MPI-ESM-LR	0.93	0.87	0.75	0.94	0.81	0.43	0.88	0.82	0.73
MPI-ESM-MR	0.94	0.86	0.72	0.93	0.82	0.50	0.91	0.80	0.71
MRI-CGCM3	0.97	0.85	0.79	0.88	0.70	0.72	0.96	0.79	0.78
NorESM1_M	0.88	0.84	0.79	0.95	0.88	0.71	0.97	0.88	0.79
6-MODEL ENSEMBLE	0.97	0.88	0.92	0.96	0.86	0.84	0.97	0.90	0.90
40-MODEL ENSEMBLE	0.95	0.83	0.91	0.92	0.78	0.81	0.96	0.83	0.90

Table A4.6 NSD-T values for years 1960 - 1999. They are evaluated for land only, sea only, and both land & sea

Models	Summer			Rainy			Winter		
	Land -only	Sea-only	Land & Sea	Land -only	Sea-only	Land & Sea	Land -only	Sea-only	Land & Sea
BCC-CSM1-1	1.13	1.19	1.16	1.20	0.91	1.06	1.34	1.06	1.25
BCC-CSM1-1-M	1.10	1.37	1.26	1.27	1.08	1.21	1.23	1.19	1.27
BNU-ESM	0.90	1.05	0.97	0.77	0.84	0.81	1.17	1.07	1.14
CanESM2	0.82	0.89	0.93	1.04	1.13	1.19	1.01	0.92	1.07
CCSM4	1.09	1.10	1.18	1.23	0.91	1.20	1.30	1.07	1.31
CESM1-BGC	1.10	1.12	1.19	1.23	0.92	1.20	1.28	1.07	1.29
CESM1-CAM5	1.05	1.15	1.17	1.19	0.96	1.19	1.13	1.00	1.17
CESM1-FASTCHEM	1.08	1.09	1.17	1.23	0.91	1.19	1.30	1.07	1.31
CESM1-WACCM	0.93	0.87	0.94	1.12	0.79	1.00	1.12	0.85	1.06
CMCC-CESM	0.99	1.41	1.14	0.92	0.92	0.81	1.14	1.18	1.07
CMCC-CM	0.97	0.97	0.94	1.42	0.89	1.16	1.12	0.88	1.09
CMCC-CMS	0.84	1.01	0.89	1.00	0.93	0.94	1.07	0.88	1.03
CNRM-CM5	0.94	1.00	1.01	1.26	1.12	1.28	1.18	1.09	1.21
CNRM-CM5-2	0.95	1.00	1.02	1.26	1.15	1.28	1.16	1.08	1.20
CSIRO-Mk3-6-0	1.15	1.61	1.32	1.11	1.26	1.00	1.44	1.39	1.34
EC-EARTH	0.84	0.67	0.80	1.16	0.56	1.05	0.94	0.66	0.91
FGOALS-g2	0.96	1.13	1.04	0.97	0.80	0.97	1.14	1.21	1.14
FIO-ESM	0.86	0.94	0.89	0.90	0.68	0.79	1.28	1.02	1.19
GFDL-CM3	0.86	1.53	1.18	0.92	0.99	0.97	1.16	1.38	1.22
GFDL-ESM2G	0.85	1.39	1.10	1.10	1.13	1.10	1.25	1.39	1.28
GFDL-ESM2M	0.86	1.35	1.08	1.08	1.09	1.03	1.25	1.31	1.24
GISS-E2-H	1.07	1.29	1.19	1.28	1.06	1.22	1.16	1.18	1.18

Table A4.6 NSD-T values for years 1960 - 1999. They are evaluated for land only, sea only, and both land & sea (Continued)

Models	Summer			Rainy			Winter		
	Land -only	Sea-only	Land & Sea	Land -only	Sea-only	Land & Sea	Land -only	Sea-only	Land & Sea
GISS-E2-H-CC	1.06	1.25	1.17	1.31	1.11	1.26	1.19	1.17	1.20
GISS-E2-R	1.15	1.33	1.31	1.75	1.61	1.73	1.06	1.27	1.15
GISS-E2-R-CC	1.16	1.33	1.32	1.78	1.65	1.76	1.06	1.28	1.16
HadCM3	1.44	1.47	1.47	1.15	0.97	1.05	1.36	1.09	1.27
HadGEM2-AO	1.06	1.11	1.04	1.06	0.99	0.95	1.25	1.15	1.18
HadGEM2-CC	1.29	1.26	1.28	1.10	0.99	0.99	1.19	0.98	1.11
HadGEM2-ES	1.29	1.22	1.26	1.08	0.96	0.96	1.17	0.97	1.10
INMCM4	1.02	0.99	1.18	1.16	1.09	1.30	1.41	1.08	1.43
IPSL-CM5A-LR	0.97	1.26	1.10	0.92	1.01	0.87	1.19	1.15	1.14
IPSL-CM5A-MR	1.03	1.25	1.14	1.03	1.04	0.95	1.26	1.10	1.19
IPSL-CM5B-LR	1.07	1.44	1.24	1.05	1.16	1.00	1.24	1.32	1.22
MIROC5	0.94	1.25	1.07	1.28	1.01	1.08	1.03	1.20	1.09
MIROC-ESM	0.77	1.01	0.85	0.82	0.84	0.73	1.03	0.97	1.01
MIROC-ESM-CHEM	0.76	1.01	0.84	0.80	0.82	0.71	1.03	0.98	1.00
MPI-ESM-LR	0.83	1.05	0.91	0.99	0.76	0.90	1.10	1.01	1.10
MPI-ESM-MR	0.83	1.09	0.93	0.95	0.79	0.88	1.13	1.00	1.11
MRI-CGCM3	1.06	1.26	1.18	1.26	0.93	1.08	1.29	1.25	1.30
NorESM1_M	1.08	1.04	1.09	1.18	0.74	0.99	1.35	1.12	1.28
6-MODEL ENSEMBLE	1.00	1.07	1.09	1.16	0.98	1.16	1.20	1.06	1.22
40-MODEL ENSEMBLE	1.00	1.17	1.10	1.13	0.99	1.07	1.19	1.10	1.17

Table A4.7 NSD-P values for years 1960 - 1999. They are evaluated for land only, sea only, and both land & sea

Models	Summer			Rainy			Winter		
	Land -only	Sea-only	Land & Sea	Land -only	Sea-only	Land & Sea	Land -only	Sea-only	Land & Sea
BCC-CSM1-1	1.37	1.43	1.41	1.44	1.04	1.13	1.32	1.41	1.35
BCC-CSM1-1-M	0.96	1.11	1.07	1.01	0.92	0.93	1.00	1.20	1.12
BNU-ESM	1.19	1.25	1.23	0.97	0.76	0.79	1.13	1.08	1.10
CanESM2	0.84	1.20	1.10	0.74	0.88	0.87	0.84	1.15	1.09
CCSM4	1.01	1.16	1.11	0.88	0.78	0.81	1.08	1.07	1.07
CESM1-BGC	0.98	1.20	1.13	0.85	0.80	0.82	1.10	1.09	1.08
CESM1-CAM5	0.99	1.11	1.08	0.83	0.76	0.76	1.03	1.08	1.08
CESM1-FASTCHEM	1.02	1.18	1.12	0.89	0.80	0.84	1.11	1.10	1.09
CESM1-WACCM	0.82	1.06	0.99	0.68	0.69	0.69	0.92	1.11	1.06
CMCC-CESM	1.41	2.27	2.02	1.26	1.23	1.24	0.97	1.56	1.35
CMCC-CM	0.76	1.37	1.20	0.99	1.53	1.51	0.73	1.38	1.19
CMCC-CMS	0.79	1.35	1.19	1.16	1.42	1.41	0.79	1.26	1.12
CNRM-CM5	1.04	1.08	1.07	0.98	0.93	0.93	0.95	0.88	0.91
CNRM-CM5-2	1.08	1.12	1.10	1.00	0.96	0.95	0.93	0.87	0.90
CSIRO-Mk3-6-0	1.26	1.90	1.72	1.23	1.31	1.29	1.35	1.91	1.70
EC-EARTH	0.74	1.19	1.07	0.86	0.90	0.89	0.78	1.12	1.05
FGOALS-g2	0.85	1.05	0.98	1.65	1.16	1.25	0.93	1.14	1.06
FIO-ESM	1.23	1.26	1.25	0.90	0.70	0.73	1.16	1.06	1.09
GFDL-CM3	0.94	1.61	1.42	0.66	0.76	0.74	0.84	1.29	1.14
GFDL-ESM2G	1.41	1.67	1.58	1.15	0.99	1.01	1.36	1.55	1.46
GFDL-ESM2M	1.34	1.57	1.49	1.06	0.94	0.96	1.28	1.41	1.35
GISS-E2-H	1.48	1.60	1.58	2.51	0.99	1.44	1.46	1.54	1.48

Table A4.7 NSD-P values for years 1960 - 1999. They are evaluated for land only, sea only, and both land & sea (Continued)

Models	Summer			Rainy			Winter		
	Land -only	Sea-only	Land & Sea	Land -only	Sea-only	Land & Sea	Land -only	Sea-only	Land & Sea
GISS-E2-H-CC	1.60	1.56	1.59	2.73	1.03	1.56	1.63	1.57	1.57
GISS-E2-R	1.43	1.38	1.41	1.65	0.96	1.12	1.35	1.43	1.38
GISS-E2-R-CC	1.43	1.38	1.40	1.67	0.97	1.13	1.35	1.43	1.38
HadCM3	1.17	1.75	1.59	0.93	1.08	1.09	1.06	1.51	1.39
HadGEM2-AO	1.26	1.85	1.67	1.31	1.40	1.39	1.13	1.64	1.45
HadGEM2-CC	2.13	3.17	2.86	1.12	1.17	1.17	0.84	1.32	1.14
HadGEM2-ES	1.32	1.97	1.77	1.12	1.16	1.17	0.92	1.62	1.36
INMCM4	1.64	1.30	1.45	1.30	0.92	1.05	1.38	1.20	1.27
IPSL-CM5A-LR	1.22	1.35	1.31	1.09	0.99	1.00	1.08	1.34	1.23
IPSL-CM5A-MR	1.42	1.37	1.39	1.44	1.06	1.12	1.19	1.29	1.24
IPSL-CM5B-LR	1.56	1.72	1.66	1.25	1.22	1.21	1.28	1.66	1.49
MIROC5	0.88	1.14	1.06	1.05	0.92	0.95	1.03	1.48	1.36
MIROC-ESM	1.16	1.57	1.44	0.90	0.90	0.90	1.02	1.44	1.29
MIROC-ESM-CHEM	1.16	1.56	1.43	0.89	0.88	0.88	1.01	1.45	1.30
MPI-ESM-LR	0.83	1.41	1.25	0.89	1.05	1.04	0.99	1.51	1.39
MPI-ESM-MR	0.79	1.53	1.35	1.14	1.13	1.14	0.95	1.56	1.42
MRI-CGCM3	1.82	1.60	1.68	1.46	1.12	1.19	1.60	1.40	1.47
NorESM1_M	0.99	1.33	1.22	0.71	0.69	0.70	1.05	1.33	1.22
6-MODEL ENSEMBLE	1.05	1.15	1.07	0.92	0.83	0.75	1.04	1.01	0.97
40-MODEL ENSEMBLE	1.18	1.47	1.23	1.16	1.00	0.74	1.10	1.34	1.05

Table A4.8 RMSE-T values for years 1960 - 1999. They are evaluated for land only, sea only, and both land & sea

Models	Summer			Rainy			Winter		
	Land -only	Sea-only	Land & Sea	Land -only	Sea-only	Land & Sea	Land -only	Sea-only	Land & Sea
BCC-CSM1-1	0.72	1.01	1.24	0.69	0.84	1.09	0.95	1.02	1.39
BCC-CSM1-1-M	0.72	1.72	1.86	0.81	1.77	1.95	0.82	1.80	1.98
BNU-ESM	0.60	0.42	0.74	0.50	0.37	0.62	0.82	0.44	0.94
CanESM2	0.67	0.99	1.19	0.53	0.87	1.02	0.60	1.09	1.25
CCSM4	0.80	0.60	1.00	0.52	0.36	0.63	1.08	0.60	1.24
CESM1-BGC	0.80	0.61	1.01	0.52	0.36	0.63	1.05	0.57	1.19
CESM1-CAM5	0.93	0.80	1.23	0.67	0.51	0.84	0.93	0.46	1.04
CESM1-FASTCHEM	0.77	0.60	0.98	0.51	0.37	0.63	1.06	0.61	1.22
CESM1-WACCM	0.69	0.42	0.80	0.51	0.33	0.60	0.73	0.49	0.88
CMCC-CESM	1.14	1.10	1.58	1.05	1.11	1.53	1.00	1.10	1.48
CMCC-CM	0.97	0.80	1.26	0.59	0.67	0.89	0.60	0.78	0.98
CMCC-CMS	0.91	0.77	1.19	0.56	0.62	0.83	0.58	0.69	0.90
CNRM-CM5	0.57	0.56	0.80	0.64	0.53	0.83	0.92	0.59	1.09
CNRM-CM5-2	0.62	0.60	0.86	0.67	0.60	0.90	0.95	0.63	1.59
CSIRO-Mk3-6-0	0.78	1.24	1.46	0.84	0.84	1.19	1.10	0.97	1.46
EC-EARTH	1.11	1.93	2.22	1.31	2.07	2.44	1.05	1.75	2.04
FGOALS-g2	0.76	1.22	1.44	0.85	1.13	1.42	1.02	1.47	1.79
FIO-ESM	0.58	0.45	0.73	0.49	0.40	0.63	0.94	0.52	1.07
GFDL-CM3	0.50	1.67	1.74	0.56	0.89	1.05	0.89	1.26	1.54
GFDL-ESM2G	0.57	1.32	1.44	0.62	0.70	0.94	1.13	1.20	1.65
GFDL-ESM2M	0.53	1.19	1.30	0.52	0.65	0.84	1.01	1.04	1.45
GISS-E2-H	0.60	1.09	1.25	0.57	0.84	1.02	0.63	0.95	1.14

Table A4.8 RMSE-T values for years 1960 - 1999. They are evaluated for land only, sea only, and both land & sea (Continued)

Models	Summer			Rainy			Winter		
	Land -only	Sea-only	Land & Sea	Land -only	Sea-only	Land & Sea	Land -only	Sea-only	Land & Sea
GISS-E2-H-CC	0.62	1.18	1.33	0.58	0.93	1.10	0.68	1.06	1.26
GISS-E2-R	0.68	1.03	1.23	1.11	1.38	1.77	0.53	1.00	1.13
GISS-E2-R-CC	0.70	1.02	1.24	1.15	1.42	1.83	0.53	1.00	1.13
HadCM3	1.16	1.19	1.66	0.69	1.09	1.29	0.97	1.24	1.57
HadGEM2-AO	0.90	1.09	1.41	0.66	0.78	1.02	0.75	0.97	1.23
HadGEM2-CC	0.91	0.89	1.27	0.47	0.52	0.70	0.74	0.72	1.03
HadGEM2-ES	0.84	0.87	1.21	0.52	0.56	0.76	0.69	0.81	1.06
INMCM4	1.55	1.23	1.98	1.31	1.48	1.97	2.03	1.33	2.42
IPSL-CM5A-LR	1.02	1.72	2.00	0.64	1.67	1.79	1.13	1.82	2.14
IPSL-CM5A-MR	0.74	0.98	1.23	0.40	0.90	0.98	1.00	0.95	1.38
IPSL-CM5B-LR	0.91	1.38	1.66	0.50	1.08	1.19	0.96	1.35	1.66
MIROC5	0.64	0.98	1.17	0.49	0.76	0.90	0.53	0.68	0.86
MIROC-ESM	0.73	1.09	1.32	0.52	1.05	1.17	0.74	1.03	1.27
MIROC-ESM-CHEM	0.76	1.05	1.30	0.52	1.00	1.13	0.71	0.99	1.22
MPI-ESM-LR	0.59	0.68	0.90	0.44	0.38	0.58	0.68	0.45	0.82
MPI-ESM-MR	0.58	0.68	0.90	0.49	0.42	0.65	0.68	0.45	0.82
MRI-CGCM3	0.79	1.06	1.32	0.63	0.91	1.10	1.14	0.91	1.46
NorESM1_M	1.04	1.16	1.56	0.70	0.99	1.21	1.31	0.89	1.58
6-MODEL ENSEMBLE	0.72	0.60	0.75	0.59	0.45	0.60	0.96	0.55	0.96
40-MODEL ENSEMBLE	0.79	1.01	0.67	0.66	0.85	0.54	0.89	0.94	0.78

Table A4.9 RMSE-P values for years 1960 - 1999. They are evaluated for land only, sea only, and both land & sea

Models	Summer			Rainy			Winter		
	Land-only	Sea-only	Land & Sea	Land-only	Sea-only	Land & Sea	Land-only	Sea-only	Land & Sea
BCC-CSM1-1	31.72	63.09	70.61	38.74	55.61	67.77	35.61	77.73	85.50
BCC-CSM1-1-M	28.63	44.20	52.66	37.70	48.91	61.76	26.23	59.47	65.00
BNU-ESM	23.82	46.34	52.11	33.54	52.32	62.15	23.71	45.98	51.73
CanESM2	24.71	54.60	59.93	39.13	47.58	61.60	30.19	49.04	57.58
CCSM4	20.40	43.26	47.83	23.74	44.71	50.62	21.95	39.50	45.19
CESM1-BGC	21.67	46.34	51.16	23.93	42.90	49.12	21.82	37.96	43.79
CESM1-CAM5	23.31	40.88	47.06	30.35	43.67	53.18	24.12	46.45	52.34
CESM1-FASTCHEM	20.59	44.12	48.69	23.45	44.87	50.63	21.96	39.97	45.61
CESM1-WACCM	22.50	39.43	45.40	29.66	44.39	53.39	24.08	49.49	55.04
CMCC-CESM	40.37	143.44	149.01	45.47	91.67	102.32	24.93	70.70	74.97
CMCC-CM	38.84	62.86	73.90	51.78	72.89	89.41	41.70	68.47	80.17
CMCC-CMS	36.53	53.06	64.42	45.08	72.27	85.18	33.65	61.97	70.52
CNRM-CM5	25.47	35.89	44.01	30.20	50.85	59.14	26.90	39.60	47.88

Table A4.9 RMSE-P values for years 1960 - 1999. They are evaluated for land only, sea only, and both land & sea (Continued)

Models	Summer			Rainy			Winter		
	Land-only	Sea-only	Land & Sea	Land-only	Sea-only	Land & Sea	Land-only	Sea-only	Land & Sea
CNRM-CM5-2	26.06	37.95	46.04	29.60	52.70	60.44	26.93	40.65	48.76
CSIRO-Mk3-6-0	34.01	98.65	104.35	33.95	84.26	90.84	32.18	95.62	100.89
EC-EARTH	34.15	49.15	59.85	38.54	57.67	69.36	30.79	50.87	59.46
FGOALS-g2	24.12	42.44	48.82	45.09	63.98	78.27	24.26	63.59	68.06
FIO-ESM	25.60	49.94	56.12	38.37	63.31	74.03	21.96	47.66	52.48
GFDL-CM3	31.78	70.34	77.18	35.95	51.95	63.18	24.23	47.68	53.48
GFDL-ESM2G	36.47	82.48	90.19	38.60	61.21	72.36	30.71	65.65	72.48
GFDL-ESM2M	29.69	70.84	76.81	37.81	53.81	65.77	25.81	54.28	60.10
GISS-E2-H	56.13	86.60	103.20	80.02	85.59	117.17	57.82	88.10	105.38
GISS-E2-H-CC	62.73	84.35	105.13	89.53	94.17	129.94	66.94	92.70	114.34
GISS-E2-R	47.60	76.93	90.46	54.49	77.85	95.03	41.40	72.05	83.10
GISS-E2-R-CC	47.35	77.22	90.58	56.12	81.53	98.98	41.21	72.02	82.98
HadCM3	38.28	107.22	113.84	42.42	104.25	112.54	27.75	94.80	98.77

Table A4.9 RMSE-P values for years 1960 - 1999. They are evaluated for land only, sea only, and both land & sea (Continued)

Models	Summer			Rainy			Winter		
	Land-only	Sea-only	Land & Sea	Land-only	Sea-only	Land & Sea	Land-only	Sea-only	Land & Sea
HadGEM2-AO	33.76	93.07	99.00	36.03	73.08	81.48	27.99	83.60	88.16
HadGEM2-CC	79.60	229.82	243.21	38.09	69.36	79.13	33.11	73.87	80.95
HadGEM2-ES	32.97	106.47	111.46	35.67	74.05	82.19	36.16	93.11	99.88
INMCM4	51.49	53.76	74.44	44.95	67.62	81.20	45.11	60.20	75.22
IPSL-CM5A-LR	38.46	62.21	73.13	42.20	59.81	73.20	32.33	56.91	65.45
IPSL-CM5A-MR	40.08	62.96	74.63	45.90	62.82	77.81	30.33	57.64	65.13
IPSL-CM5B-LR	42.49	79.05	89.75	41.74	65.81	77.94	34.07	83.26	89.96
MIROC5	19.75	38.30	43.09	32.63	68.40	75.78	25.79	77.49	81.67
MIROC-ESM	24.01	69.56	73.59	44.64	94.17	104.22	25.68	73.96	78.29
MIROC-ESM-CHEM	23.73	68.57	72.56	44.58	91.78	102.03	25.26	72.67	76.93
MPI-ESM-LR	33.64	53.79	63.44	41.44	74.47	85.23	35.75	74.51	82.64
MPI-ESM-MR	37.76	62.32	72.87	43.25	72.58	84.48	37.31	79.79	88.08
MRI-CGCM3	60.62	72.73	94.68	38.67	67.29	77.61	52.28	67.01	84.99

Table A4.9 RMSE-P values for years 1960 - 1999. They are evaluated for land only, sea only, and both land & sea (Continued)

Models	Summer			Rainy			Winter		
	Land-only	Sea-only	Land & Sea	Land - only	Sea-only	Land & Sea	Land-only	Sea-only	Land & Sea
NorESM1_M	23.73	50.24	55.56	28.80	54.20	61.38	19.68	50.48	54.18
6-MODEL ENSEMBLE	23.46	41.78	37.36	28.56	47.86	46.61	24.24	41.69	37.98
40-MODEL ENSEMBLE	34.87	68.86	47.72	40.80	66.01	47.25	31.74	64.41	38.97

Table A4.10 Var, RMSE, Trend and ENSO between observations and model simulations of mean annual temperature for years 1991 – 1999

Models	VAR	RMSE	Trend	ENSO
Mean reference	0.31	-	0.16	0.28
BCC-CSM1-1	0.30	0.26	0.72	0.56
BCC-CSM1-1-M	0.31	0.57	0.69	0.38
BNU-ESM	0.41	0.60	0.69	0.40
CanESM2	0.28	0.40	0.63	0.49
CCSM4	0.32	3.20	0.82	0.44
CESM1-BGC	0.40	1.49	0.75	0.31
CESM1-CAM5	0.27	1.75	0.35	0.14
CESM1-FASTCHEM	0.33	1.43	0.84	0.48
CESM1-WACCM	0.40	0.84	0.77	0.30
CMCC-CESM	0.46	1.56	0.45	-0.18
CMCC-CM	0.44	0.33	0.49	0.21
CMCC-CMS	0.42	0.47	0.16	0.30
CNRM-CM5	0.18	1.42	0.35	0.12
CNRM-CM5-2	0.34	1.56	0.35	0.19
CSIRO-Mk3-6-0	0.18	0.68	-0.03	0.40
EC-EARTH	0.24	2.83	0.71	0.63
FGOALS-g2	0.24	2.00	0.61	0.17

Table A4.10 Var, RMSE, Trend and ENSO between observations and model simulations of mean annual temperature for years 1991 – 1999 (Continued)

Models	VAR	RMSE	Trend	ENSO
FIO-ESM	0.28	0.45	0.76	0.57
GFDL-CM3	0.23	1.14	-0.02	0.46
GFDL-ESM2G	0.37	1.30	0.41	0.31
GFDL-ESM2M	0.52	1.00	0.41	0.24
GISS-E2-H	0.16	0.36	-0.01	0.17
GISS-E2-H-CC	0.34	0.38	0.52	0.20
GISS-E2-R	0.16	0.28	0.35	0.62
GISS-E2-R-CC	0.31	0.39	0.29	0.33
HadCM3	0.20	0.20	0.42	0.50
HadGEM2-AO	0.35	0.82	-0.06	0.29
HadGEM2-CC	0.35	0.52	0.05	0.38
HadGEM2-ES	0.23	0.22	-0.05	0.27
INMCM4	0.34	3.46	0.70	0.24
IPSL-CM5A-LR	0.27	1.30	0.77	0.72
IPSL-CM5A-MR	0.28	0.66	0.75	0.51
IPSL-CM5B-LR	0.31	1.32	0.47	0.40
MIROC5	0.22	0.37	0.06	0.45
MIROC-ESM	0.32	0.61	0.62	0.47
MIROC-ESM-CHEM	0.46	0.57	0.60	0.35
MPI-ESM-LR	0.34	0.45	0.72	0.49
MPI-ESM-MR	0.33	0.34	0.72	0.52
MRI-CGCM3	0.20	1.58	0.24	0.43
NorESM1_M	0.21	1.70	0.30	0.31
6-MODEL ENSEMBLE	0.32	1.67	0.55	0.27
40-MODEL ENSEMBLE	0.31	1.02	0.46	0.37

Table A4.11 Var, RMSE, Trend and ENSO between observations and model simulations of mean annual precipitation for years 1991 – 1999

Row	CV	RMSE	Trend	ENSO
Mean reference	0.13	-	5.26	-0.10
BCC-CSM1-1	0.10	221.04	0.41	0.04
BCC-CSM1-1-M	0.11	470.59	-1.06	0.00
BNU-ESM	0.13	172.04	1.38	-0.04
CanESM2	0.05	475.29	1.97	0.49
CCSM4	0.06	145.68	-0.55	-0.02
CESM1-BGC	0.14	199.66	0.81	-0.08
CESM1-CAM5	0.10	194.57	13.62	-0.12
CESM1-FASTCHEM	0.09	161.09	-1.92	0.48
CESM1-WACCM	0.10	275.96	-0.22	-0.07

Table A4.11 Var, RMSE, Trend and ENSO between observations and model simulations of mean annual precipitation for years 1991 – 1999 (Continued)

Row	CV	RMSE	Trend	ENSO
CMCC-CESM	0.12	176.76	-0.57	0.26
CMCC-CM	0.16	917.65	-2.52	0.33
CMCC-CMS	0.16	643.69	0.71	-0.09
CNRM-CM5	0.05	240.72	3.04	-0.21
CNRM-CM5-2	0.14	246.03	4.17	0.19
CSIRO-Mk3-6-0	0.06	197.17	4.09	-0.21
EC-EARTH	0.04	497.44	-3.43	0.02
FGOALS-g2	0.05	210.87	-0.68	-0.07
FIO-ESM	0.08	204.85	-0.89	0.57
GFDL-CM3	0.06	400.03	10.52	-0.03
GFDL-ESM2G	0.14	486.37	-2.07	0.03
GFDL-ESM2M	0.20	340.20	1.50	-0.14
GISS-E2-H	0.04	805.62	0.97	-0.01
GISS-E2-H-CC	0.15	970.07	3.33	0.00
GISS-E2-R	0.03	755.46	2.65	0.62
GISS-E2-R-CC	0.13	866.48	3.91	-0.02
HadCM3	0.04	138.41	1.29	-0.13
HadGEM2-AO	0.13	314.29	1.13	0.01
HadGEM2-CC	0.13	416.84	4.70	0.38
HadGEM2-ES	0.07	321.53	3.46	-0.12
INMCM4	0.11	645.93	6.40	-0.04
IPSL-CM5A-LR	0.05	216.06	-1.01	-0.01
IPSL-CM5A-MR	0.08	146.75	-0.73	-0.05
IPSL-CM5B-LR	0.17	234.80	-1.71	0.06
MIROC5	0.07	123.49	6.70	0.45
MIROC-ESM	0.06	244.25	6.17	-0.06
MIROC-ESM-CHEM	0.10	257.47	5.78	-0.02
MPI-ESM-LR	0.08	466.23	-3.85	-0.02
MPI-ESM-MR	0.09	471.71	-2.44	0.52
MRI-CGCM3	0.09	347.03	14.61	0.00
NorESM1_M	0.08	229.58	4.18	-0.03
6-MODEL ENSEMBLE	0.05	590.37	3.70	-0.05
40-MODEL ENSEMBLE	0.02	548.92	2.16	0.07

APPENDICES B

The additional part was added to respond to the committees' suggestion and comments. As there are currently over 60 GCMs in CMIP6, it would take too much time to use them all to evaluate their performance. Due to time constraints, the CMIP6 GCMs, which were previously among the top three performing tropical models to be released in 2019-2021, were selected for climate simulation performance evaluation at Southeast Asia. Moreover, the CNRM-CM-2 was selected to examine its performance in this additional study because it was confirmed as the best model with performance above Southeast Asia in this thesis. Therefore, in this additional study, the performance of 12 GCMs (CMIP5-6) was evaluated in simulating the historical temperature and precipitation at Southeast Asia. The three sub-periods were studied based on the temperature trend between 1901 and 2014: 1901 to 1940 (P1), 1941 to 1970(P2) and 1971 to 2014(P3), and the long-term climate from 1901 to 2014 (P4).

The results of these new analyzes are used to answer queries and are listed in the Appendices section. As a result, certain responses to analysis-related queries refer to the findings of this additional part.

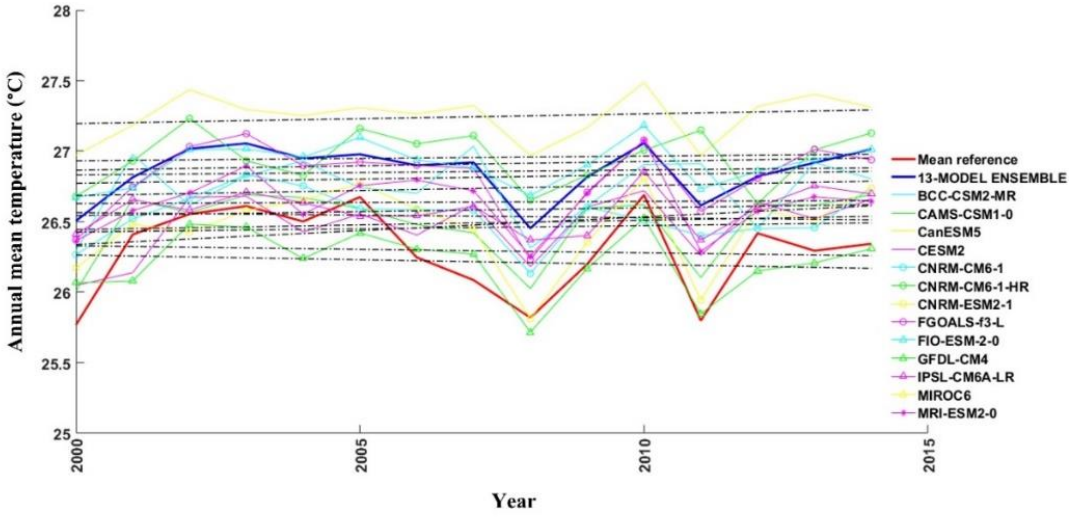

Figure A.1 Time series of the trend in annual mean temperature for the year 2000 to 2014

Figure A1 shows the temperature trend over the last 15 years. The annual mean temperature trend over Thailand for the years 2000 to 2014 is shown in the graph below (). The annual temperature trend of reference data is -0.005 °C/15 years, while all GCMs have trend values between -0.010 and 0.019 °C/15 year. Given these trend values, the length of this research period is not sufficient to show a clear trend value. This preliminary result suggest that using trend metrics to estimate climate change in less than 15 years is inappropriate.

Second, new assessments by selecting a new group of CMIP5-6 GCMs that were previously among the top three GCMs in tropical areas published between 2019 and 2021. The sub-periods of the trend were studied using the three main periods prone to temperature changes: 1901 to 1940, 1941 to 1970, and 1971 to 2014 (Figure A2). Examination of climate change at Southeast Asia using these GCM models also revealed that the temperature and precipitation variations in the three period are significantly affected by global temperature change (Figure A3 and Figure A4). Hence, temperature and precipitation sub-trends in Southeast Asia using these three time periods and these results were also examined in more details.

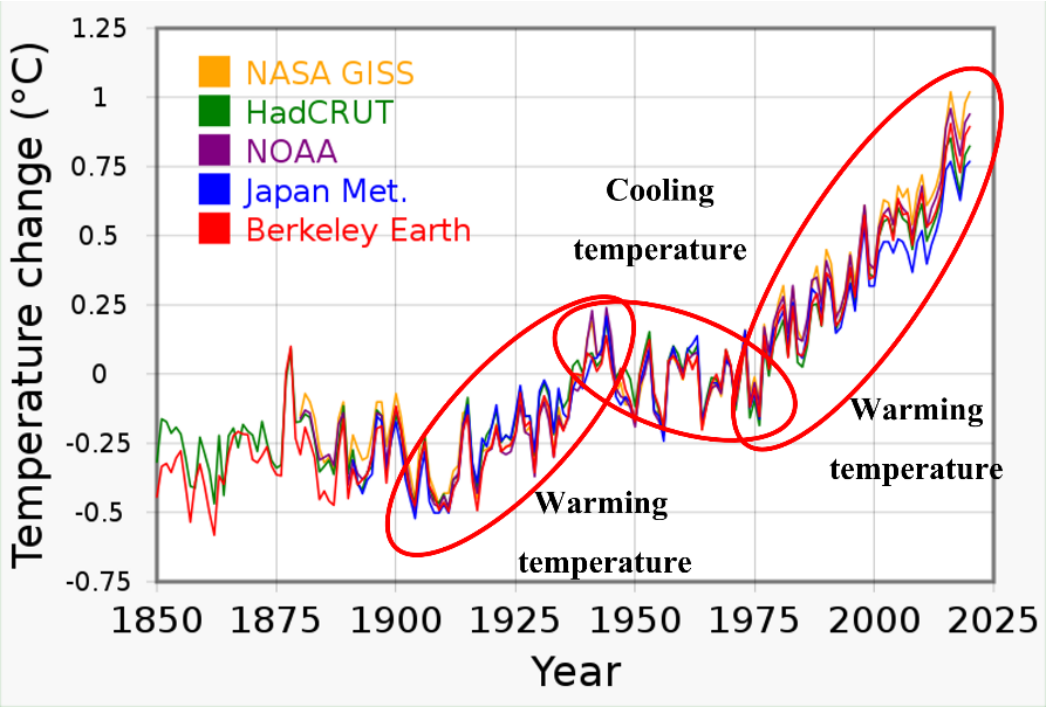

Figure A.2 Global Average Temperature Changes (NASA/NOAA, 2020)

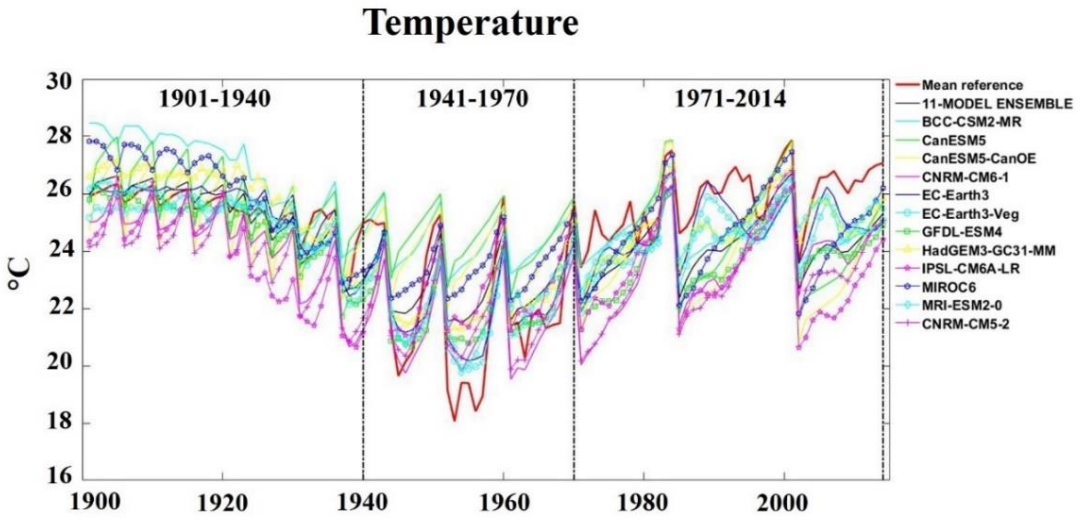

Figure A.3 The time series of mean annual temperature over the period 1901 to 2014 for Southeast Asia.

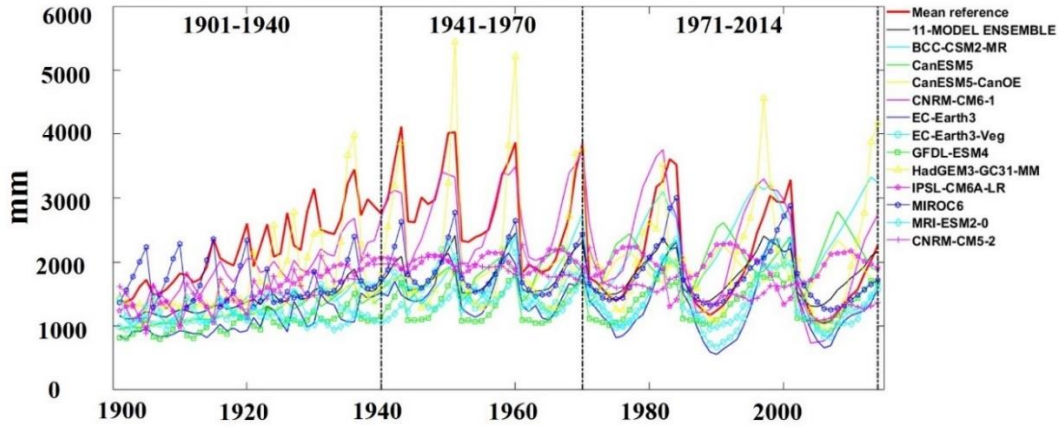

Figure A.4 The time series of mean annual of precipitation over the period from 1901 to 2014 for Southeast Asia.

Table A1 shows trend values for both variables from 1901 to 1940, 1941 to 1970, and 1971 to 2014. For temperature, the results in almost all GCMs indicated a decreasing trend from 1941 to 1970 and an increasing trend from 1901 to 1940 and 1971 to 2014, which is consistent with the mean reference. However, although GCMs can capture the trend direction, the magnitude of the trend value of the GCMs differs significantly from the mean reference. For precipitation, the mean reference revealed an increasing precipitation trend during the periods 1901 to 1940 and 1941 to 1970, but

a decreasing precipitation trend during 1971 to 2014. Considering these sub-periods, the results show a significant relationship between the trends of temperature and precipitation at Southeast Asia. When temperature shows a decreasing trend, precipitation shows a significant increasing trend. The mean annual trends of temperature and precipitation in the different periods were shown in Figure A5 and Figure A6, respectively, in the Appendix.

From the analysis of the results for the short-term period, the larger the time interval for the analysis (e.g., 30 to 45 years), the better the reference data and GCMs capture the trends in temperature and precipitation. The findings of this additional study demonstrate that trend metrics can be used to analyze climatic trends over a short time period, but it is conceivable that a longer time period than 30 years is needed.

Table A1 Trend-T and Trend-P mean annual temperature and precipitation for year 1901 to 1940, 1941 to 1970, and 1971 to 2014

Models	Temperature (°C)			Precipitation (%)		
	1901-1940	1941-1970	1971-2014	1901-1940	1941-1970	1971-2014
Mean reference	0.09	-0.09	0.58	0.48	2.31	-1.36
BCC-CSM2-MR	0.31	-0.01	0.70	-1.61	2.45	1.46
CanESM5	0.35	-0.08	1.29	0.30	2.04	-0.13
CanESM5-CanOE	0.27	-0.08	1.11	0.10	3.07	-0.02
CNRM-CM6-1	0.19	-0.11	0.69	-0.99	2.79	3.18
EC-Earth3	0.46	-0.08	0.74	0.63	2.09	0.17
EC-Earth3-Veg	0.38	-0.15	0.72	-0.52	3.93	-0.32
GFDL-ESM4	0.31	-0.23	0.67	0.86	1.94	4.11
HadGEM3-GC31-MM	0.32	-0.32	1.07	-2.99	1.74	-2.24
IPSL-CM6A-LR	0.29	0.04	0.81	-1.45	0.67	-0.08
MIROC6	0.26	-0.08	0.45	-0.05	2.35	0.57
MRI-ESM2-0	0.24	-0.14	0.67	-0.06	5.32	4.82
11-MODEL ENSEMBLE	0.31	-0.11	0.81	-0.52	2.57	0.85

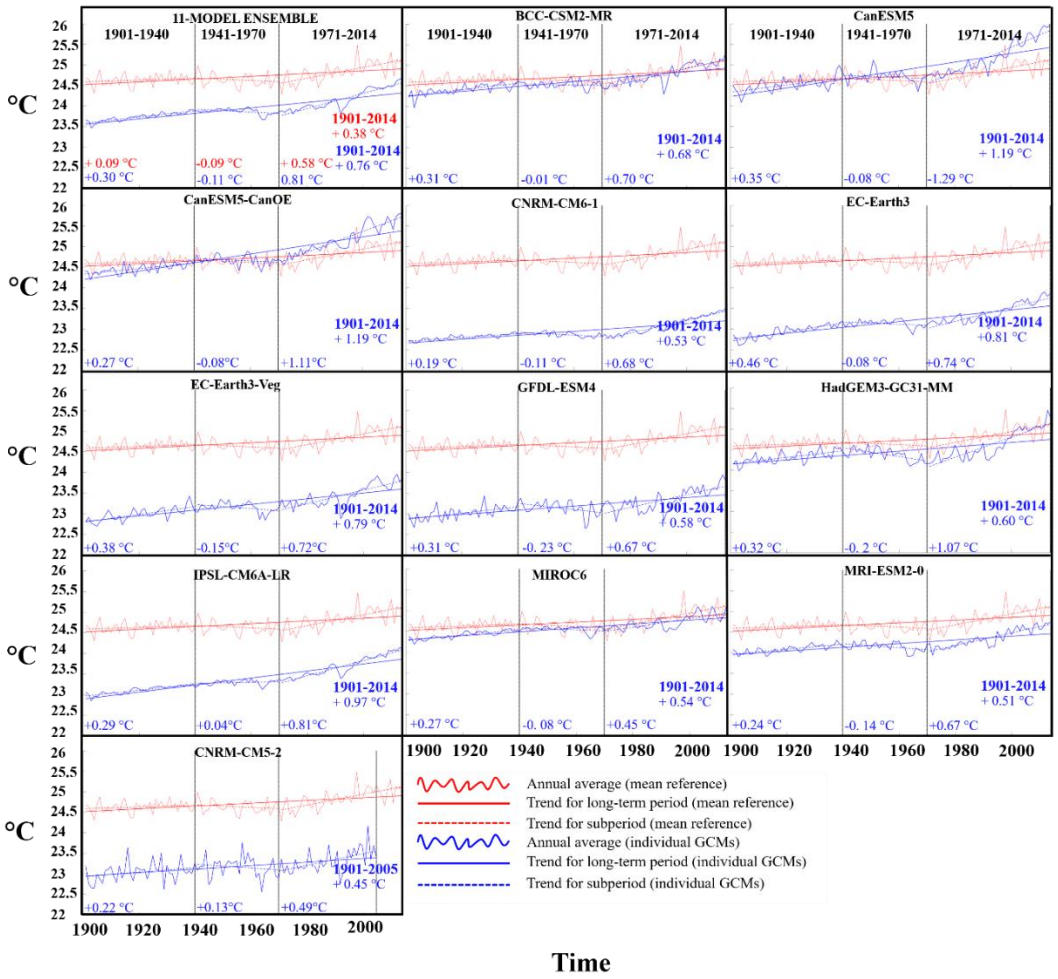

Figure A.5 Time series of mean annual temperature trend (Trend-T) for year 1901 to 1940, 1941 to 1970, 1971 to 2014, and 1901 to 2014 of mean reference (red line) and individual GCMs (blue line).

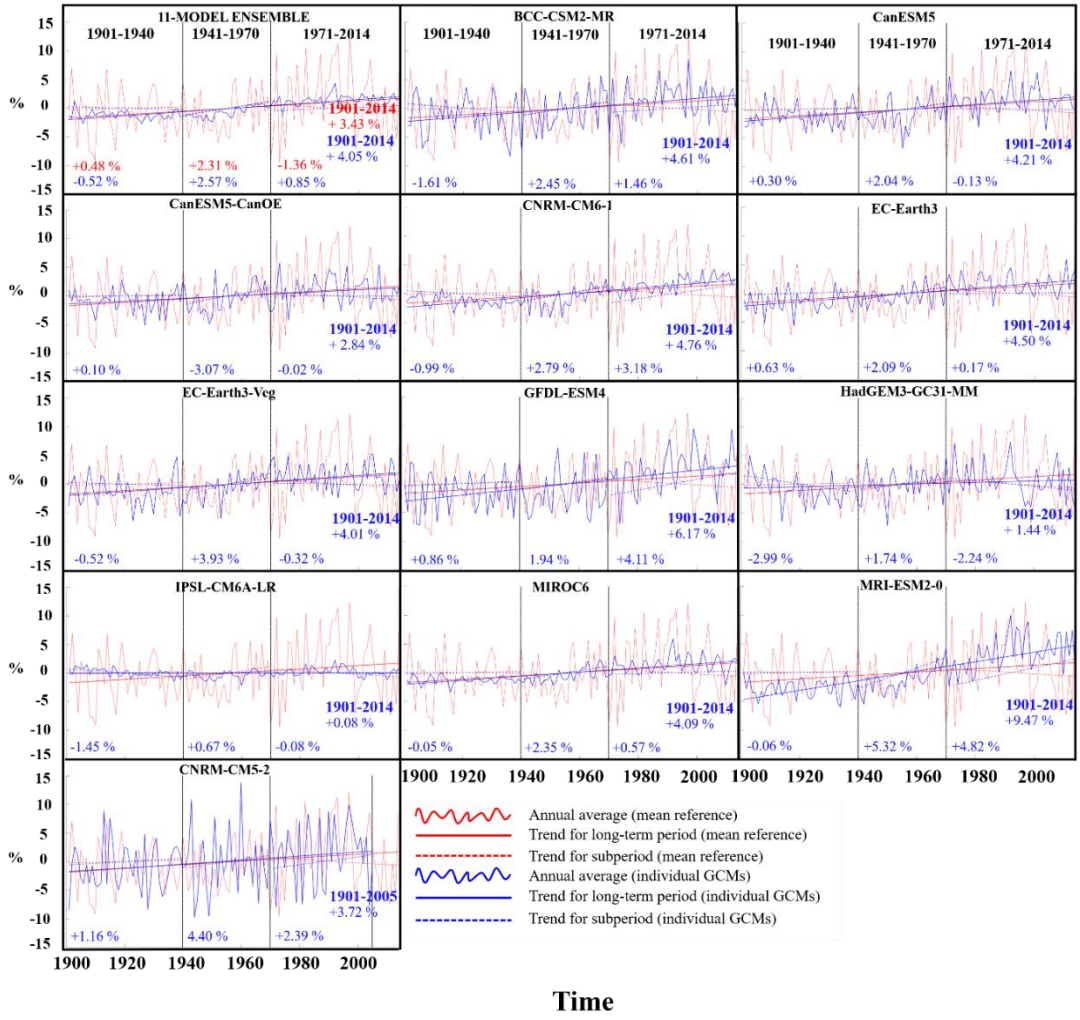

Figure A.6 Time series of the mean annual precipitation trend (Trend-P) for the years 1901 to 1940, 1941 to 1970, 1971 to 2014, and 1901 to 2014 of mean reference (red line) and individual GCMs (blue line)

In the additional study, the ENSO metric was used to evaluate 11 CMIP6 GCMs for simulating temperature and precipitation in both short-term and long-term time periods. The ENSO values of each model for the years 1901 to 1940, 1941 to 1970, 1971 to 2014, 1901 to 2014 are shown in Table A2.

Table A2 Correlation coefficient of winter temperature with Niño 3.4 index and that of winter precipitation with Niño 3.4 index for 1901 to 1940, 1941 to 1970, 1971 to 2014, 1901 to 2014

Models	Temperature				Precipitation			
	1901-1940	1941-1970	1971-2014	1901-2014	1901-1940	1941-1970	1971-2014	1901-2014
Mean reference	0.28	0.35	0.23	0.23	-0.11	-0.08	-0.11	-0.09
BCC-CSM2-MR	0.14	0.16	0.40	0.42	-0.09	-0.04	-0.05	-0.08
CanESM5	0.51	0.24	0.65	0.70	-0.10	-0.10	-0.03	-0.12
CanESM5-CanOE	0.25	0.23	-0.20	0.64	0.00	0.10	-0.01	-0.04
CNRM-CM6-1	0.04	-0.20	0.46	0.43	0.04	-0.01	-0.04	-0.12
EC-Earth3	0.58	0.53	0.78	0.74	-0.20	-0.18	-0.11	-0.29
EC-Earth3-Veg	0.48	0.50	0.78	0.72	-0.17	-0.19	-0.10	-0.22
GFDL-ESM4	0.42	0.45	0.60	0.52	-0.11	-0.08	-0.07	-0.11
HadGEM3-GC31-MM	0.27	0.43	0.54	0.48	-0.04	-0.04	0.02	-0.04
IPSL-CM6A-LR	0.40	0.46	0.78	0.86	0.03	0.10	0.12	0.13
MIROC6	0.56	0.53	0.66	0.71	-0.03	-0.06	-0.10	-0.20
MRI-ESM2-0	0.30	0.41	0.44	0.46	-0.07	-0.11	-0.04	-0.20
11-MODEL ENSEMBLE	0.62	0.60	0.86	0.81	-0.07	0.02	0.00	-0.25

After considering the evaluation results, the difference in ENSO values between all models and the reference data of temperature evaluation for the short-term period of 1901 to 1940, 1941 to 1970, 1971 to 2014 ranged from 0.01 to 0.34, 0.06 to 0.55, 0.17 to 0.63, and that for the long-term period of 1901 to 2014 ranged from 0.19 to 0.63, respectively. Whereas the difference of ENSO values between all models and the reference data of precipitation evaluation for the short-term period of 1901 to 1940, 1941 to 1970, 1971 to 2014 ranged from 0 to 0.15, 0 to 0.18, 0 to 0.23, and that for the long-term period of 1901 to 2014 ranged from 0.01 to 0.22, respectively. These results indicate that ENSO metrics can be used to assess models over a 30-year period because they can simulate the interaction between the atmosphere and oceans in the study area and the Nino 3.4 index region.

It was also found that the period 1971 to 2014 is the period when El Nino and La Nina events had an impact on climate simulations. This is due to the similarity in the range of ENSO values between all models and the references data for

the 1971 to 2014 and 1901 to 2014 periods, while ENSO values for the other sub-periods had a smaller range. Therefore, these preliminary results from additional research suggest that the 20th century climate modeling errors were partially influenced by the El Nino and La Nina phenomena for the 1970.

VITAE

Name Suchada Kamworapan

Student ID 5730430001

Educational Attainment

Degree	Name of Institute	Year of Graduation
Bachelor's degree of science (Environmental Geoinformatics)	Prince of Songkla University, Phuket Campus, Thailand	2014

List of Publication and Proceeding

Kamworapan, S., and Surussavadee, C. (2019). "Evaluation of CMIP5 global climate models for simulating climatological temperature and precipitation for Southeast Asia." Advances in Meteorology, 2019.

International conference:

Kamworapan, S., & Surussavadee, C. (2017, November). "Performance of CMIP5 global climate models for climate simulation in Southeast Asia." In TENCON 2017-2017 IEEE Region 10 Conference (pp. 718-722). IEEE.